

**Effect of Desorption Purge Gas Oxygen Impurity on Heel Formation During  
Regeneration of Beaded Activated Carbon Saturated with Organic Vapors**

by

Seyed Mojtaba Hashemi

A thesis submitted in partial fulfillment for the requirements for the degree of

Master of Science

in

ENVIRONMENTAL ENGINEERING

Department of Civil and Environmental Engineering

University of Alberta

© Seyed Mojtaba Hashemi, 2017

## Abstract

Irreversible adsorption or heel formation during cyclic adsorption/regeneration of high molecular weight volatile organic compounds (VOCs) onto activated carbon decreases its adsorption capacity and lifetime. The effect of regeneration purge gas oxygen impurity on activated carbon performance, specifically during successive adsorption/regeneration cycles was investigated. 5-cycle adsorption/regeneration tests were performed on microporous beaded activated carbon (BAC) using 11 different aliphatic and aromatic organic compounds representative of VOCs produced from painting booths. Nitrogen with different oxygen concentrations ( $\leq 5$  to 20,000 ppm) was used as regeneration purge gas during thermal desorption of 1,2,4-trimethylbenzene (TMB). Cumulative heel formation increased from 0.5% to 15.4% as the oxygen concentration in the desorption purge gas increased from  $\leq 5$  ppm to 20,000 ppm, respectively, in case of TMB adsorption. For regeneration of BAC saturated with all other VOCs, nitrogen with two levels of oxygen impurity ( $\leq 5$  ppm and 10,000 ppm) was used as regeneration purge gas. At 10,000 ppm oxygen concentration, the cumulative heel was 0.7-3.2% for aliphatic compounds and 0-13% for aromatic compounds while at  $\leq 5$  ppm, it was 0.3-1.3% for aliphatic compounds and 0.0-4.6% for aromatic compounds. Overall, regeneration of alkyl-aromatics was impacted by presence of oxygen in the purge gas to a greater degree compared to aliphatic compounds. Thermogravimetric analysis of the regenerated samples showed desorption of species at high temperatures (400-600°C) which shows that these compounds are strongly attached to the adsorbent surface. The results suggest that the effect of regeneration purge gas oxygen impurities on the irreversible adsorption of VOCs is dependent on the nature of the adsorbate- likely its tendency to react with oxygen. The results from this study help explain the heel formation mechanism and how it relates to regeneration purge gas purity.

## **Dedication**

I would like to dedicate this thesis to my lovely parents, Jalal and Maryam, for their continuous support and encouragement.

## **Acknowledgement**

I would like to express my gratitude to Dr. Zaher Hashisho for his supervision, guidance and support through my research. This work could not have been accomplished without his guidance, knowledge, and passion.

I also would like to acknowledge financial support from Ford Motor Company and the Natural Sciences and Engineering Research Council (NSERC) of Canada.

And lastly, I would like to thank my colleagues in the Air Quality Characterization and Control Lab: Masoud Jahandar Lashaki, Pooya Shariaty, Mohammad Feizbakhshan, Saeed Niknaddaf, Imranul Islam Laskar, Abedeh Gholidoust, Nastaran Mosavari, Monisha Alam and Biniyam Amdebrhan.

# Table of Contents

1. CHAPTER 1: Introduction .....	1
1.1 Introduction .....	2
1.1.1 Background .....	2
1.1.2 VOCs emission abatement techniques.....	3
1.2 Objectives.....	4
1.3 Thesis Outline .....	5
References.....	6
2. CHAPTER 2: Literature Review .....	8
2.1 Adsorption.....	9
2.1.1 Reversibility of Adsorption.....	9
2.2 Adsorbent Material.....	10
2.3 Regeneration.....	12
2.3.1 Thermal Regeneration.....	13
2.3.2 Chemical Regeneration.....	13
2.3.3 Effect of Thermal Regeneration Parameters.....	15
References.....	20
3. CHAPTER 3: Regeneration of Beaded Activated Carbon (BAC) Saturated with 1,2,4-trimethylbenzene (TMB) with Oxygen-containing Purge Gas .....	23
3.1 Introduction .....	24

3.2	Materials and Methods .....	26
3.2.1	Adsorbent and adsorbate .....	26
3.2.2	Experimental setup and methods .....	27
3.2.3	BAC characterization.....	29
3.3	Results and Discussion.....	30
3.4	Conclusions .....	41
	References .....	42
4.	CHAPTER 4: Heel Buildup During Thermal Desorption of Volatile Organic Compounds off Beaded Activated Carbon in Presence of Oxygen Impurity .....	44
4.1	Introduction .....	45
4.2	Materials and Methods .....	48
4.2.1	Adsorbent.....	48
4.2.2	Adsorbates.....	49
4.2.3	Experimental setup and methods .....	50
4.2.4	BAC characterization.....	52
4.3	Results and Discussion.....	53
4.4	Conclusions .....	69
	References .....	70
5.	CHAPTER 5: Conclusions and Recommendations.....	73
5.1	Conclusions .....	74

5.2 Recommendations .....	75
Bibliography .....	76
Appendices.....	81
Appendix A: Mass balance cumulative heel tables of Chapter 3 .....	81
Appendix B: Adsorption breakthrough curves of Chapter 4 .....	85
Appendix C: Mass balance cumulative heel tables of Chapter 4.....	96

## List of Tables

<b>Table 3-1.</b> Characterization of regenerated samples .....	36
<b>Table 4-1.</b> Summary of studies on adsorption and regeneration on activated carbon .....	48
<b>Table 4-2.</b> Adsorbate structures and physical properties .....	49
<b>Table 4-3.</b> Characterization results of virgin and regenerated BAC .....	62



## List of Figures

<b>Figure 1-1.</b> Classification of VOCs treatment techniques [1].....	4
<b>Figure 3-1.</b> Schematic of the adsorption/regeneration setup.....	28
<b>Figure 3-2.</b> TMB Adsorption breakthrough curves at varying oxygen concentrations in the desorption purge gas .....	32
<b>Figure 3-3.</b> (a) Cumulative and first cycle mass balance heel results (b) Adsorption capacity of the adsorbent for the first and fifth cycle at different levels of O <sub>2</sub> impurity.....	34
<b>Figure 3-4.</b> DTG analysis of samples regenerated at different oxygen in the purge gas .....	38
<b>Figure 3-5.</b> Pore size distribution of BAC samples regenerated after 5-cycle TMB adsorption/regeneration at different levels of oxygen impurity in the purge gas .....	40
<b>Figure 3-6.</b> Cumulative heel vs. (a) Micropore volume, and (b) Surface area .....	40
<b>Figure 4-1.</b> Schematic of the adsorption/regeneration setup.....	53
<b>Figure 4-2.</b> Breakthrough reduction times (first adsorption cycle compared to the fifth cycle) for different adsorbates at two levels of oxygen impurity in the purge gas.. .....	55
<b>Figure 4-3.</b> Mass balance cumulative (5-cycle) heel results .....	58
<b>Figure 4-4.</b> Surface oxygen concentration of regenerated samples .....	63
<b>Figure 4-5.</b> DTG analysis of 5-cycle BAC samples regenerated with 10,000 ppm O <sub>2</sub> in N <sub>2</sub> purge gas .....	65
<b>Figure 4-6.</b> DTG analysis of 5-cycle BAC samples regenerated with $\leq 5$ ppm O <sub>2</sub> in N <sub>2</sub> purge gas .....	65
<b>Figure 4-7.</b> DTG analysis of 5-cycle BAC samples saturated with different adsorbates and regenerated at two levels of oxygen concentration in the purge gas .....	67
<b>Figure 4-8.</b> PSD of BAC samples regenerated with 10,000 ppm O <sub>2</sub> in N <sub>2</sub> purge gas .....	68

## **1. CHAPTER 1: Introduction**

## **1.1 Introduction**

### **1.1.1 Background**

Volatile Organic Compounds (VOCs) include degreasers, solvent thinners, cleaners, lubricants, and liquid fuels [1]. A multitude of definitions for VOCs exist among different regulatory systems depending on how VOCs affect the surrounding environment. Environment Canada defines VOCs under Schedule 1 (item 65) of the Canadian Environmental Protection Act (CEPA), as organic compounds having high vapor pressure that contain one or more carbon atoms and readily vaporize to the atmosphere. This definition excludes substances such as methane, ethane, methyl acetate and methyl chloride [2]. The US Environmental Protection Agency (EPA) defines VOCs as any compound of carbon, excluding carbon monoxide, carbon dioxide, carbonic acid, metallic carbides or carbonates and ammonium carbonate, which takes part in atmospheric photochemical reactions, except those designated by EPA as having negligible photochemical reactivity [3]. The World Health Organization defines VOCs as any organic compounds having a boiling point of in the range from (50-100°C) to (240-260°C), corresponding to a saturation vapor pressure of greater than 102 kPa at 25°C [4].

The main sources of VOCs emissions can be categorized in two groups: biogenic sources and anthropogenic sources. The major biogenic sources include woods, crops, oceans, and volcanos [5]. Oil and natural gas production, petroleum refining, paint production, and pulp and paper industry are examples of the main anthropogenic sources of VOCs emissions [6].

The effect of VOCs on human health and the environment is a matter of concern. Many VOCs are toxic and can cause headaches, eye and nose irritations, nausea and damage to the liver and nervous system [7]. Some VOCs are precursors to tropospheric ozone formation and some

deplete the stratospheric ozone layer [8]. Thus, it is crucial to control VOCs emissions to meet the environmental regulations.

### **1.1.2 VOCs emission abatement techniques**

VOCs abatement techniques can be classified into two categories namely (i) process and equipment modification and (ii) add-on control techniques. In the first group the process equipment, raw material or the process itself are modified such that the production of VOCs is minimized, while in the second group an additional control method is used to regulate emissions. Even though the former is the most efficient way of emissions control, it is more often than not impossible to change the process conditions or equipment. The techniques in the second category are further classified into two sub-categories: destruction-based and recovery-based techniques [1].

Destruction-based techniques are used when recovery of the removed compounds is not necessary or economical. The removed compounds are converted to other non-hazardous chemical compounds such as  $\text{CO}_2$  and  $\text{H}_2\text{O}$ . Common destruction techniques include oxidation and biofiltration [9].

Recovery methods remove the organic compounds in such way that they can be recovered for reuse. The most common recovery techniques are absorption, adsorption, condensation, and membrane separation [1, 10]. A tree diagram of different VOCs treatment techniques is shown in Figure 1-1.

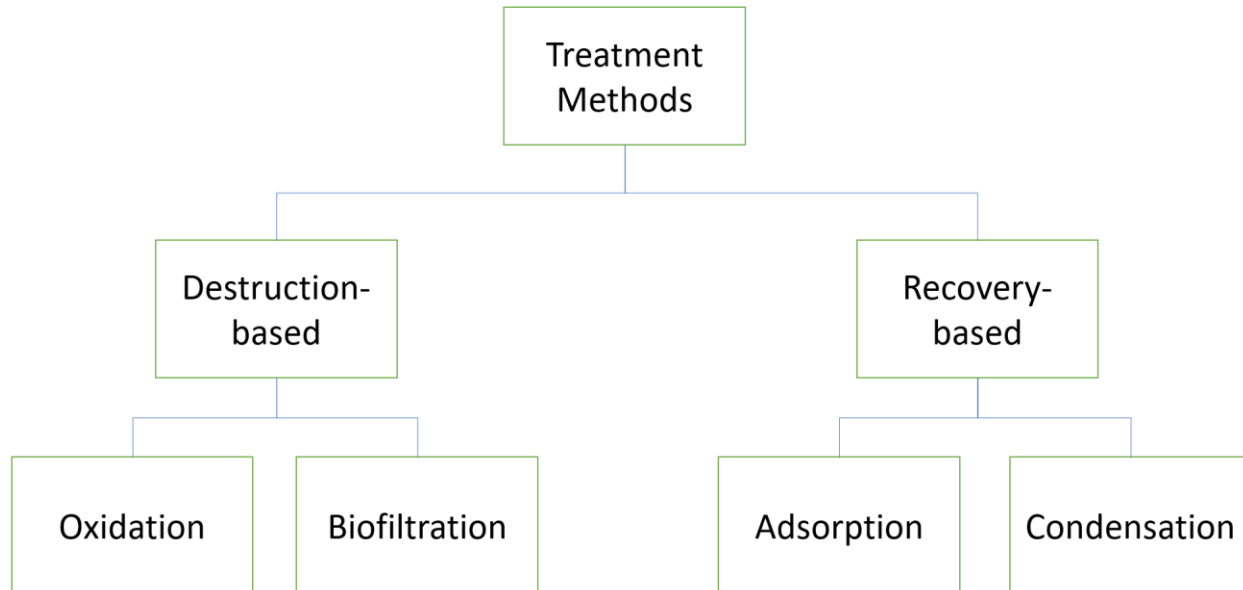


Figure 1-1. Classification of VOCs treatment techniques [1]

Adsorption on activated carbon is an established and promising method for capturing VOCs from polluted streams. Adsorption must be coupled with regeneration to allow reuse of the carbon for an economically feasible application [11]. Activated carbon can be regenerated by different means such as thermal [12], extractive [13], chemical [14], electrochemical [15], and biological [16]. Thermal desorption at temperatures of  $< 300^{\circ}\text{C}$  is industrially used for regeneration of adsorbents loaded with gas phase compounds [17]. The successive adsorption-regeneration cycles when regeneration is performed by means of elevating the temperature of the adsorbent bed, are referred to as thermal swing adsorption (TSA) [18].

## 1.2 Objectives

The goal of this study is to investigate the effect of purge gas oxygen impurity on irreversible adsorption of gas phase organic compounds on BAC. Eleven compounds including 6 aromatic and

5 aliphatic compounds were tested for their adsorption capacity and regeneration efficiency.

Therefore, the objectives of this study are:

- 1 to investigate the effect of purge gas oxygen impurity on regeneration efficiency of BAC saturated with TMB
- 2 to elucidate how oxygen impurity in the purge gas affects regeneration of different adsorbates with different functionalities and structures

Presence of oxygen in purge gas may trigger chemical reactions between oxygen and the adsorbate which may result in higher heel formation for particular compounds. On the other hand, using low purity nitrogen may reduce the operation costs significantly. This results in a tradeoff between operating costs and permissible heel formation. Studying the effect of purge gas impurity on heel helps optimizing the regeneration process as well as gaining insight into the different behaviors of VOCs in presence of oxygen.

### **1.3 Thesis Outline**

This thesis consists of five chapters which will contribute to the overall goal of this research. Chapter 1 provides an introduction to the background, significance and motivation of this research. Chapter 2 provides a general literature review about adsorption, adsorbent material, regeneration, and heel formation. Chapter 3 investigates the effect of regeneration purge gas oxygen impurity on irreversible adsorption of TMB. Chapter 4 compares the effect of purge gas oxygen impurity for different adsorbates, and chapter 5 includes conclusions of this research as well as recommendations for future work.

## References

1. Khan, F.I. and A. Kr. Ghoshal, *Removal of Volatile Organic Compounds from polluted air*. Journal of Loss Prevention in the Process Industries, 2000. **13**(6): p. 527-545.
2. CEPA. *Definition of Volatile Organic Compounds (VOCs)*. 1999 2016-01-04 [cited 2016 06/06]; Available from: <https://www.ec.gc.ca/inrp-npri/default.asp?lang=En&n=EF5C823B-1>.
3. USEPA. *Technical Overview of Volatile Organic Compounds*. 2016 17/3/2016 [cited 2016 28/11/2016]; Available from: <https://www.epa.gov/indoor-air-quality-iaq/technical-overview-volatile-organic-compounds>.
4. ISO, *ISO 16000-6*, in *Indoor air — Part 6: Determination of volatile organic compounds in indoor and test chamber air by active sampling on Tenax TA sorbent, thermal desorption and gas chromatography using MS or MS-FID*. 2011.
5. Guenther, A., *A global model of natural volatile organic compound emissions*. Journal of geophysical research, 1995. **100**: p. 8873-8892.
6. Piccot, S.D., J.J. Watson, and J.W. Jones, *A global inventory of volatile organic compound emissions from anthropogenic sources*. Journal of Geophysical Research, 1992. **97**(D9): p. 9897-9912.
7. USEPA. *Volatile Organic Compounds Emissions*. 2014 [cited 2016 06-06]; Available from: <https://cfpub.epa.gov/roe/indicator.cfm?i=23>.
8. Bowman, F.M. and J.H. Seinfeld, *Atmospheric chemistry of alternate fuels and reformulated gasoline components*. Progress in Energy and Combustion Science, 1995. **21**(5): p. 387-417.
9. Parmar, G.R. and N.N. Rao, *Emerging Control Technologies for Volatile Organic Compounds*. Critical Reviews in Environmental Science and Technology, 2009: p. 41-78.
10. Berenjian, A., N. Chan, and H.J. Malmiri, *Volatile Organic Compounds removal methods: A review*. American Journal of Biochemistry and Biotechnology, 2012. **8**(4): p. 220-229.
11. Carratalá-Abril, J., et al., *Regeneration of activated carbons saturated with benzene or toluene using an oxygen-containing atmosphere*. Chemical Engineering Science, 2010. **65**(6): p. 2190-2198.

12. Sabio, E., et al., *Thermal regeneration of activated carbon saturated with p-nitrophenol*. Carbon, 2004. **42**(11): p. 2285-2293.
13. Cooney, D.O., A. Nagerl, and A.L. Hines, *Solvent regeneration of activated carbon*. Water Research, 1983. **17**(4): p. 403-410.
14. Martin, R.J. and W.J. Ng, *The repeated exhaustion and chemical regeneration of activated carbon*. Water Research, 1987. **21**(8): p. 961-965.
15. Zhang, H., *Regeneration of exhausted activated carbon by electrochemical method*. Chemical Engineering Journal, 2002. **85**(1): p. 81-85.
16. Dobrevski, I. and L. Zvezdova, *Biological regeneration of activated carbon*. Water Science and Technology, 1989. **21**(1): p. 141-143.
17. Salvador, F., et al., *Regeneration of carbonaceous adsorbents. Part I: Thermal Regeneration*. Microporous and Mesoporous Materials, 2015. **202**: p. 259-276.
18. Hwang, K.S., et al., *Adsorption and thermal regeneration of methylene chloride vapor on an activated carbon bed*. Chemical Engineering Science, 1997. **52**(7): p. 1111-1123.



## **2. CHAPTER 2: Literature Review**

## **2.1 Adsorption**

Adsorption is the use of certain solids' ability of selectively concentrating specific substances from a gaseous or a liquid stream onto their surfaces. In the context of gaseous separations adsorption is used for removing humidity, odors, and impurities from industrial gas streams. Adsorption is typically categorized as physical adsorption (physisorption) or chemical adsorption (chemisorption) [1].

Physical adsorption is readily reversible and is the result of van der Waals forces of attraction between the adsorbent particles and the adsorbate molecules. For example, when forces of attraction between a solid and a gas are greater than those between the gas molecules, the gas will condense on the surface of the solids even at pressures lower than its vapor pressure at the corresponding temperature. Industrial operations exploit this reversibility to recover the adsorbent for reuse, or for recovery of adsorbed species [1].

Chemisorption however, involves stronger forces of attraction between the adsorbent and the adsorbate, i.e. chemical bonds. These forces of attraction are much greater than those of physical adsorption. The phenomenon is usually irreversible and upon desorption the original compound may have chemically changed. Both phenomena can occur simultaneously, while at higher temperatures substances that would normally physically adsorb, may chemisorb to the surface [1].

### **2.1.1 Reversibility of Adsorption**

Desorption is the result of changes in operating conditions such as a decrease in liquid phase concentration or displacement of adsorbed compounds by competitive adsorption [2]. Adsorption can be categorized into reversible adsorption and irreversible adsorption. Reversible

adsorption is when adsorbate and adsorbent are held together by van der Waals forces and/or weaker charge-transfer complexes that happen at other adsorption sites [3].

On the other hand, irreversible adsorption is a stronger interaction between the adsorbate and the adsorbent and can be explained by two mechanisms [2]. One is bonding on adsorbate molecules to specific functional groups on active sites of carbon surface which results in covalent bonding [2, 3]. The strength of this interaction is dependent on the type of surface functional groups and the adsorbate [2]. Therefore, researchers have attributed irreversible adsorption to chemisorption, the degree of which is proportional to the number of high-energy bonds [3-5]. The second mechanism is the polymerization of phenolic compounds onto activated carbon due to the presence of oxygen [2, 6-8]. Aromatic compounds that undergo oxidative coupling reaction may be irreversibly attached to surface of the adsorbent [9, 10]. Oxidative coupling is also dependent on the carbon activation process [2]. Researchers observed a higher degree of irreversible adsorption for thermally activated carbon [2, 8]. They explained this by the affinity of thermally activated carbon towards oxygen and modifications in surface chemistry [2].

In a study by Snoeyink et al. [11] researchers observed that only 50% of the adsorbed phenol is desorbed from granular activated carbon. However, Schultz obtained full recovery of carbon (100% reversibility) for phenol adsorbed on powdered activated carbon from a different manufacturer. These results indicate that irreversible adsorption depends on the adsorbate as well as the adsorbent [3].

## **2.2 Adsorbent Material**

Porous carbonaceous materials have excellent adsorbent properties such as large surface area and high adsorption capacity. These factors make materials such as activated carbons (ACs) ideal

for use in diverse applications such as treatment of liquid streams [12, 13], gas streams [14], as well as storage of valuable gases [15]. Activated carbon comes in different shapes and sizes depending on the application it is being used for. Different shapes of activated carbon include extruded activated carbon (EAC), Granular activated carbon (GAC) [16], powder activated carbon (PAC) [17], beaded activated carbon (BAC) [4], and activated carbon fiber cloth [5].

Adsorption behaviour of AC is dictated by its physical and chemical properties such as pore size distribution, surface functional groups, and ash content. Pore size distribution is influenced by the material from which the AC is extracted as well as the activation procedure [18, 19]. Surface functional groups are another factor that affects the adsorption properties of AC. The surface of the AC contains oxygen and nitrogen groups which impact its surface functionality [18, 19].

Lillo-Rodenas et al. [19] investigated the effect of pore size distribution and surface oxygen groups on adsorption capacity of activated carbons. They tested ten activated carbons prepared by different activation techniques and different precursors. Adsorption was performed at  $298 \pm 1$  K and the concentration of the VOC (Benzene and toluene) was 200 ppmv in helium gas stream. They found that adsorption capacity is higher for toluene than for benzene, in agreement with the relative pressures of the compounds ( $5.4 \times 10^{-3}$  and  $1.6 \times 10^{-3}$ , respectively). Their results indicate that adsorption capacity varies depending on the type of AC used and that it correlates to the micropore volume obtained from CO<sub>2</sub> adsorption. They attributed adsorption of benzene to narrow micropores ( $< 0.7$  nm) only, while for toluene total micropore volume was found to be a better correlation. To study the effect of surface oxygen groups, they heated the ACs in an inert atmosphere (helium) up to 1173 K to remove the surface oxygen groups, whereas the porosity remains nearly unchanged by this treatment. They found that ACs with less surface oxygen groups have higher adsorption capacity as compared to untreated ones. The effect of physicochemical

properties of GAC on adsorption of o-xylene was investigated by Li et al. [18]. They treated GAC prepared from coconut shell with alkalis and acids and performed adsorption tests at 22-27°C using dry air flow containing 2176-2239 mg/m<sup>3</sup> of adsorbate. Alkali-treated GAC was found to have higher adsorption capacity than untreated GAC, whereas acid-treated GAC reduced the adsorption capacity. Alkali treatment resulted in increase in surface area and pore volume, and elimination of total oxygen containing functional groups. On the other hand, acid treatment showed the opposite trend. They concluded that surface area, porosity, and surface chemistry of the adsorbent are determining factors of adsorption capacity and increase in surface area, total pore volume, and surface hydrophobicity favorably affect the adsorption capacity.

Pevida et al. [14] studied the effect of surface modification of ACs on CO<sub>2</sub> adsorption. They modified two commercial ACs by heat treating them at 200-800°C with gaseous ammonia, resulting in an increase in their basic character by adding nitrogen-functionalities to the carbon. CO<sub>2</sub> adsorption capacity at 25°C was found to be higher for the modified ACs as compared to the original carbons. Their results showed that CO<sub>2</sub> adsorption capacity is related to specific nitrogen-functionalities that increase the CO<sub>2</sub>-adsorbent affinity, rather than the total nitrogen content of the adsorbent. Thus, they concluded that to increase CO<sub>2</sub> capture, surface modifications of commercial ACs should be focused on nitrogen-functionalities that promote CO<sub>2</sub> capture without altering the texture of the adsorbent.

## **2.3 Regeneration**

Cyclic adsorption systems are usually followed by in situ thermal regeneration to remove the adsorbate from the adsorbent. The progressive accumulation of the adsorbate on the adsorbent pores results in gradual reduction of the adsorbent's adsorption capacity. The main purpose of regeneration is to revitalize the adsorbent and recover its original adsorption capacity [20].

Regeneration must maintain the porous structure of the adsorbent as well as eliminating the adsorbate [4].

### **2.3.1 Thermal Regeneration**

There are several methods for adsorbent regeneration, including thermal, chemical, microbial, and vacuum regeneration. Thermal regeneration is the most common regeneration method and is categorized into traditional method which is accomplished by purging the adsorbent bed with a hot purge gas or steam [21], and the more novel methods which include microwave, ultrasound, and use of electrical current [22-24]. The regeneration purge gas is usually an inert gas (such as N<sub>2</sub>) to prevent any reaction between the gas and the desorbed species [20]. Microwave regeneration exposes the adsorbent to microwaves to heat the adsorbent and can have much higher heating rates than traditional regeneration [23]. Resistive heating passes an electrical current through the adsorbent to heat the bed [5].

### **2.3.2 Chemical Regeneration**

Chemical Regeneration techniques were first introduced as alternatives to thermal regeneration to reduce energy requirements and improve the regeneration efficiency [25]. Chemical regeneration techniques including solvent, NaOH, Wet Air, and Thermal Oxidative Regeneration have been studied and optimized. Regeneration with liquid water is a simple way of regenerating carbonaceous adsorbents in which water acts as a solvent that extracts the retained adsorbate and regenerates the adsorbent [25]. However, regeneration with cold liquid water is not very efficient because water is a poor solvent of organic materials [26]. Moreover, using water as the regenerating agent means that pollutants are transferred from the original stream to water which then needs to be treated as well [25]. Other solvent alternatives such as NaCl or NaNO<sub>3</sub> have been

experimented and found to increase the extraction efficiency of arsenic adsorbed on GAC from 10% to 100% [27]. Increased temperature works in favour of the regeneration efficiency in two ways: I) it enhances desorption, and II) it increases the solubility of organic compounds in water [28, 29] .

Solvent regeneration restores adsorbents that contain strongly attached adsorbates that proceed from polluted liquid streams through contact with organic solvents [25]. This method offers advantages in some aspects over thermal regeneration such as no mass loss, no damage to the porous structure of carbon, and easy recovery of adsorbates [30, 31]. However, it also has severe disadvantages by increasing the costs, as well as toxicity of the compounds which makes solvent regeneration not an environmentally friendly technique [32]. Basically, adsorbate molecules are displaced by solvent molecules, which results in solvent molecules being retained on the surface and the pores of carbon. The retention of the solvent molecules on the carbon results in lower adsorption capacity for the following cycle because it prevents the adsorption of the pollutant in the following cycle. Thus, the retained solvent needs to be removed to achieve the maximum capacity during subsequent cycles [25]. This is usually done by purging the solvent with hot N<sub>2</sub> [33], cold liquid water [30], hot water [32], or steam [34].

Another regeneration method is supercritical regeneration. When fluids surpass their critical point, they undergo significant changes. Their viscosity and dielectric constant reduce while their diffusivity increases [35]. These changes make them excellent solvents for organic compounds and consequently potential activated carbon regeneration agents [25]. Supercritical regeneration offers two advantages over solvent regeneration: I) the employed fluids, CO<sub>2</sub> and water, are more environmental friendly compared to organic solvents, and II) removal of the retained solvent is not required, because supercritical solvents do not remain on the surface of

carbon during extraction of the adsorbate, thus, eliminating the need for a final solvent removal step [25]. On the other hand, the severe conditions to achieve the supercritical state pose an important disadvantage to this method, especially for water with  $P_c = 221\text{bar}$  and  $T_c = 374^\circ\text{C}$ . Most researchers use  $\text{CO}_2$  as solvent since it has more reasonable critical conditions ( $P_c = 74\text{bar}$ ,  $T_c = 31^\circ\text{C}$ ) [25, 36, 37].

Oxidative regeneration offers a great advantage over other methods since it not only revitalizes the exhausted ACs, but also destroys the pollutants by oxidative treatment. Oxidative regeneration includes a degrading/reacting stage. Researches of oxidative regeneration can be distinguished by the fact that whether or not they employ  $\text{O}_2$  as the regeneration agent [38, 39]. If  $\text{O}_2$  is not present, other agents such as hydrogen peroxide ( $\text{H}_2\text{O}_2$ ) may be used [25].

### **2.3.3 Effect of Thermal Regeneration Parameters**

Thermal regeneration efficiency is affected by factors such as the regeneration temperature [5, 40, 41], regeneration time [40], purge gas composition [4, 42], purge gas flow rate, and heating rate [5].

Effect of regeneration temperature was studied by Jahandar Lashaki et al. [41]. They regenerated BAC saturated with a mixture of organic compounds at two temperatures ( $288^\circ\text{C}$  and  $400^\circ\text{C}$ ). Their results indicate that heel formation reduced by 61% at the higher temperature ( $400^\circ\text{C}$ ) possibly due to desorption of chemicals from narrow micropores. BET surface area and pore volume of the adsorbent decreased proportional to the cumulative heel. They measured the decrease in pore volume and found it to be higher than the calculated value which is due to pore blockage by compounds with large kinetic diameter. For example, naphthalene, which is one of the major contributors to heel has a kinetic diameter of  $6.1\text{\AA}$  which is larger than the narrow



micropores and could block these pores and make them inaccessible to other adsorbates. They suggested that another mechanism for heel formation could be oligomerization of adsorbates and resulting in materials that are more difficult to desorb.

Niknaddaf et al. [5] studied the regeneration of a 1,2,4-trimethylbenzene (TMB) on three activated carbon fiber cloths namely ACFC10, ACFC15, and ACFC20, with increasing pore width and volume. They regenerated the samples at two temperatures (288°C and 400°C). They observed that as opposed to the previous works, heel formation increases as the regeneration temperature increases. They proposed that this is due to the high heating rate ( $\sim 70^{\circ}\text{C}/\text{min}$ ) and that TMB goes under thermal degradation during rapid adsorption heating. Regeneration at 288°C resulted in 83% adsorption capacity loss for ACFC10, while ACFC15 and ACFC20 only lost 5% and 9% of their adsorption capacity respectively. They proposed that the narrow pores of ACFC10 are blocked by species produced from thermal degradation of TMB during regeneration. For ACFC15 and ACFC20 however, due to having larger pores they continue to adsorb additional species over subsequent cycles despite having similar amounts of heel. However, according to Niknaddaf et al.'s results, regeneration at 400°C resulted in adsorption capacity loss of 93%, 51%, and 50%, for ACFC10, ACFC15, and ACFC20 respectively.

Chang et al. [40] investigated the regeneration of silica gel at different temperatures and varying regeneration times. The objective of their study was to test the commercial silica gel and silica gel with improved transport properties for their performance in adsorption dehumidification process. They varied the regeneration time from 10 mins to 3 hrs and observed that as the regeneration time increases the breakthrough curve shifts to the right meaning that less heel is formed and regeneration efficiency is improved. The breakthrough curves for 2hr and 3hr regeneration times are almost coincident showing that after about 2 hours all the species are

desorbed from silica gel and complete regeneration is achieved. The commercial and modified silica gel with similar surface area but different mass transfer resistances were tested to see the effect of mass transfer resistance. They concluded that the modified silica gel requires higher regeneration temperature and longer regeneration time to reach a specific uptake in the adsorption and dehumidification process.

The type of purge gas used may affect the regeneration efficiency and the cost of operation. Many researchers and industries have used high purity nitrogen as the regeneration purge gas [5, 43, 44].

Carratala et al. [42] studied adsorption and regeneration of benzene and toluene on various activated carbons (5 different adsorbents with different porous texture, surface chemistry, and reactivity). Regeneration was performed in an inert atmosphere (He) and an oxygen containing atmosphere (20% O<sub>2</sub> in He) to compare regeneration efficiencies. Their results showed that benzene and toluene adsorption capacities do not change significantly after successive helium regeneration cycles for all adsorbents, while regeneration in presence of oxygen reduces the adsorption capacity of successive cycles in case of particular adsorbents, due to the presence of carbon gasification catalysts (potassium salts) from their preparation procedure. They justified that this is due to porosity modification and increase in surface oxygen groups of adsorbent when regenerated in an oxygen containing atmosphere. They also reported that optimum temperature for regeneration of benzene is 250-300°C while for toluene 300-350°C is the optimum temperature. Their results indicate that for regeneration of ACs saturated with toluene the porous texture of some of the tested ACs show a significant change, especially the chemically activated ACs that have gone under agglomeration process during preparation procedure. They concluded that the

modification in porosity and surface chemistry of the adsorbents is sufficient to explain the changes in adsorption capacities of the ACs with successive cycles.

Vidic and Suidan [45] studied adsorption of different organic compounds (o-cresol, phenol, o-chlorophenol, 3-ethylphenol, trichloroethylene, and natural organic matter) on granular activated carbon (GAC) in aqueous phase focusing on the effect of presence of molecular oxygen. Their experimental data indicate that the adsorption capacity of GAC significantly increases for five of the six compounds studied. They reported that this increase under oxic conditions is due to polymerization of adsorbate on the surface of carbon. However, according to their results the adsorption capacity of GAC for aliphatic compounds (trichloroethylene) is not significantly influenced by the presence of molecular oxygen. They analyzed extracts from the carbons with GC-MS and found out that noticeable amounts of dimers, trimers, and tetramers of o-cresol are detected in the extracts from the GAC used in oxic conditions while for anoxic conditions only traces of dimers were detected. The results of their research showed that presence of carbon surface is necessary for catalyzing the polymerization reaction since no polymerization was observed in the blank experiments.

Polymerization of aromatic compounds in presence of molecular oxygen has been reported in the literature by multiple researchers [6, 7, 10]. Boocock et al. [7] irradiated a mixture of atomic oxygen and benzene in a reactor at 25°C. Analysis of the products of the reaction indicated presence of phenol (13%), but the major product was found to be a polymeric compound. Researchers were unable to identify the structure of this compound. Brendt et al. [6] studied reaction of oxygen atoms with benzene in the gas phase. The experiments were conducted in the conditions of 50-100 mbar pressure and  $295 \pm 2$  K temperature. Concentration of O<sub>2</sub> in the carrier gas was in the range of  $(7.7-84) \times 10^{14}$  molecule/cm<sup>3</sup>. They reported that the primary products of

the reaction are phenol, benzene oxide/oxepin, and a not identified compound possibly with the formula  $C_5H_6O$ .

Thermal desorption behaviour of aliphatic and aromatic compounds on granular activated carbon (GAC) with nitrogen purge gas was studied by Liu et al. [44]. They reported that thermal desorption of simple low molecular weight alkanes is characterized by a single broad derivative weight loss. They characterized this peak as physical adsorption and stated that no residue was found on the carbon surface after desorption. Higher molecular weight alkanes show a broad three-stage desorption curve. For these compounds the first peak corresponds to simple desorption and after this peak compounds undergo thermal cracking and the products are desorbed subsequently. Aromatic compounds with an alkyl side chain such as butylbenzene show DTG curves of single-step physisorption. Aromatics with side chains greater than  $C_5$  desorb similar to higher molecular weight alkanes. They concluded that behaviour of aromatic compounds with alkyl side chains is predicted by the number of carbons in the side chain.

To summarize, thermal regeneration is the most common technique for gas phase adsorption/regeneration process. However, irreversible adsorption is a challenge for use of this technique. Irreversible adsorption or heel formation reduces the adsorption capacity of the adsorbent over successive cycles. Thus, it is important to study the parameters affecting this phenomenon to minimize heel formation. Regeneration temperature and purge gas flow rate have been extensively studied, however, there is still room for investigation of the effect of regeneration purge gas.

## References

1. Treybal, R.E., Mass-Transfer Operations. 3 ed. 1981. 784.
2. Aktaş, Ö. and F. Çeçen, Bioregeneration of activated carbon: A review. *International Biodeterioration & Biodegradation*, 2007. 59(4): p. 257-272.
3. Yonge, D.R., et al., Single-solute irreversible adsorption on granular activated carbon. *Environmental Science and Technology*, 1985. 19(8): p. 690-694.
4. Jahandar Lashaki, M., et al., Effect of desorption purge gas oxygen impurity on irreversible adsorption of organic vapors. *Carbon*, 2016. 99: p. 310-317.
5. Niknaddaf, S., et al., Heel formation during volatile organic compound desorption from activated carbon fiber cloth. *Carbon*, 2016. 96: p. 131-138.
6. Berndt, T. and O. Böge, Reaction of O(3P) Atoms with Benzene, in *Zeitschrift für Physikalische Chemie/International journal of research in physical chemistry and chemical physics*. 2004. p. 391.
7. Boocock, G. and R.J. Cvetanović, Reaction of oxygen atoms with benzene. *Canadian Journal of Chemistry*, 1961. 39(12): p. 2436-2443.
8. De Jonge, R.J., A.M. Breure, and J.G. Van An del, Reversibility of adsorption of aromatic compounds onto powdered activated carbon (PAC). *Water Research*, 1996. 30(4): p. 883-892.
9. Grant, T.M. and C.J. King, Mechanism of irreversible adsorption of phenolic compounds by activated carbons. *Industrial and Engineering Chemistry Research*, 1990. 29(2): p. 264-271.
10. Vidic, R.D., M.T. Suidan, and R.C. Brenner, Oxidative coupling of phenols on activated carbon: impact on adsorption equilibrium. *Environmental Science & Technology*, 1993. 27(10): p. 2079-2085.
11. Snoeyink, V.L., W.J. Weber Jr, and H.B. Mark Jr, Sorption of phenol and nitrophenol by active carbon. *Environmental science and technology*, 1969. 3(10): p. 918-926.
12. Miyake, Y., et al., Activated carbon adsorption of trichloroethylene (TCE) vapor stripped from TCE-contaminated water. *Water Research*, 2003. 37(8): p. 1852-1858.
13. Yin, C.Y., M.K. Aroua, and W.M.A.W. Daud, Review of modifications of activated carbon for enhancing contaminant uptakes from aqueous solutions. *Separation and Purification Technology*, 2007. 52(3): p. 403-415.
14. Pevida, C., et al., Surface modification of activated carbons for CO<sub>2</sub> capture. *Applied Surface Science*, 2008. 254(22): p. 7165-7172.
15. Huang, C.C., H.M. Chen, and C.H. Chen, Hydrogen adsorption on modified activated carbon. *International Journal of Hydrogen Energy*, 2010. 35(7): p. 2777-2780.

16. Walker, G.M. and L.R. Weatherley, Adsorption of acid dyes on to granular activated carbon in fixed beds. *Water Research*, 1997. 31(8): p. 2093-2101.
17. Boehler, M., et al., Removal of micropollutants in municipal wastewater treatment plants by powder-activated carbon. *Water Science and Technology*, 2012. 66(10): p. 2115-2121.
18. Li, L., S. Liu, and J. Liu, Surface modification of coconut shell based activated carbon for the improvement of hydrophobic VOC removal. *Journal of Hazardous Materials*, 2011. 192(2): p. 683-690.
19. Lillo-Ródenas, M.A., D. Cazorla-Amorós, and A. Linares-Solano, Behaviour of activated carbons with different pore size distributions and surface oxygen groups for benzene and toluene adsorption at low concentrations. *Carbon*, 2005. 43(8): p. 1758-1767.
20. Salvador, F., et al., Regeneration of carbonaceous adsorbents. Part I: Thermal Regeneration. *Microporous and Mesoporous Materials*, 2015. 202: p. 259-276.
21. Friday, D.K. and M.D. LeVan, Hot purge gas regeneration of adsorption beds with solute condensation: Experimental studies. *AIChE Journal*, 1985. 31(8): p. 1322-1328.
22. Ania, C.O., et al., Microwave-assisted regeneration of activated carbons loaded with pharmaceuticals. *Water Research*, 2007. 41(15): p. 3299-3306.
23. Fayaz, M., et al., Using microwave heating to improve the desorption efficiency of high molecular weight VOC from beaded activated carbon. *Environmental Science and Technology*, 2015. 49(7): p. 4536-4542.
24. Ondon, B.S., et al., Effect of microwave heating on the regeneration of modified activated carbons saturated with phenol. *Applied Water Science*, 2014. 4(4): p. 333-339.
25. Salvador, F., et al., Regeneration of carbonaceous adsorbents. Part II: Chemical, Microbiological and Vacuum Regeneration. *Microporous and Mesoporous Materials*, 2015. 202(C): p. 277-296.
26. Chatzopoulos, D., A. Varma, and R.L. Irvine, Activated carbon adsorption and desorption of toluene in the aqueous phase. *AIChE Journal*, 1993. 39(12): p. 2027-2041.
27. Di Natale, F., A. Erto, and A. Lancia, Desorption of arsenic from exhaust activated carbons used for water purification. *Journal of Hazardous Materials*, 2013. 260: p. 451-458.
28. Martin, R.J. and W.J. Ng, Chemical regeneration of exhausted activated carbon-I. *Water Research*, 1984. 18(1): p. 59-73.
29. Martin, R.J. and W.J. Ng, Chemical regeneration of exhausted activated carbon-II. *Water Research*, 1985. 19(12): p. 1527-1535.
30. Cooney, D.O., A. Nagerl, and A.L. Hines, Solvent regeneration of activated carbon. *Water Research*, 1983. 17(4): p. 403-410.
31. Guo, D., et al., Different solvents for the regeneration of the exhausted activated carbon used in the treatment of coking wastewater. *Journal of Hazardous Materials*, 2011. 186(2-3): p. 1788-1793.

32. Martin, R.J. and W.J. Ng, The repeated exhaustion and chemical regeneration of activated carbon. *Water Research*, 1987. 21(8): p. 961-965.
33. Tamon, H., et al., Solvent Regeneration of Spent Activated Carbon in Wastewater Treatment. *JOURNAL OF CHEMICAL ENGINEERING OF JAPAN*, 1990. 23(4): p. 426-432.
34. Sutikno, T. and K.J. Himmelstein, Desorption of phenol from activated carbon by solvent regeneration. *Industrial & Engineering Chemistry Fundamentals*, 1983. 22(4): p. 420-425.
35. Salvador, F., et al., Study of the energetic heterogeneity of the adsorption of phenol onto activated carbons by TPD under supercritical conditions. *Applied Surface Science*, 2005. 252(3): p. 641-646.
36. Ryu, Y.-K., K.-L. Kim, and C.-H. Lee, Adsorption and Desorption of n-Hexane, Methyl Ethyl Ketone, and Toluene on an Activated Carbon Fiber from Supercritical Carbon Dioxide. *Industrial & Engineering Chemistry Research*, 2000. 39(7): p. 2510-2518.
37. Tan, C.-S. and P.-L. Lee, Supercritical CO<sub>2</sub> desorption of toluene from activated carbon in rotating packed bed. *The Journal of Supercritical Fluids*, 2008. 46(2): p. 99-104.
38. Harriott, P. and A.T.-Y. Cheng, Kinetics of spent activated carbon regeneration. *AIChE Journal*, 1988. 34(10): p. 1656-1662.
39. Sabio, E., et al., Thermal regeneration of activated carbon saturated with p-nitrophenol. *Carbon*, 2004. 42(11): p. 2285-2293.
40. Chang, K.S., H.C. Wang, and T.W. Chung, Effect of regeneration conditions on the adsorption dehumidification process in packed silica gel beds. *Applied Thermal Engineering*, 2004. 24(5-6): p. 735-742.
41. Lashaki, M.J., et al., Effect of adsorption and regeneration temperature on irreversible adsorption of organic vapors on beaded activated carbon. *Environmental Science and Technology*, 2012. 46(7): p. 4083-4090.
42. Carratalá-Abril, J., et al., Regeneration of activated carbons saturated with benzene or toluene using an oxygen-containing atmosphere. *Chemical Engineering Science*, 2010. 65(6): p. 2190-2198.
43. Hwang, K.S., et al., Adsorption and thermal regeneration of methylene chloride vapor on an activated carbon bed. *Chemical Engineering Science*, 1997. 52(7): p. 1111-1123.
44. Liu, P.K.T., S.M. Feltch, and N.J. Wagner, Thermal desorption behavior of aliphatic and aromatic hydrocarbons loaded on activated carbon. *Industrial and Engineering Chemistry Research*, 1987. 26(8): p. 1540-1545.
45. Vidic, R.D. and M.T. Suidan, Role of dissolved oxygen on the adsorptive capacity of activated carbon for synthetic and natural organic matter. *Environmental Science and Technology*, 1991. 25(9): p. 1612-1618.

**3. CHAPTER 3: Regeneration of Beaded Activated Carbon  
(BAC) Saturated with 1,2,4-trimethylbenzene (TMB) with  
Oxygen-containing Purge Gas**



### 3.1 Introduction

Adsorption on activated carbon is an established method for capturing volatile organic compounds (VOCs) from industrial gas streams [1-5]. Adsorption is typically followed with regeneration to allow reuse of the adsorbent [1, 2, 5]. Thermal desorption at temperatures of  $< 300^{\circ}\text{C}$  is industrially used for regeneration of adsorbents loaded with gas phase compounds [2, 4].

Ideal regeneration will remove all of the adsorbed species from the adsorbent, however, in reality some of the adsorbates remain inside the adsorbent pores after regeneration, in the form of heel. Irreversible adsorption or heel build up is a challenge during regeneration of activated carbon, since it reduces the lifetime as well as the adsorption capacity of activated carbon during successive cycles [3, 6-8]. Previous studies have extensively investigated irreversible adsorption mechanisms in the aqueous phase [3, 6, 8-10], but few researchers have studied the gas phase [2, 11]. Some heel formation mechanisms include strong physical adsorption [12], chemical adsorption [13], oligomerization [3] and adsorbate decomposition [14].

During regeneration, an inert gas is purged over the adsorbent bed to help remove the desorbed species. The type of purge gas used for regeneration can affect not only heel formation, but also the cost of operation. Many researchers as well as industries have used high purity  $\text{N}_2$  as the regeneration purge gas [4, 15, 16]. Impurities in the purge gas may affect the regeneration efficiency. These impurities are mainly oxygen; however, traces of  $\text{CO}_2$  and  $\text{H}_2\text{O}$  exist despite being negligible [2]. Presence of oxygen even at very low concentrations may increase heel formation as it triggers chemical reactions with the adsorbate and/or adsorbent at elevated temperatures [2,17].

Previous researchers have investigated the effect of presence of oxygen in the purge gas to some extent. Carratala et al. [11] studied adsorption and desorption of benzene and phenol on five different activated carbons. Regeneration was performed at 250-350°C in an inert atmosphere (He) and an oxygen containing atmosphere (20% O<sub>2</sub> in He) to compare regeneration efficiencies. They observed that benzene and toluene adsorption capacities remain unchanged after successive helium regeneration cycles for all activated carbons, while regeneration in presence of oxygen reduces the adsorption capacity for both benzene and toluene over successive cycles in case of particular activated carbons due to the presence of carbon gasification catalysts (potassium salts) from their preparation procedure. They attributed this reduction to porosity modification and increase in surface oxygen groups.

Jahandar Lashaki et al. [2] adsorbed a mixture of volatile organic compounds on activated carbon and regenerated the carbon at 288°C using nitrogen purge gas with different levels of oxygen impurity (from  $\leq 5$  ppm to 10,000 ppm). They observed that heel formation after five successive cycles is exaggerated at higher O<sub>2</sub> concentrations (from 19.5% to 25.6% at  $\leq 5$  ppm and 10,000 ppm respectively). They attributed heel formation to a combination of physisorption and chemisorption, the latter being the dominant mechanism at higher O<sub>2</sub> concentrations. They also investigated the effect of long-term exposure (50-cycles) of samples to purge gas oxygen and observed that at high O<sub>2</sub> concentration (5000 ppm) chemisorption is the main heel formation mechanism, in agreement with the short-term exposure results, while no evidence of chemisorption was observed at low O<sub>2</sub> concentration (50 ppm).

Vidic and Suidan [8] investigated the effect of molecular oxygen during adsorption of different organic compounds on granular activated carbon (GAC) in aqueous phase. Their experimental data indicate that the adsorption capacity of GAC significantly increases for five of

the six compounds studied. They reported that this increase under oxic conditions is due to polymerization of adsorbate on the surface of carbon. However, according to their results the adsorptive capacity of GAC for aliphatic compounds is not significantly influenced by presence of molecular oxygen. They observed noticeable amounts of dimers, trimers, and tetramers of o-cresol in the extracts from the GAC used in oxic conditions, while for anoxic conditions only traces of dimers were detected. The results of their research showed that presence of carbon surface is necessary for catalyzing the polymerization reaction since no polymerization was observed in the blank experiments.

The objective of this work is to investigate the effect of oxygen in the regeneration purge gas during thermal regeneration of BAC saturated with TMB. It will be shown in this study that oxygen impurity in the regeneration purge gas adversely affects the regeneration efficiency of BAC, due to entrapment of species in the carbon pores. This effect is most likely due to formation of polymeric by-products from chemical reaction between oxygen and TMB. The presence of oxygen alone (with no adsorbate), cannot justify the observed trends.

## **3.2 Materials and Methods**

### **3.2.1 Adsorbent and adsorbate**

Beaded activated carbon (BAC; G-70R; Kureha Corporation) was used as the adsorbent for all experiments. The BAC has high microporosity (88%), narrow particle size distribution (average particle diameter 0.7 mm, 99% mass between 0.6 and 0.84 mm), and very low ash content (< 0.05%) [18]. BAC was preheated at 200°C for 2 hrs before use to remove adsorbed impurities. 1,2,4-trimethylbenzene (TMB, 98%, Acros Organics) was used as adsorbate for all experiments.

TMB has a boiling point of 171°C and a kinetic diameter of 0.61 nm [19], thus filling up the narrow micropores during adsorption.

### **3.2.2 Experimental setup and methods**

The experimental setup is described in detail elsewhere [2], and is briefly reviewed (Figure 3-1). The setup consists of an adsorption/regeneration tube, an adsorbate generation system, a heat application module, a gas concentration measurement system, and a data acquisition and control (DAC) system. The adsorption/regeneration setup is a stainless-steel tube filled with 4.0-4.1 g of BAC. Glass wool was used at the top and bottom of the tube to provide support for the BAC. The temperature was maintained at  $23 \pm 2^\circ\text{C}$  during adsorption. A k-type thermocouple was used to control the temperature of the adsorbent bed during adsorption and regeneration. The adsorbate was injected into a dry air stream of 10 SLPM using a syringe pump, generating a VOC concentration of 500 ppm. The outlet concentration during adsorption was intermittently measured using a flame ionization detector (FID; Baseline-Mocon Inc. series 9000) to obtain breakthrough curves. Adsorption experiments were carried out for 2 hours allowing enough time for exhaustion of the adsorbent.

Regeneration of the adsorbent was performed at  $288^\circ\text{C}$ . Heat was provided using a heating tape wrapped around the reactor and an insulation tape minimizing the heat loss. The regeneration temperature was controlled using a DAC system with a LabVIEW program (National Instruments) and a data logger (National Instruments, Compact DAQ) equipped with analog input and output modules. During regeneration, the adsorption/regeneration tube was heated for 3 hours after which heating was stopped and the tube was allowed to cool down to room temperature. The adsorbent bed was purged with 1 SLPM (Standard Liters Per Minute) total flow of gas, containing nitrogen with different levels of oxygen impurity ( $\leq 5, 208, 625, 1250, 2500, 5000, 10000, \text{ and } 20000 \text{ ppm}$ ).

To generate these gas streams, ultra-high purity nitrogen and air were mixed using a 1 SLPM mass flow controller (Alicat Scientific) for N<sub>2</sub> (accuracy of  $\pm 3$  SCCM) and a 100 SCCM (Standard Cubic Centimeters per Minute) mass flow controller (Alicat Scientific) for air ( $\pm 0.3$  SCCM). The grade 4.8 (99.9984% purity) N<sub>2</sub> gas cylinder contained a maximum of 5 ppm O<sub>2</sub> and was used as the purge gas for the  $\leq 5$  ppm O<sub>2</sub> experiment.

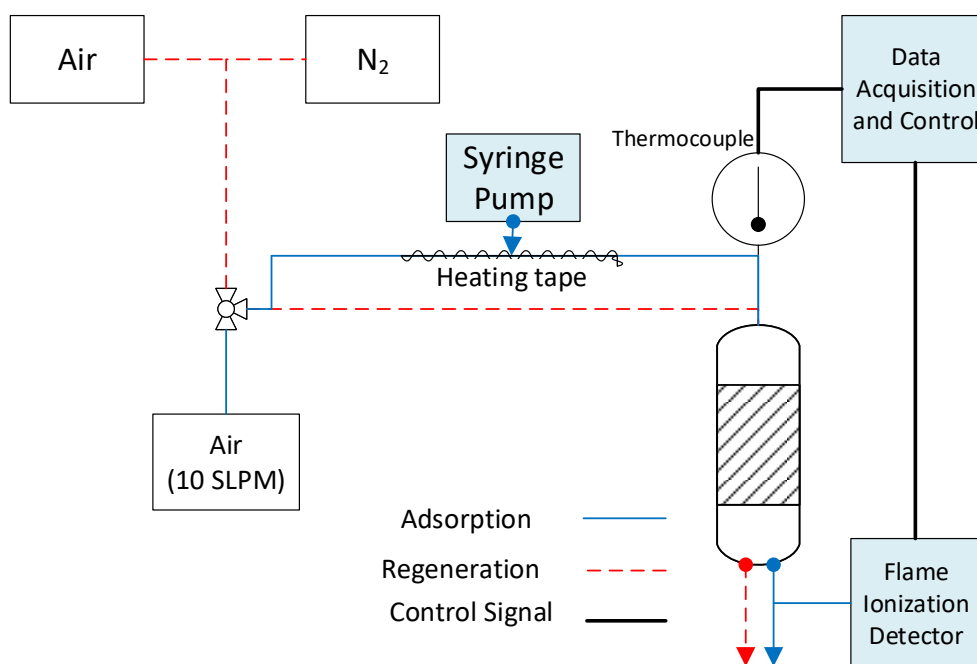


Figure 3-1. Schematic of the adsorption/regeneration setup

Heel formation and adsorption capacity were quantified using gravimetric analysis. The difference between initial weight of the reactor and weight of the reactor after the first adsorption cycle represents amount of VOC adsorbed during the first adsorption cycle. Adsorption capacities are normalized by dividing the amount of VOC adsorbed by the weight of the BAC and reported as percentages. Adsorption capacity calculations for the next cycles were carried out in the same

fashion. The difference between the weight of the reactor after the (n-1)<sup>th</sup> regeneration cycle and after the n<sup>th</sup> regeneration cycle represents the amount of heel during the n<sup>th</sup> cycle. Heel is also reported as percentage relative to the initial BAC weight.

Adsorption capacity (%)

$$= \frac{\text{Tube weight after adsorption} - \text{Tube weight before adsorption}}{\text{Weight of virgin BAC}} \times 100$$

Mass balance cumulative heel (%)

$$= \frac{\text{Tube weight after last regeneration cycle} - \text{Tube weight before 1}^{\text{st}} \text{ adsorption cycle}}{\text{Weight of virgin BAC}} \times 100$$

### 3.2.3 BAC characterization

#### 3.2.3.1 Micropore surface analysis

Virgin BAC samples and BAC samples after 5-cycle experiments were analyzed to determine Brunauer-Emmett-Teller (BET) surface area and pore size distribution using a micropore surface analyzer (iQ2MP, Quantachrome). Adsorption of N<sub>2</sub> was performed at -196°C with relative pressure (p/p<sub>0</sub>) ranging from 10<sup>-7</sup> to 1. 30-50 mg of sample was placed in a 6 mm cell and degassed for 5h at 150°C to remove any moisture. BET surface area and micropore volume were determined from relative pressures ranging from 0.01 to 0.07 and 0.2 to 0.5, respectively. V-t model was used to obtain micropore volume, and pore size distribution (PSD) was obtained using the quenched solid density functional theory (QSDFT) model for slit-shaped pores.

### **3.2.3.2 Thermogravimetric analysis**

Thermal stability of the virgin and regenerated samples were assessed using derivative thermogravimetric (DTG) analysis (TGA/DSC 1, Mettler Toledo). Samples were heated to 900°C at a heating rate of 2°C/min while being purged with 50 SCCM of nitrogen.

### **3.2.3.3 X-ray photoelectron spectroscopy (XPS) analysis**

Surface elemental composition (C, O, and N) was determined with XPS using an AXIS 165 spectrometer (Kratos Analytical). High resolution scans of binding energy with signal to noise ratio of greater than 10 were obtained ranging from 1100 eV to 0 with analyzer pass energy of 20 eV and a step of 0.1 eV. The XPS scans were processed with CasaXPS software and the results are reported in atomic concentrations.

## **3.3 Results and Discussion**

Adsorption breakthrough curves of 5-cycle experiments are shown in Figure 3-2. First cycle breakthrough times ( $t_{5\%}$ , when the outlet concentration equals 5% of the inlet concentration) are within the same range ( $59 \pm 2$  mins) for all experiments, since BAC has not been exposed to O<sub>2</sub> yet. Regeneration at  $\leq 5$  ppm O<sub>2</sub> does not change the breakthrough time over 5 cycles considerably ( $< 2\%$ ), indicating that the adsorbent maintains its adsorption capacity through successive cycling which is consistent with the mass balance results. This is consistent with previous studies completed under similar conditions [4, 11, 20]. Figure 3-2 shows that as the oxygen concentration in the purge gas increases, the breakthrough curve shifts to the left, indicating shorter breakthrough time over successive cycles. In addition, the gap between the first cycle and fifth cycle breakthrough curves increases with the concentration of oxygen in the purge gas (Figure 3-2). For regeneration at 20,000 ppm O<sub>2</sub> impurity, 5<sup>th</sup> cycle breakthrough time decreased by 29% compared

to the 1<sup>st</sup> cycle. This early breakthrough is due to heel build up which reduces the adsorption capacity of the adsorbent over successive cycles and results in shorter breakthrough time. Two blank 5-cycle adsorption/regeneration experiments were performed with air (with no VOC) as adsorption gas and nitrogen containing  $\leq 5$  and 20,000 ppm O<sub>2</sub> as regeneration purge gas. No heel was observed for these experiments proving that presence of O<sub>2</sub> alone is not sufficient to explain the aforementioned trends (heel buildup). This means that presence of O<sub>2</sub> as well as TMB is necessary to observe heel buildup and that heel buildup most likely involves reactions between O<sub>2</sub> in the purge gas and TMB.



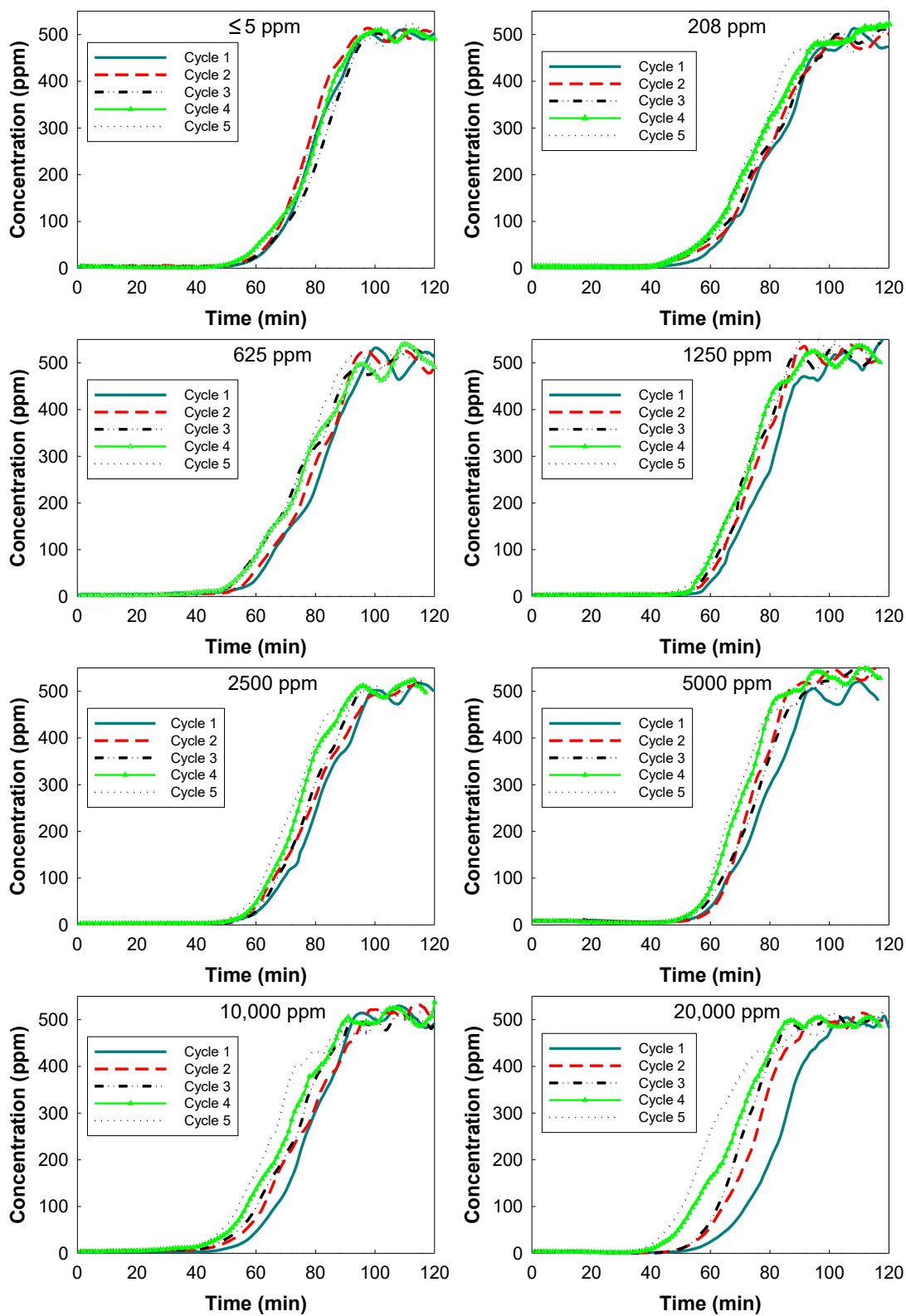


Figure 3-2. TMB Adsorption breakthrough curves at varying oxygen concentrations in the desorption purge gas

Mass balance heel results are presented in Figure 3-3a for all experiments (detailed tables are presented in Appendix A). Increased O<sub>2</sub> concentration in the purge gas results in excessive heel formation, increasing the heel from 0.5% to 15.8% for  $\leq 5$  and 20,000 ppm O<sub>2</sub> concentration, respectively. Comparison of the first cycle and cumulative (five-cycle) heel shows that heel is building up over successive cycles, i.e. each cycle contributes to the total heel. This shows that heel buildup is a progressive process and the use of BAC in successive cycles deteriorates the adsorbent after every cycle and exhausts it over time.

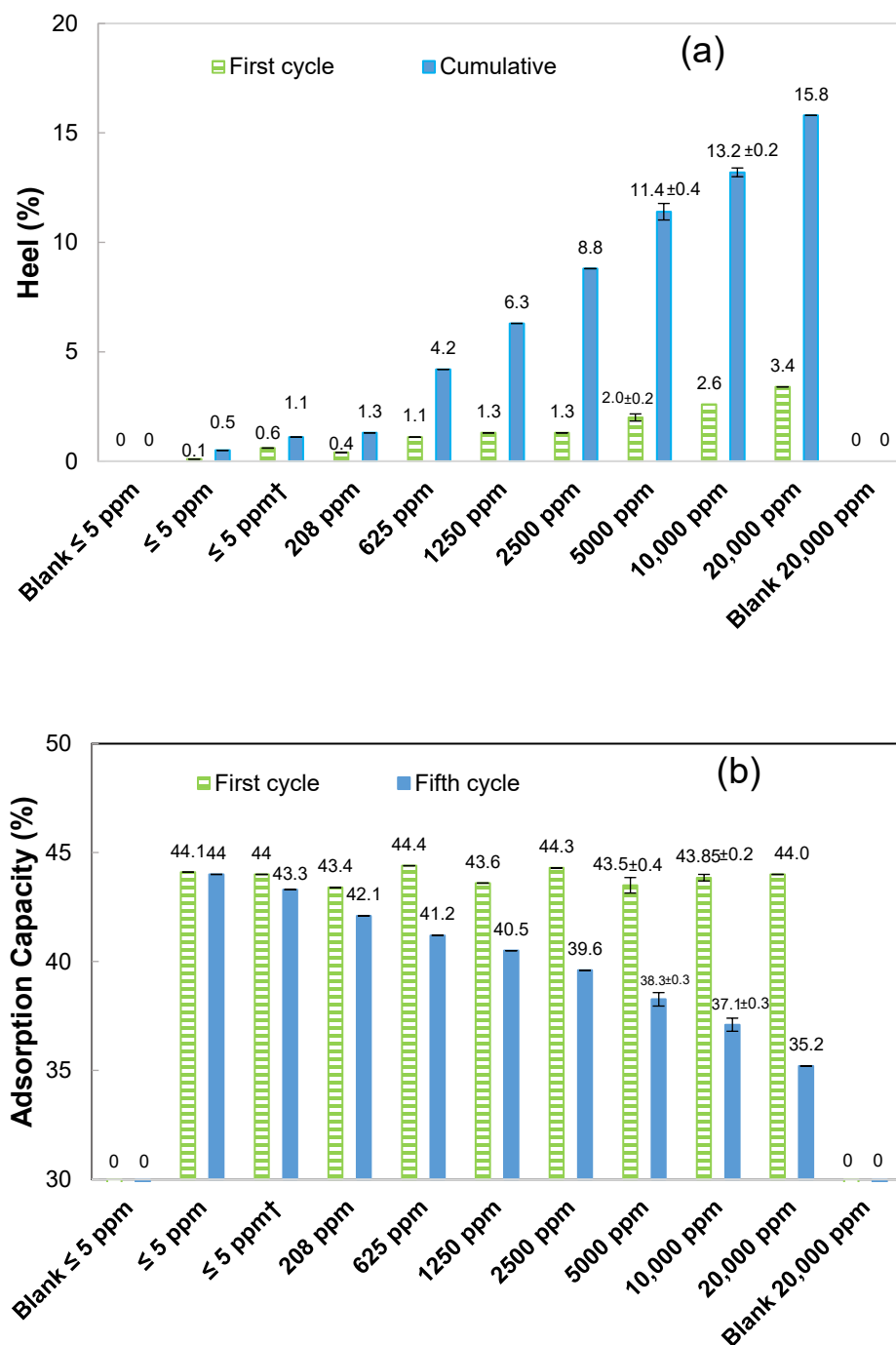


Figure 3-3. (a) Cumulative and first cycle mass balance heel results of 5-cycle adsorption/regeneration of TMB at different levels of O<sub>2</sub> impurity in the purge gas (b) Adsorption capacity of the adsorbent for the first and fifth cycle at different levels of O<sub>2</sub> impurity. † 5 cycles of blank adsorption with regeneration at 10,000 ppm O<sub>2</sub> in purge gas followed by 5 cycles of TMB adsorption with regeneration at ≤ 5 ppm O<sub>2</sub> concentration in the purge gas.

Adsorption capacities of 5-cycle experiments are presented in Figure 3-3b. First cycle adsorption capacities are similar for all experiments since BAC has not yet been exposed to oxygen during the first adsorption cycle. Increased O<sub>2</sub> concentration in the purge gas results in lower adsorption capacity during the next cycles. Jahandar Lashaki et al. [2] observed a similar trend for a mixture of VOCs. This is consistent with the heel values presented in Figure 3-3a. After each regeneration cycle, part of the adsorbate remains in the BAC pores which reduces their availability for future adsorption cycles and results in lower adsorption capacity. The reduction in adsorption capacity during the  $n^{\text{th}}$  cycle is expected to be greater than or equal to the amount of heel formed up to the  $(n-1)^{\text{th}}$  cycle, due to pore blockage. However, this is not what is observed in the results. For the 20,000 ppm experiment heel was found to be 13.0% up to the 4<sup>th</sup> cycle, while the adsorption capacity reduction was only 8.8% for the 5<sup>th</sup> adsorption cycle. Two possibilities may justify this observation: 1) there is greater pore volume available for adsorption, thus resulting in higher adsorption capacity; or 2) the pore volume is the same (or even lower) but greater mass is adsorbed on the carbon. In order to investigate the first hypothesis, surface analysis experiments were carried out to find the total pore volume, micropore volume, and surface area of the samples (Table 3-1). No increase in total pore volume is observed which rules out the first hypothesis. For the second hypothesis to be true the same volume must be occupied by more mass. This is possible if the density of the heel is greater than the density of the adsorbate, resulting in a greater mass occupying the same volume. Even though there is no direct method of measuring the density of the heel, studying the chemical reactions involved helps clarifying the picture. Presence of O<sub>2</sub> in the purge gas triggers chemical reactions between oxygen and the adsorbate/adsorbent. To figure out whether reaction of oxygen with the adsorbate or the adsorbent plays the major role in heel formation, a blank experiment was designed and completed. 5-cycle blank adsorption with air (no

TMB injection) was carried out on BAC with regeneration in 10,000 ppm O<sub>2</sub> in the purge gas at 288°C. This was followed by additional 5 cycles of TMB adsorption (on the same BAC) and regeneration at 288°C with  $\leq 5$  ppm O<sub>2</sub> in the purge gas. Comparison of the results of this experiment with the results of the 10,000 ppm O<sub>2</sub> experiment shows whether the reaction between oxygen and the adsorbate, or the reaction between oxygen and the adsorbent plays the major role in heel formation. Heel was found to be 1.1% compared to 13.4% for the 10,000 ppm O<sub>2</sub> test and 0.5% for the 5 ppm O<sub>2</sub> test. This shows that presence of oxygen in absence of TMB does not significantly increase the heel, confirming that the reaction between oxygen and TMB is the major contributor to heel formation. This reaction may produce by-products that are possibly denser than TMB itself, and thus result in a greater mass occupying the pores for future cycles.

Table 3-1. Characterization of regenerated samples

Carbon Description	Carbon Sample	Physical Properties			Chemical Properties		
		BET Surface Area (m <sup>2</sup> /g)	Micropore Volume (cm <sup>3</sup> /g)	Total Pore Volume (cm <sup>3</sup> /g)	C (%)	O (%)	N (%)
Virgin	Kureha	1371	0.50	0.57	93.0	7.0	0.0
Blank Tests	$\leq 5$ ppm	1345	0.48	0.56	91.6	7.9	0.3
	10,000 ppm	1323	0.48	0.57	91.9	7.6	0.3
BAC after 5 Ads/Reg. cycles	$\leq 5$ ppm	1305	0.47	0.56	95.4	4.6	0
	208 ppm	1263	0.46	0.51	94.4	5.6	0
	625 ppm	1176	0.44	0.48	94.6	5.4	0
	1250 ppm	1091	0.39	0.45	93.7	6.3	0
	2500 ppm	1064	0.39	0.45	94.2	5.8	0
	5000 ppm	1063	0.38	0.45	92.4	7.6	0
	10,000 ppm	978	0.34	0.44	92.9	7.1	0
	20,000 ppm	892	0.31	0.39	91.6	8.4	0

The reaction of aromatic compounds with oxygen was studied by Boocock et al. [21] and Berndt et al. [22] Both researchers reported that the major product of the reaction of benzene with

atomic oxygen is a polymeric compound. Boocock et al. [21] produced atomic oxygen by mercury photosensitized decomposition of nitrous oxide, and irradiated the mixture of atomic oxygen and benzene in a reactor at 25°C. Analysis of the reaction products showed presence of phenol (13%), but the major product was found to be a polymeric compound. Researchers were unable to identify the structure of this compound. Brendt et al. [22] investigated the gas-phase reaction of oxygen atoms with benzene at 50-100 mbar pressure and  $295 \pm 2$  K temperature. Concentration of O<sub>2</sub> in the carrier gas was in the range of  $(7.7-84) \times 10^{14}$  molecule/cm<sup>3</sup>. They reported that the primary products of the reaction are phenol, benzene oxide/oxepin, and a not identified compound possibly with the formula C<sub>5</sub>H<sub>6</sub>O. In our case, this polymeric compound is possibly the by-product of the reaction of TMB and O<sub>2</sub>. This compound is the major contributor to heel and cannot escape the pores due to its larger size.

DTG results of the virgin and 5-cycle BAC samples are shown in Figure 3-4. Heating of the samples results in gradual desorption of the remaining heel inside the pores. The stronger the interaction between the heel and the adsorbent, the higher the required temperature to break the molecules free. The first peak is observed at around 40°C which is due to desorption of any adsorbed moisture [2, 14]. Since samples were heated to 288°C during regeneration, no species are desorbed until after this temperature. The second and third peaks are observed at about 400°C and 550°C respectively. The species that are being desorbed at these temperatures are strongly attached to the surface and are not removed during regeneration. Both peaks are progressively amplified with higher O<sub>2</sub> concentrations; however, the 550°C peak displays a greater amplification. This suggests that in presence of more O<sub>2</sub> the chemical reaction between oxygen and TMB is enhanced resulting in more highly stable compounds that require more energy to desorb. The peaks at 400°C and 550°C are not observed for the  $\leq 5$  ppm sample which rules out the possibility of

physisorption being the heel formation mechanism. This means that the compounds being desorbed at these temperatures are either strongly attached to the surface with a chemical bound, or are the products of a chemical reaction between TMB and oxygen which then adsorbs on to the carbon. In either case, we categorize this interaction as chemisorption. In summary, at low  $O_2$  concentration ( $\leq 5$  ppm) no noticeable heel was formed while at higher  $O_2$  concentrations ( $\geq 208$  ppm) chemisorption was the main mechanism contributing to heel. A final peak is observed at about  $800^\circ\text{C}$  which is due to carbon loss.

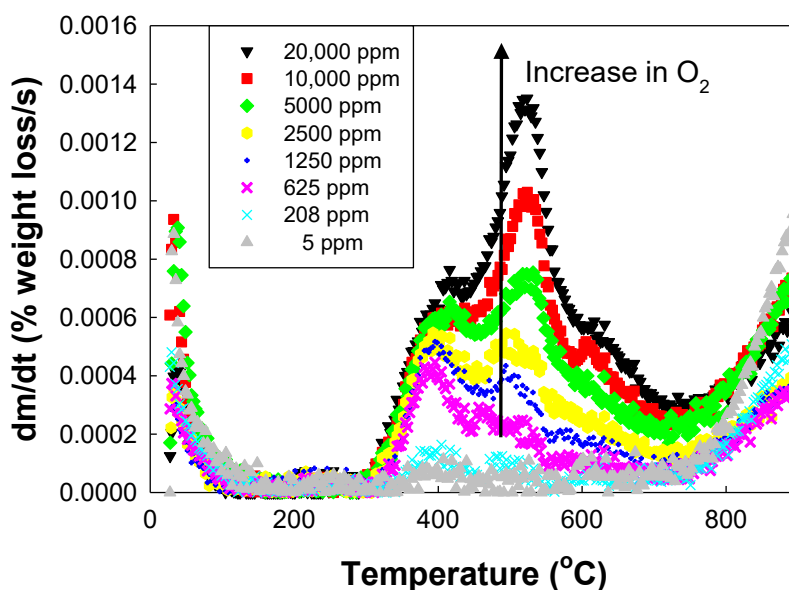


Figure 3-4. DTG analysis of samples regenerated at different oxygen concentrations in the purge gas

XPS analysis were performed on all samples to determine surface elemental compositions (Table 3-1). Surface oxygen concentration increased with increasing  $O_2$  concentration in the purge gas. This could be due to the reaction of oxygen with TMB which produces oxygen containing compounds or chemisorption of oxygen from the purge gas on the surface of BAC. Virgin BAC surface  $O_2$  concentration was higher than some of the regenerated samples. This is possibly due to

the adsorption of moisture from the atmosphere on virgin BAC which increases the surface O<sub>2</sub> concentration. Two blank adsorption (no adsorbate) experiments on virgin BAC showed no significant increase in surface oxygen, indicating that oxygen in purge gas alone does not alter the chemical properties of BAC.

Surface analysis were performed on all samples to measure BET surface area, micropore volume, and total pore volume. Lower BET surface area, micropore volume and total pore volume were observed for regenerated samples compared to virgin BAC. This is in agreement with mass balance heel results. Increased heel leaves some of the adsorption sites occupied after regeneration, resulting in less vacant sites available for N<sub>2</sub> adsorption. Similar reduction in micropore volume and total pore volume were observed which shows that formation of heel is mostly in micropores, which make up more than 88% of the virgin BACs pore volume [2]. This is also supported by the PSD results presented in Figure 3-5 which shows that reduction of pore volume is mostly in the < 20 Å range which is the micropore range. The amount of heel can be well correlated with the reduction in surface area and micropore volume, while the total pore volume is not a good indicator of the amount of heel formed (Figure 3-6). This is because heel is mostly formed in the micropores, thus, any increase in heel results in reduction of the micropore volume. The correlation is not as accurate for the total pore volume since at the concentrations used, adsorption and heel occur mainly in the mesopores. Similar trends are reported in previous research [20].



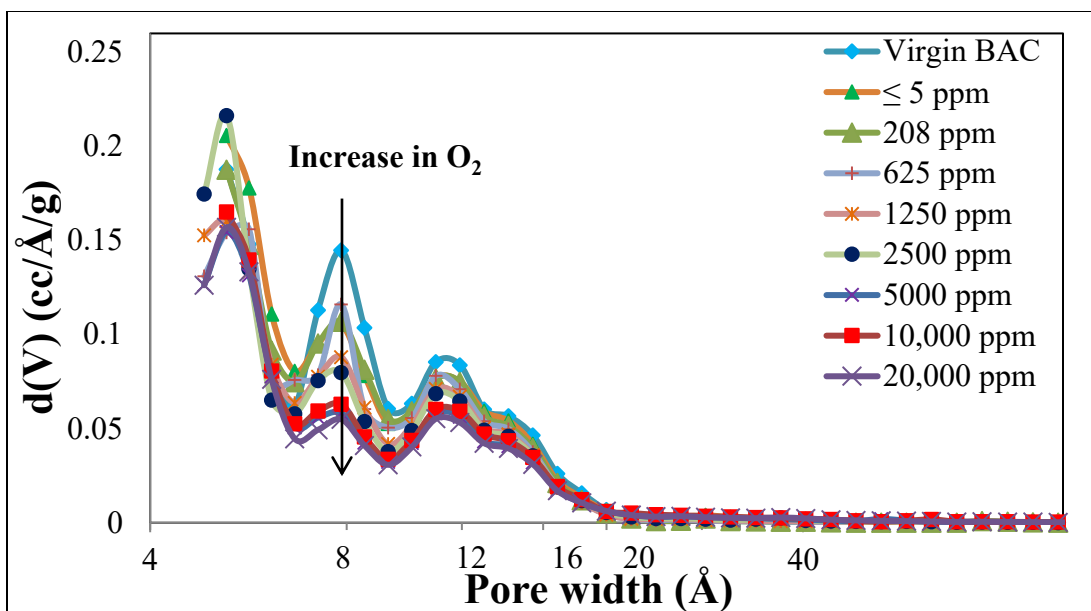


Figure 3-5. Pore size distribution of BAC samples regenerated after 5-cycle TMB adsorption/regeneration at different levels of oxygen impurity in the purge gas

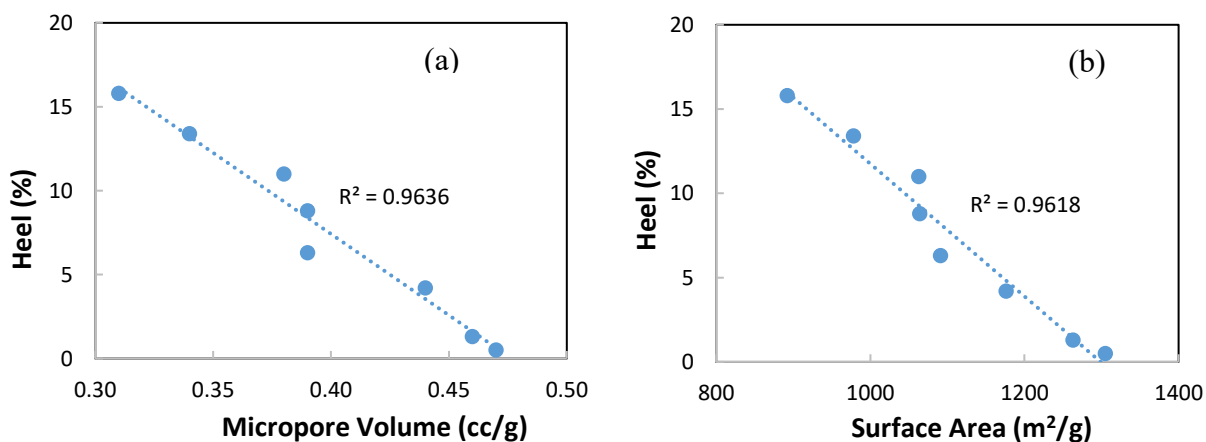


Figure 3-6. Cumulative heel vs. (a) Micropore volume, and (b) Surface area

The findings of this research help explain heel formation mechanisms and how they relate to purge gas impurity. Further research to investigate the effect of purge gas impurity on adsorption of other volatile organic compounds as well as other adsorbents could be helpful in understanding the phenomenon more thoroughly. The results presented here suggest that purge gas impurity increase heel formation during adsorption of TMB on BAC resulting in lower adsorption capacity and regeneration efficiency in successive cycles.

### 3.4 Conclusions

Adsorption/regeneration of 1,2,4-trimethylbenzene on beaded activated carbon in an oxygen containing atmosphere was studied. Increased oxygen concentration in the purge gas (208-20,000 ppm) resulted in greater heel accumulation, lower adsorption capacity, shorter breakthrough time, and loss of BET surface area of the adsorbent. Thermogravimetric analysis results indicate that chemisorption of TMB is the major heel formation mechanism. Presence of O<sub>2</sub> in the purge gas triggers chemical reactions between oxygen and TMB which leads to extensive heel formation, possibly due to formation of polymeric by-products that are trapped inside the pores. The results of this study show that presence of oxygen in the purge gas adversely affects the performance of the adsorption/regeneration system and shed light on heel formation mechanisms during adsorption/regeneration of volatile organic compounds.

## References

1. Ania, C.O., et al., *Microwave-induced regeneration of activated carbons polluted with phenol. A comparison with conventional thermal regeneration*. Carbon, 2004. **42**(7): p. 1383-1387.
2. Jahandar Lashaki, M., et al., *Effect of desorption purge gas oxygen impurity on irreversible adsorption of organic vapors*. Carbon, 2016. **99**: p. 310-317.
3. Lu, Q. and G.A. Sorial, *Adsorption of phenolics on activated carbon - Impact of pore size and molecular oxygen*. Chemosphere, 2004. **55**(5): p. 671-679.
4. Niknaddaf, S., et al., *Heel formation during volatile organic compound desorption from activated carbon fiber cloth*. Carbon, 2016. **96**: p. 131-138.
5. Salvador, F., et al., *Regeneration of carbonaceous adsorbents. Part I: Thermal Regeneration*. Microporous and Mesoporous Materials, 2015. **202**: p. 259-276.
6. Dąbrowski, A., et al., *Adsorption of phenolic compounds by activated carbon—a critical review*. Chemosphere, 2005. **58**(8): p. 1049-1070.
7. Dias, J.M., et al., *Waste materials for activated carbon preparation and its use in aqueous-phase treatment: A review*. Journal of Environmental Management, 2007. **85**(4): p. 833-846.
8. Vidic, R.D. and M.T. Suidan, *Role of dissolved oxygen on the adsorptive capacity of activated carbon for synthetic and natural organic matter*. Environmental Science and Technology, 1991. **25**(9): p. 1612-1618.
9. Vidic, R.D., M.T. Suidan, and R.C. Brenner, *Oxidative coupling of phenols on activated carbon: impact on adsorption equilibrium*. Environmental Science & Technology, 1993. **27**(10): p. 2079-2085.
10. Yonge, D.R., et al., *Single-solute irreversible adsorption on granular activated carbon*. Environmental Science and Technology, 1985. **19**(8): p. 690-694.
11. Carratalá-Abril, J., et al., *Regeneration of activated carbons saturated with benzene or toluene using an oxygen-containing atmosphere*. Chemical Engineering Science, 2010. **65**(6): p. 2190-2198.

12. Rzepka, M., P. Lamp, and M.A. de la Casa-Lillo, *Physisorption of Hydrogen on Microporous Carbon and Carbon Nanotubes*. The Journal of Physical Chemistry B, 1998. **102**(52): p. 10894-10898.
13. Welham, N.J., V. Berbenni, and P.G. Chapman, *Increased chemisorption onto activated carbon after ball-milling*. Carbon, 2002. **40**(13): p. 2307-2315.
14. Çalışkan, E., et al., *Low temperature regeneration of activated carbons using microwaves: Revising conventional wisdom*. Journal of Environmental Management, 2012. **102**: p. 134-140.
15. Hwang, K.S., et al., *Adsorption and thermal regeneration of methylene chloride vapor on an activated carbon bed*. Chemical Engineering Science, 1997. **52**(7): p. 1111-1123.
16. Liu, P.K.T., S.M. Feltch, and N.J. Wagner, *Thermal desorption behavior of aliphatic and aromatic hydrocarbons loaded on activated carbon*. Industrial and Engineering Chemistry Research, 1987. **26**(8): p. 1540-1545.
17. GEO-CENTERS, I., *The Reaction of Oxygen-Nitrogen Mixtures with Granular Activated Carbons Below The Spontaneous Ignition Temperature*. 1984.
18. Kureha Corporation Website. Available from: [www.kureha.com/pdfs/Kureha-BAC-Bead-Activated-Carbon.pdf](http://www.kureha.com/pdfs/Kureha-BAC-Bead-Activated-Carbon.pdf).
19. Barrie, J.K.P.j., *Recent advances in zeolite science*. 1989: Elsevier.
20. Lashaki, M.J., et al., *Effect of Adsorption and Regeneration Temperature on Irreversible Adsorption of Organic Vapors on Beaded Activated Carbon*. Environmental Science & Technology, 2012. **46**(7): p. 4083-4090.
21. Boocock, G. and R.J. Cvetanović, *Reaction of oxygen atoms with benzene*. Canadian Journal of Chemistry, 1961. **39**(12): p. 2436-2443.
22. Berndt, T. and O. Böge, *Reaction of O(3P) Atoms with Benzene*, in *Zeitschrift für Physikalische Chemie/International journal of research in physical chemistry and chemical physics*. 2004. p. 391.

**4. CHAPTER 4: Heel Buildup During Thermal Desorption  
of Volatile Organic Compounds off Beaded Activated  
Carbon in Presence of Oxygen Impurity**

## 4.1 Introduction

Paint solvents contain volatile organic compounds (VOCs) that can be emitted to the atmosphere during painting operations. Spraying operations are the main emission source of VOCs during automobile manufacturing process since the paint booth air carries away the solvents and overspray paint. The VOCs include a wide range of aromatic and aliphatic hydrocarbons, with different functionalities such as ketones, esters, and alcohols [1].

Adsorption on activated carbon has long been used for removal of VOCs from industrial gas streams [2-4]. Activated carbon is a very effective adsorbent owing to its high porosity and surface area [3, 5]. Thermal regeneration with hot purge gas is widely used to regenerate activated carbon and recover the adsorbate. In this method, the adsorbent bed is purged with a hot inert gas to carry away the desorbed compounds [6-8]. High purity nitrogen is typically used as the regeneration purge gas [9, 10].

Ideal regeneration recovers the original adsorption capacity of the adsorbent, as well as maintaining the porous structure of the adsorbent [11]. However, this is not always possible due to challenges such as heel formation. Heel formation, i.e. the accumulation of non-desorbed adsorbates on the adsorbent over successive adsorption/regeneration cycles, reduces the adsorption capacity and lifetime of the adsorbent [7, 12]. Heel formation can be attributed to different mechanisms including strong physical adsorption [12], chemisorption [12], adsorbate decomposition [5, 13], and oligomerization [14, 15].

Thermal regeneration has been investigated by researchers in an attempt to optimize the regeneration parameters including temperature (T) [7, 8, 16], regeneration time (t), purge gas flow rate [17], and purge gas type [12, 18, 19]. The choice of regeneration purge gas used is a

determining factor of the cost of the process. Purifying nitrogen (as a common regeneration purge gas) from 95% to 99.5%, 99.99%, and 99.999%, increases the power consumption from 37 to 56, 93, and 149 kW respectively, for production of 100 standard cubic feet per minute of nitrogen [20]. Therefore, using lower purity nitrogen reduces the electricity costs, while it may result in heel buildup [12]. Jahandar Lashaki et al. [12] investigated the effect of regeneration purge gas oxygen impurity on regeneration of beaded activated carbon (BAC) saturated with a mixture of VOCs. They concluded that as the oxygen impurity in the purge gas increases from  $\leq 5$  ppm to 10,000 ppm, the 5-cycle cumulative heel increases from 19.1% to 25.6%, respectively. Heel was found to be due to a combination of strong physisorption and chemisorption. Carratala et al. [18] regenerated different activated carbons saturated with benzene or toluene, in presence and absence of oxygen to understand how oxygen affects the regeneration efficiency. They found that regeneration of activated carbons saturated with benzene at temperatures of 250-350 °C, in presence of a purge gas with similar oxygen concentration as that of air, shows very good regeneration efficiency after several cycles. In contrast, they observed that regeneration of activated carbons saturated with toluene in presence of oxygen-containing purge gas require higher temperatures (300-350 °C) and most activated carbons showed a reduction in regeneration efficiency with cycling.

Liu et al. [10] studied the thermal desorption behaviour of aromatic and aliphatic compounds on activated carbon. They classified the thermal desorption behaviour of the tested hydrocarbons as type I, vaporization, type II, decomposition, and type III, decomposition followed by char formation. Compounds belonging to the first type have low molecular weight and are physisorbed to the AC. These compounds show no residue on the carbon after desorption. Low molecular weight alkanes (C<sub>4</sub>-C<sub>8</sub>) and aromatics with small side chains (C<sub>1</sub> and C<sub>4</sub> side chain)

belong to this group. Type II compounds undergo cracking reactions at high temperatures and the newly formed compounds are desorbed upon formation. High molecular weight alkanes ( $C_{10}$  and  $C_{18}$ ) and aromatics with large side chains ( $C_6$  and  $C_{12}$  side chain) are categorized in this class. Type III compounds differ from type II in that a carbonaceous residue is formed after the decomposition step. Compound structure plays the dominant role in distinguishing between type II and type III, e.g., 1,7-octadiene with conjugated double bonds was found to have type III behaviour. They proposed that aromatics with alkyl side chains desorb in the same fashion as simple alkanes. Their behaviour is determined by the number of carbons in the side chain. They also concluded that for a homologous series such as alkanes, alkenes, or aromatics, compounds can be classified as type I according to their boiling point. However, this criterion cannot distinguish between type II and type III.

Similarly, Suzuki et al. [21] tested 32 single component organic compounds and classified them into three groups similar to Liu et al. [10], however, based on a different basis. They proposed that the main factors predicting the desorption behaviour of the compounds are the boiling point and the aromatic carbon content (number of aromatic carbons/total number of carbons).

Table 4-1 summarizes the studies on adsorption and regeneration of organic compounds on different types of activated carbon. The studies were selected to represent different types of VOCs, low inlet VOC concentrations and moderate regeneration temperatures, most commonly found in industrial applications. The number of studies investigating the effect of presence of oxygen in the regeneration purge gas is limited. To the best of our knowledge only two studies have investigated this topic [12, 18].



Table 4-1. Summary of studies on adsorption and regeneration on activated carbon

Reference	Adsorbent	Adsorbate	Concentration (ppm)	Purge Gas	Desorption	
					T(°C)	t(min)
[19]	ACFC*	1,2,4-TMB	500	N <sub>2</sub>	288, 400	130
[18]	GAC <sup>ψ</sup>	Methylene chloride	1,000-4,000	N <sub>2</sub>	Up to 177	75
[20]	GAC	Multiple organic compounds	No information	N <sub>2</sub>	220-425	No information
[21]	BAC	Mixture of VOCs	500	10,000 ppm O <sub>2</sub> in N <sub>2</sub>	288	180
[22]	PAC <sup>†</sup>	Benzene	2,000-5,000	N <sub>2</sub>	260	140
[11]	GAC, PAC	Benzene, toluene	200	20% O <sub>2</sub> in He	250-350	48-70
[23]	GAC	Acetone, Toluene	~4600	N <sub>2</sub>	120-150	70-120

\*Activated Carbon Fibre Cloth, <sup>ψ</sup>Granular Activated Carbon, <sup>†</sup>Powdered Activated Carbon

The focus of the present work is to elucidate the effect of presence of oxygen in the regeneration purge gas on thermal desorption behavior of single component organic compounds. 11 compounds were tested in 5-cycle adsorption/regeneration experiments. Activated carbon samples were characterized to quantify heel formation and irreversible adsorption.

## 4.2 Materials and Methods

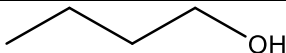
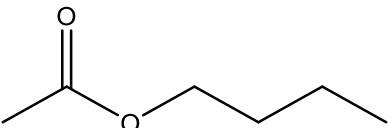
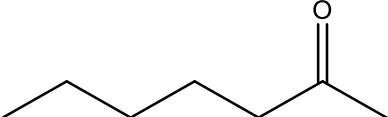
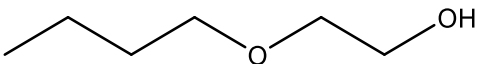

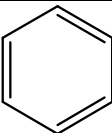
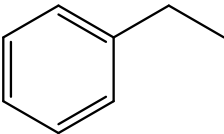
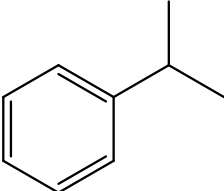
### 4.2.1 Adsorbent

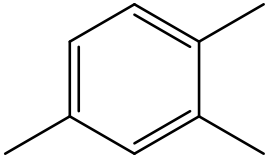
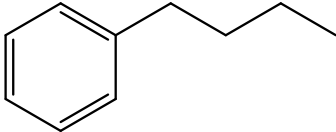
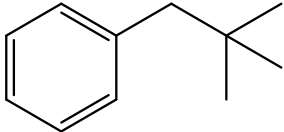
The adsorbent used in this study is beaded activated carbon from Kureha Corporation (BAC; G-70R). Kureha BAC is highly microporous (88%) and has a narrow particle size distribution (average particle diameter 0.7 mm, 99% mass between 0.6 and 0.84 mm). The ash content of the BAC is very low with less than 0.05% ash [23]. Prior to the first adsorption cycle BAC was preheated at 200°C for 2 hrs to remove adsorbed impurities during manufacture, transportation, and storage.

## 4.2.2 Adsorbates

11 organic compounds were tested in single component adsorption/regeneration experiments. Table 4-2 presents the chemical structure and physical properties of the tested compounds. The selected compounds represent a wide range of boiling point (80–185 °C) as well as different functionalities including aromatic and aliphatic compounds. The selected compounds are used as surrogates for VOCs produced from automotive painting booth air streams.

Table 4-2. Adsorbate structures and physical properties

Compound	Structure	Molecular weight	Boiling point (°C)	Vapor pressure (25°C) mm Hg
1-butanol		74.1	117	8.5
n-butyl acetate		116.2	126	11.5
2-heptanone		114.2	151	4.7
2-butoxyethanol		118.2	171	0.6
n-decane		142.3	174	1.6
benzene		78.1	80	100
ethylbenzene		106.2	136	9.2
isopropylbenzene		120.2	152	4.5

1,2,4-trimethylbenzene (TMB)		120.2	169	2.1
butylbenzene		134.2	183	1.1
neopentylbenzene		148.3	185	1.0

### 4.2.3 Experimental setup and methods

The experimental setup used for this study has been thoroughly explained elsewhere [12] and will be shortly reviewed here (Figure 4-1). Adsorption/regeneration experiments were carried out in a stainless-steel tube.  $4.05 \pm 0.05$  g of BAC was weighed and placed in the adsorption tube. The VOC laden stream with the target concentration (500 ppm) was generated using a syringe pump that injects the VOC at a specified rate into a 10 standard litre per minute (SLPM) air stream. The VOC laden stream concentration was monitored using a flame ionization detector (FID; Baseline-Mocon Inc. series 9000). After a steady concentration of 500 ppm was reached, the VOC laden stream was directed into the adsorption tube to start adsorption, and the tube outlet concentration was monitored with the FID. The temperature during adsorption was measured and maintained at  $23 \pm 2^\circ\text{C}$  using a k-type thermocouple inserted into the center of the BAC bed. Injection was stopped after a steady concentration was reached at the outlet of the tube (500 ppm). Adsorbate injection was continued for 2 hrs for all of the adsorbates except for 1-butanol and isopropylbenzene which required 2.5 hrs to reach steady outlet concentration.

During regeneration, heat was provided using a heating tape wrapped around the tube. Heat loss was minimized by wrapping a layer of insulation taper around the heating tape. The temperature

during regeneration was maintained at 288°C for 3 hrs (including the initial ramp), after which heating was stopped and the tube was allowed to cool down to room temperature. The tube was purged with 1 SLPM flow of gas at two different levels of oxygen impurity ( $\leq 5$  ppm and 10,000 ppm) for each adsorbate. Compressed nitrogen (99.9984% pure, Praxair) was used as the  $\leq 5$  ppm purge gas, and the 10,000 ppm oxygen concentration purge gas was produced by mixing the compressed nitrogen with compressed air (99.9999% pure, Praxair). Two mass flow controllers were used for mixing of nitrogen and air: a 100 standard cubic centimeter per minute (SCCM) mass flow controller with  $\pm 0.3$  SCCM accuracy (Alicat Scientific) for air, and a 1 SLPM mass flow controller with accuracy of  $\pm 3$  SCCM (Alicat Scientific) for N<sub>2</sub>.

Two blank experiments (air without VOC) were also performed to see the effect of oxygen in the purge gas on surface properties of the activated carbon. For these experiments, no VOC was injected into the air stream and the activated carbon bed was purged with air during adsorption. The regeneration conditions for the blank experiments were similar to other experiments. Samples were regenerated at 288°C with nitrogen purge gas containing  $\leq 5$  ppm and 10,000 ppm oxygen concentration.

Adsorption capacity and heel formation were quantified with gravimetric measurements. The adsorption/regeneration tube was weighed before the first adsorption cycle, after each adsorption cycle, and after each regeneration cycle. Heel formation and adsorption capacity were calculated according to the following equations:

Adsorption capacity (%)

$$= \frac{\text{Tube weight after adsorption} - \text{Tube weight before adsorption}}{\text{Weight of virgin BAC}} \times 100$$

Mass balance cumulative heel (%)

$$= \frac{\text{Tube weight after last regeneration cycle} - \text{Tube weight before 1}^{\text{st}} \text{ adsorption cycle}}{\text{Weight of virgin BAC}} \times 100$$

#### 4.2.4 BAC characterization

The virgin and regenerated BAC samples were tested with a micropore surface analyzer (iQ2MP, Quantachrome) to determine the Brunauer-Emmett-Teller (BET) surface area. Micropore volume was calculated using the v-t model, and the pore size distribution using the quenched solid density functional theory (QSDFT). 30-50 mg of sample was placed in a 6mm cell and outgassed for 5h at 150°C to remove and adsorbed moisture. After degassing, adsorption of N<sub>2</sub> was performed at -196°C with relative pressure (p/p<sub>0</sub>) ranging from 10<sup>-7</sup> to 1.

Samples were tested for their thermal stability with thermogravimetric analysis (TGA/DSC 1, Mettler Toledo) by heating up to 900°C at a heating rate of 2°C/min. The slow heating rate provides enough time for the desorbing compounds to diffuse through the pores, and thus, improves peak resolution. Samples were purged with 50 SCCM of nitrogen during heating to carry away the desorbed compounds.

X-ray photoelectron spectroscopy (XPS; AXIS 165 spectrometer, Kratos Analytical) was performed on all samples to determine surface elemental composition. The instrument has a resolution of 0.55 eV for Ag 3d and 0.70 eV for Au 4f peaks. XPS scans were processed using CasaXPS Software and the results are reported in atomic concentration.

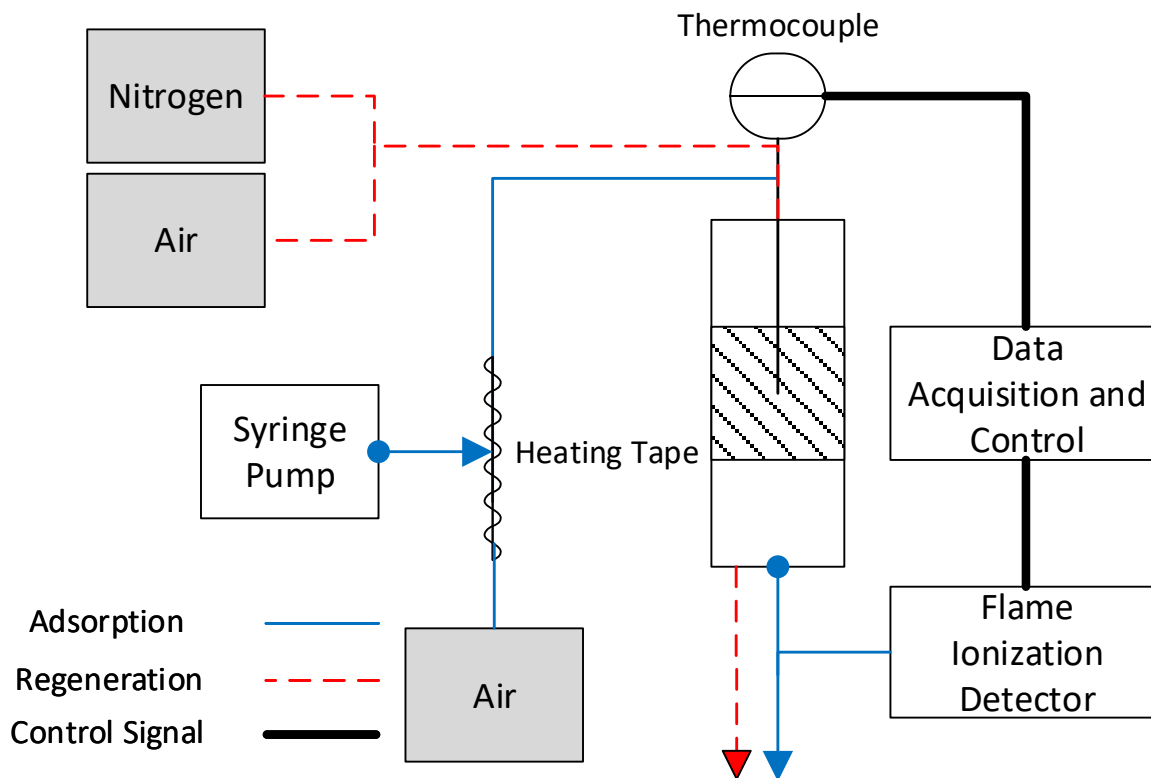


Figure 4-1. Schematic of the adsorption/regeneration setup

### 4.3 Results and Discussion

Accumulation of non-desorbed species after each regeneration cycle decreases the adsorption capacity in subsequent cycles due to availability of fewer adsorption sites. Therefore, the adsorbent is saturated with the adsorbate earlier and the breakthrough time is reduced from one cycle to the next. Figure 4-2 depicts the reduction in breakthrough time over a 5-cycle adsorption/regeneration process, i.e. the difference in breakthrough time between the first and fifth adsorption cycles. Breakthrough curves for all of the experiments are presented in Appendix B. Breakthrough time reductions are greater at higher oxygen impurity in the purge gas for all adsorbates except for n-butyl acetate and 2-butoxyethanol. This is consistent with the mass balance cumulative heel results

discussed later (Figure 4-3). The highest reduction in breakthrough time is for isopropylbenzene at 10,000 ppm oxygen concentration in the purge gas (21 mins) although it has lower cumulative heel percentage than TMB (Figure 4-3), which shows that different adsorbates reduce the breakthrough time to different degrees. To explain this, we should note that BAC is saturated and breakthrough is reached when all pores are occupied by the adsorbate and there are no more pores available for adsorption. Availability of pores for adsorption is quantified by the pore volume (Table 4-3). As discussed later, different adsorbates reduce the pore volume to different degrees due to pore blockage based on their size, and consequently, breakthrough time for different adsorbates is reduced to different degrees as well. It should also be pointed out that for a single adsorbate, reduction in breakthrough time is not proportional to cumulative heel at the two levels of oxygen impurity. For example, breakthrough time reduction for isopropylbenzene is 2 mins and 21 mins for  $\leq 5$  ppm and 10,000 ppm oxygen concentration in the purge gas respectively, while cumulative heel is 4.6% and 11.2 % for the two experiments respectively. This is due to the different nature of heel for the two experiments. At the higher oxygen concentration, the adsorbate engages in a chemical reaction with oxygen and produces products that result in pore blockage and consequently reduction of pore volume and breakthrough time. This reaction will be discussed in detail later.

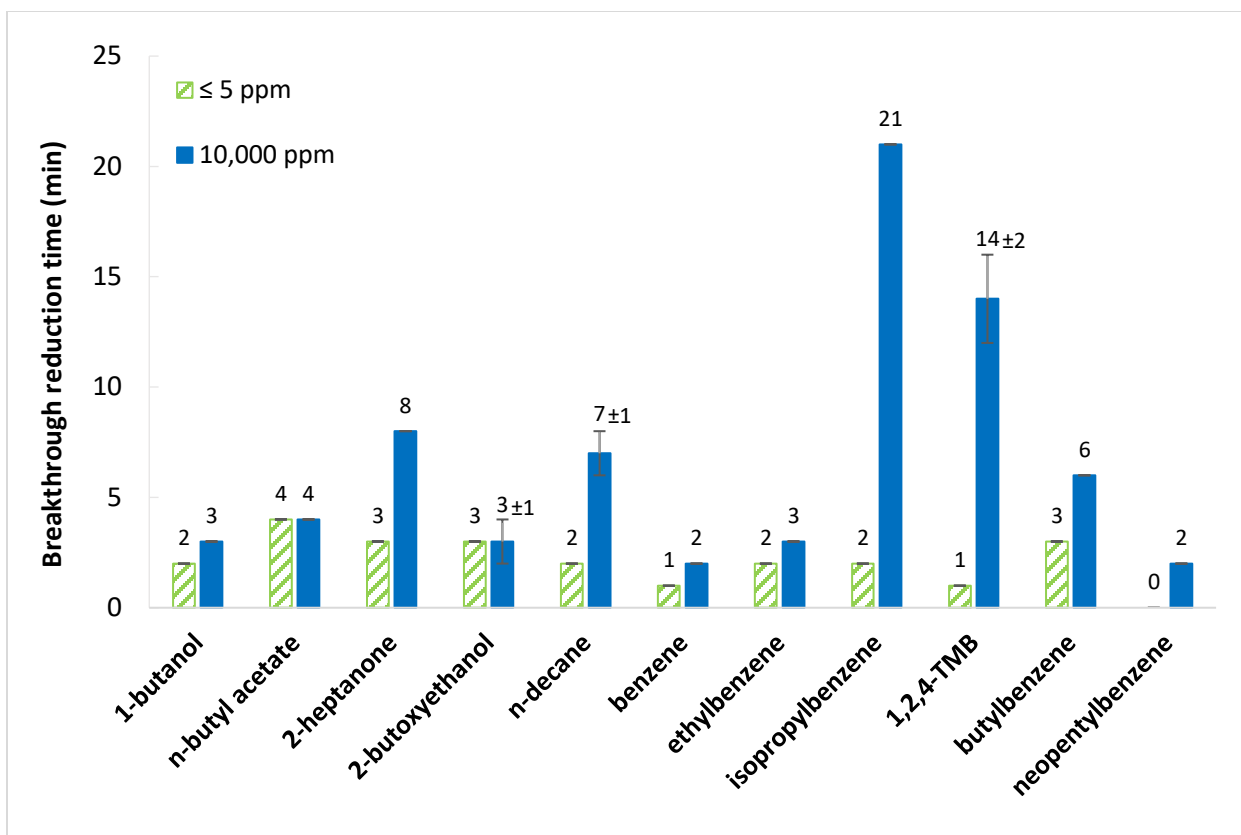


Figure 4-2. Breakthrough reduction times (first adsorption cycle compared to the fifth cycle) for different adsorbates at two levels of oxygen impurity in the purge gas. Select tests were duplicated and the uncertainties are shown with error bars (XX±YY where XX is the mean of the values for the repeated experiments and YY is the standard deviation).

Figure 4-3 shows the 5-cycle cumulative mass balance heel results for different adsorbates at two levels of oxygen concentration in the purge gas ( $\leq 5$  ppm and 10,000 ppm). Detailed mass balance tables are presented in Appendix C. For all adsorbates, cumulative heel at 10,000 ppm oxygen concentration is greater than or equal to the heel at  $\leq 5$  ppm. Aromatic adsorbates seem to be affected by the presence of oxygen in the purge gas to a greater degree as compared to aliphatic adsorbates. n-butyl acetate and 2-butoxyethanol depicted similar amounts of heel in both oxygen concentrations, independent of the presence of oxygen in the purge gas, while 2-heptanone and n-decane showed a noticeable increase (from 0.5% to 2.9%, and 0.7% to 3.4% at  $\leq 5$  ppm and 10,000



ppm, respectively). Liu et al. [10] suggested that high molecular weight alkanes undergo cracking at high temperatures. In case of n-decane, the cracking reaction in presence of oxygen may produce products that are not able to escape the pores of the carbon and result in excess heel formation compared to regeneration with pure nitrogen ( $\leq 5$  ppm  $O_2$  in  $N_2$ ). Similarly, the excess heel formation in presence of  $O_2$  for 2-heptanone suggests that the adsorbate engages in a chemical reaction with oxygen which results in higher heel formation. The chemical reactivity of the compounds with oxygen as well as the boiling point seem to be the deciding parameters predicting the amount of cumulative heel of aliphatic compounds. On the other hand, the effect of oxygen in the regeneration purge gas is notable for three out of the six aromatic compounds tested, namely, isopropylbenzene, 1,2,4 TMB, and butylbenzene. Benzene, ethylbenzene, and neopentylbenzene show low cumulative mass balance heel even at 10,000 ppm oxygen concentration. Liu et al. [10] predicted the thermal desorption behaviour of aromatic compounds according to the number of carbons in their side chain. Suzuki et al. [21] classified organic compounds only by their boiling point and aromatic carbon content to predict their desorption behaviour. However, neither of these criteria hold true for the results of the present work, because the presence of oxygen in the purge gas possibly triggers chemical reactions between oxygen and the adsorbates, thus, introducing a new variable that affects the desorption behavior. In such conditions, desorption behaviour and heel formation cannot be predicted solely by the boiling point and the aromatic carbon content.

The reaction of benzene with atomic oxygen was studied by previous researchers [24, 25]. They found that the main products of the reaction of oxygen with benzene are phenol and a polymeric compound. Phenol represents some 13% of the products, while the polymeric compound is the major product of the reaction. According to our results, however, regeneration efficiency of benzene is far better than other aromatics. This is possibly due to the low boiling

point of benzene (80°C) which allows it to vaporize and leave the pores before the chemical reaction initiates. On the other hand, aromatics with side chains offer a high enough boiling point (136-183°C) for the chemical reaction to initiate while the adsorbed molecules are still inside the pores, and thus, heel formation for these compounds is higher at 10,000 ppm oxygen concentration compared to  $\leq 5$  ppm. Heel formation for ethylbenzene increases from 0.1% to 1.5% at  $\leq 5$  ppm oxygen concentration and 10,000 ppm oxygen concentration, respectively. Even though heel increases by 1,500%, regeneration efficiency is still satisfactory at 10,000 ppm because the baseline heel at  $\leq 5$  ppm is too small. This suggests that boiling point of ethylbenzene (136°C) is still not high enough, so most of the adsorbed molecules escape before they can react with oxygen. However, for isopropylbenzene the heel at 10,000 ppm increased to 11.2% compared to 4.6% at  $\leq 5$  ppm purge gas oxygen concentration. Isopropylbenzene, having a high enough boiling point (152°C), reacts with oxygen at the regeneration temperature to possibly produce polymeric compounds similar to what is reported in the literature [24, 25], which are perhaps the major contributors to heel. TMB and butylbenzene depict a similar trend as isopropylbenzene, however, neopentylbenzene does not follow a similar behaviour.

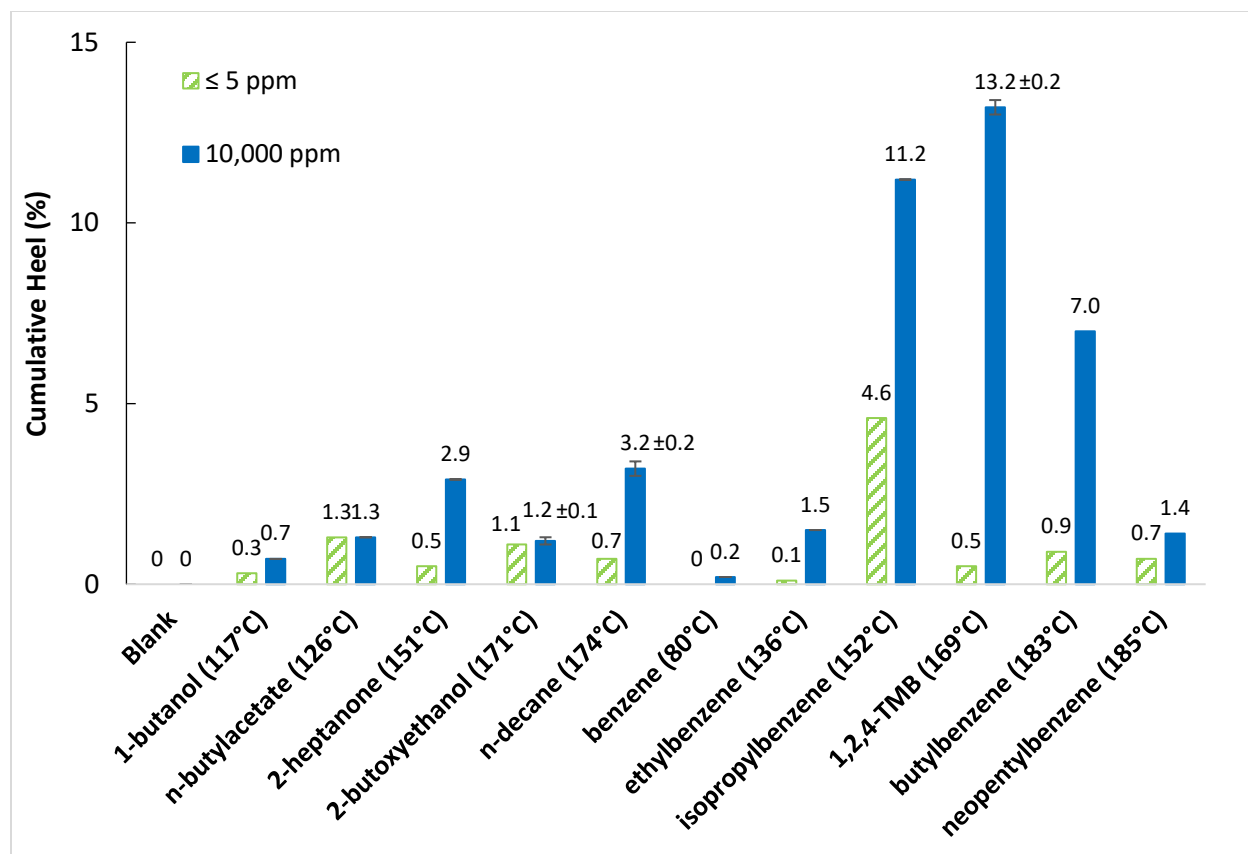
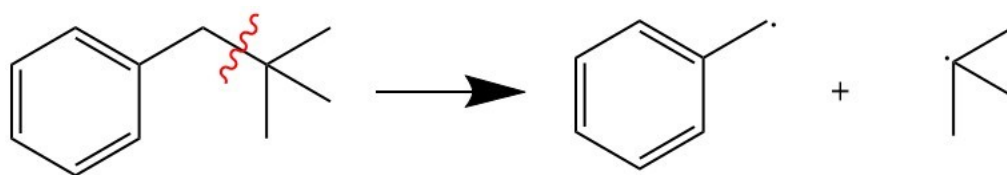
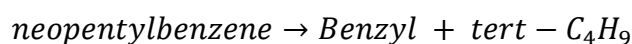


Figure 4-3. Mass balance cumulative (5-cycle) heel results. Select tests were duplicated and uncertainties are shown with error bars (XX±YY where XX is the mean of the values for the repeated experiments and YY is the standard deviation).

To better understand the desorption behaviour of neopentylbenzene, it is useful to study the structure of aromatics with alkyl side chains and the bond energy between the alkyl group and the aromatic ring, as well as the bond energy between the carbons in the alkyl group. The alkyl group may be attached to the aromatic ring at three different types of carbon: 1) primary carbon such as in ethylbenzene and butylbenzene, 2) secondary carbon such as in isopropylbenzene, and 3) tertiary carbon such as in *tert*-butylbenzene. The bond dissociation energy of a primary carbon is higher than a secondary carbon, and a secondary carbon is higher than a tertiary carbon ( $E_{\text{primary}} > E_{\text{secondary}} > E_{\text{tertiary}}$ ) [26]. Furthermore, electron donating groups attached to a carbon, reduce the

bond energy between that carbon and a neighbouring element because the produced radical is more stable [26], e.g., the bond between the tertiary carbon and a neighbouring carbon in neopentylbenzene is easier to break than the C-C bonds in *n*-pentylbenzene. Therefore, the bond between the tertiary carbon and the carbon attached to the benzene ring in neopentylbenzene, has lower dissociation energy than the C-C bonds in butylbenzene or isopropylbenzene. Accordingly, the lower heel formation of neopentylbenzene can be explained. The regeneration temperature provides enough heat to possibly break the C-C bond between the tertiary carbon and the carbon attached to the benzene ring. This reaction has been reported in the literature [27] and proceeds as shown below:



This makes the regeneration behaviour of neopentylbenzene somewhat between the two products of the reaction since neopentylbenzene itself does not engage in reactions with O<sub>2</sub> while the products may be involved in reaction with oxygen at elevated temperatures. Therefore, in this case, the behaviour of aromatics with alkyl side chains that are prone to be decomposed before engaging in reaction with oxygen, is expected to be similar to the behaviour of the alkyl side chain. This was first proposed by Liu et al. [10] to predict the desorption behaviour of aromatic compounds with side chains. But our results suggest that in presence of oxygen, this can only be used when the compound decomposes before initiating reaction with oxygen. Otherwise, the chemical reaction between oxygen and the compound results in a different behaviour.

All in all, heel formation for aromatic compounds is a function of the chemical reactivity of the compound as well as the boiling point. Adsorbates with low boiling points (such as benzene, 80°C) escape the pores before the initiation of the chemical reaction. However, when the boiling point of the compound is high enough (136-183°C for the compounds tested in this study), some of the adsorbate still remains in the pores of activated carbon at higher temperatures, resulting in a chemical reaction between the adsorbate and oxygen. In such cases, the products of this chemical reaction are the main contributors to heel and result in higher heel formation. As the boiling point increases however, the possibility of decomposition of the compound and breakage of the bond between the benzene ring and the side chain rises. For these compounds, heel formation is similar to the behaviour of the alkyl side chain.

Table 4-3 presents characterization results of virgin and regenerated activated carbons. Two blank experiments (air without VOC) were run to see the effect of oxygen in the purge gas on surface properties and surface chemistry of BAC. The results indicate that presence of oxygen alone does not noticeably change the surface properties or the surface chemistry of the BAC. Figure 4-4 shows the surface oxygen atomic percentage of the regenerated samples. All samples regenerated at 10,000 ppm O<sub>2</sub> in N<sub>2</sub> depicted higher surface oxygen content compared to the samples regenerated at  $\leq 5$  ppm O<sub>2</sub> in N<sub>2</sub>. This is possibly due to adsorption of oxygen in the purge gas on the carbon. For compounds with oxygen in their chemical structure (such as heptanone, butanol, etc.), or compounds that react with the oxygen in the purge gas, it could also be due to the oxygen in the heel remained in the pores of the carbon [12].

BET surface area, micropore volume, and total pore volume of the samples were calculated and are presented in Table 4-3. The results indicate that surface area and pore volume decrease with increasing heel. This is because some of the adsorbed species remain in the pores of the BAC

even after regeneration. This results in fewer adsorption sites available for N<sub>2</sub> adsorption when measuring the surface area and micropore volume using the surface analyzer. Different adsorbates affect the physical properties of the regenerated BAC to different extents. The change in micropore volume and surface area per 1% of mass balance cumulative heel can be calculated for different adsorbates. For example, for TMB, 1% of heel reduces the surface area and micropore volume by 26 m<sup>2</sup>/g and 0.010 cm<sup>3</sup>/g respectively, while for isopropylbenzene surface area and micropore volume are reduced by 34 m<sup>2</sup>/g and 0.013 cm<sup>3</sup>/g, respectively. This is due to the different structures of the compounds resulting in some compounds blocking the pores of the BAC and reducing the physical properties more than others. Similar trends were observed by Jahandar Lashaki et al. [12].

Table 4-3. Characterization results of virgin and regenerated BAC

Carbon Description	Carbon Sample		Structural properties			Surface composition	
			BET Surface Area (m <sup>2</sup> /g)	Micropore Volume (cm <sup>3</sup> /g)	Total Pore Volume (cm <sup>3</sup> /g)	C (%)	O (%)
Virgin	Kureha		1371	0.50	0.57	93.0	7.0
Blank Tests	≤ 5 ppm		1345	0.48	0.56	92.1	7.9
	10,000 ppm		1323	0.48	0.57	92.4	7.6
BAC after 5 Ads/Reg. cycles at full loading	1-butanol	≤ 5 ppm	1307	0.45	0.58	93.1	6.9
		10,000 ppm	1278	0.45	0.55	92.5	7.5
	n-butyl acetate	≤ 5 ppm	1184	0.42	0.48	94.1	5.9
		10,000 ppm	1096	0.40	0.46	92.2	7.8
	2-heptanone	≤ 5 ppm	1316	0.48	0.54	93.1	6.1
		10,000 ppm	1200	0.44	0.49	90.1	9.9
	2-butoxyethanol	≤ 5 ppm	1283	0.46	0.52	92.8	7.2
		10,000 ppm	1280	0.45	0.54	91.7	8.3
	n-decane	≤ 5 ppm	1320	0.48	0.55	93.8	6.2
		10,000 ppm	1180	0.40	0.52	91.9(91.5)	8.1(8.5)
	benzene	≤ 5 ppm	1375	0.50	0.57	94.1	5.9
		10,000 ppm	1343	0.50	0.54	93.7	6.3
	ethylbenzene	≤ 5 ppm	1208	0.44	0.50	94.6	5.4
		10,000 ppm	1118	0.40	0.46	94.4	5.6
	isopropylbenzene	≤ 5 ppm	1137	0.41	0.46	94.0	6.0
		10,000 ppm	942	0.34	0.40	90.5	9.5
	1,2,4 TMB	≤ 5 ppm	1305	0.47	0.56	95.4	4.6
		10,000 ppm	978	0.34	0.44	92.9	7.1
	butylbenzene	≤ 5 ppm	1131	0.41	0.47	94.8	5.2
		10,000 ppm	1147	0.42	0.48	92.2	7.8
	neopentylbenzene	≤ 5 ppm	1255	0.45	0.52	94.8	5.2
		10,000 ppm	1297	0.48	0.53	93.0	7.0

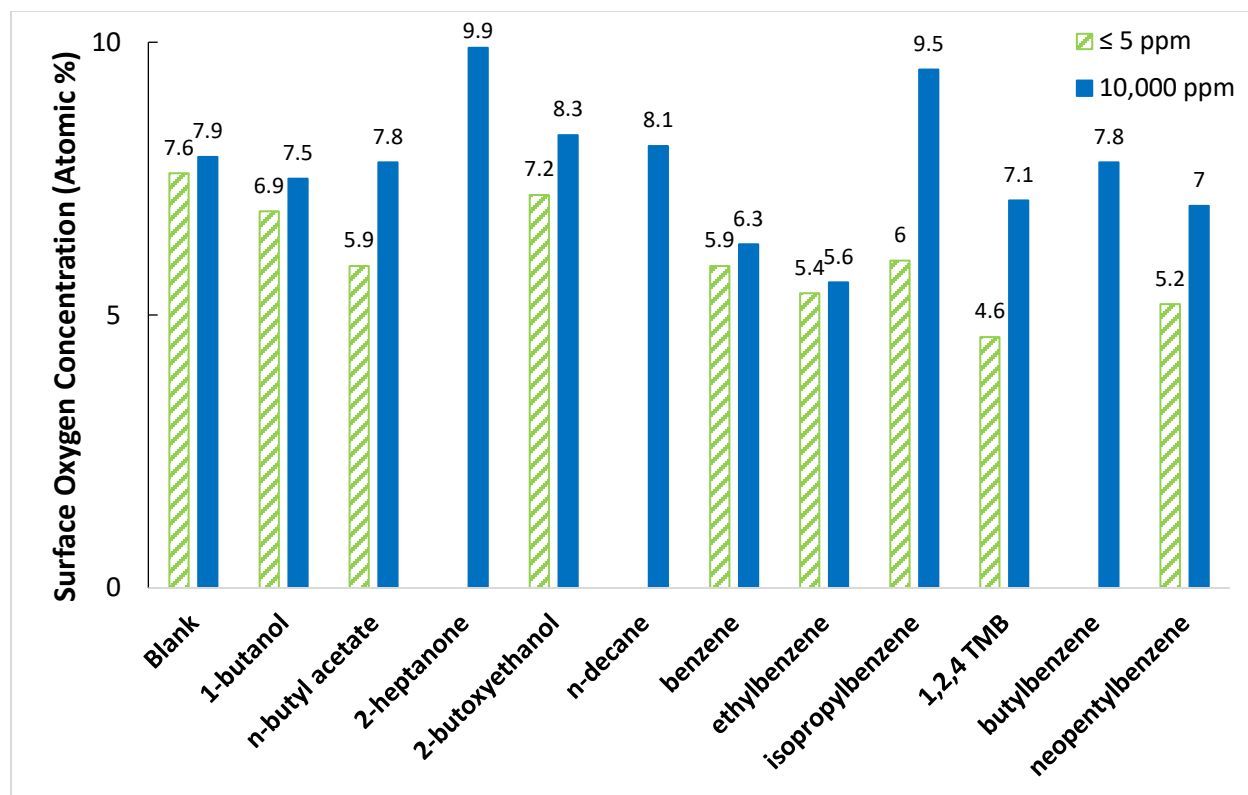


Figure 4-4. Surface oxygen concentration of regenerated samples

Figure 4-5 and Figure 4-6 show the DTG analysis of the regenerated and virgin samples for the 10,000 ppm and  $\leq 5$  ppm experiments, respectively, and Figure 4-7 shows the individual DTG analysis for select adsorbates at the two levels of oxygen impurity in the purge gas. All samples show a first peak at a temperature of about 40°C which is due to desorption of adsorbed moisture [5]. There is a flat region from about 100°C to 288°C (regeneration temperature) in which no desorption is observed since any compound that can be vaporized at this temperature has already escaped the pores during the last regeneration cycle. The second peak is observed at about 400°C and has a higher magnitude for compounds with higher heel formation. In order to determine whether the compounds being desorbed at this temperature are chemisorbed or physisorbed to the BAC, a comparison between the  $\leq 5$  ppm and 10,000 ppm experiments could



be helpful. If this peak ( $400^{\circ}\text{C}$ ) is due to physisorption, a similar peak must be observed for the  $\leq 5$  ppm experiment. If a similar peak is not observed, this means that either a chemical reaction is occurring between oxygen and the adsorbate, the products of which are adsorbed to the carbon, or the adsorbate is chemisorbed to the surface of the BAC. In either case, the interaction is categorized as chemisorption because there is either a chemical bond between the adsorbate and the adsorbent or there is a chemical reaction occurring during the adsorption/regeneration process. Three of the adsorbates (2-butoxyethanol, n-decane, neopentylbenzene) show similar peaks for the  $\leq 5$  ppm and 10,000 ppm experiments while others are flat in that temperature range (around  $400^{\circ}\text{C}$ ). According to the discussion above, these three compounds are physisorbed while others are chemisorbed to the surface of the BAC.

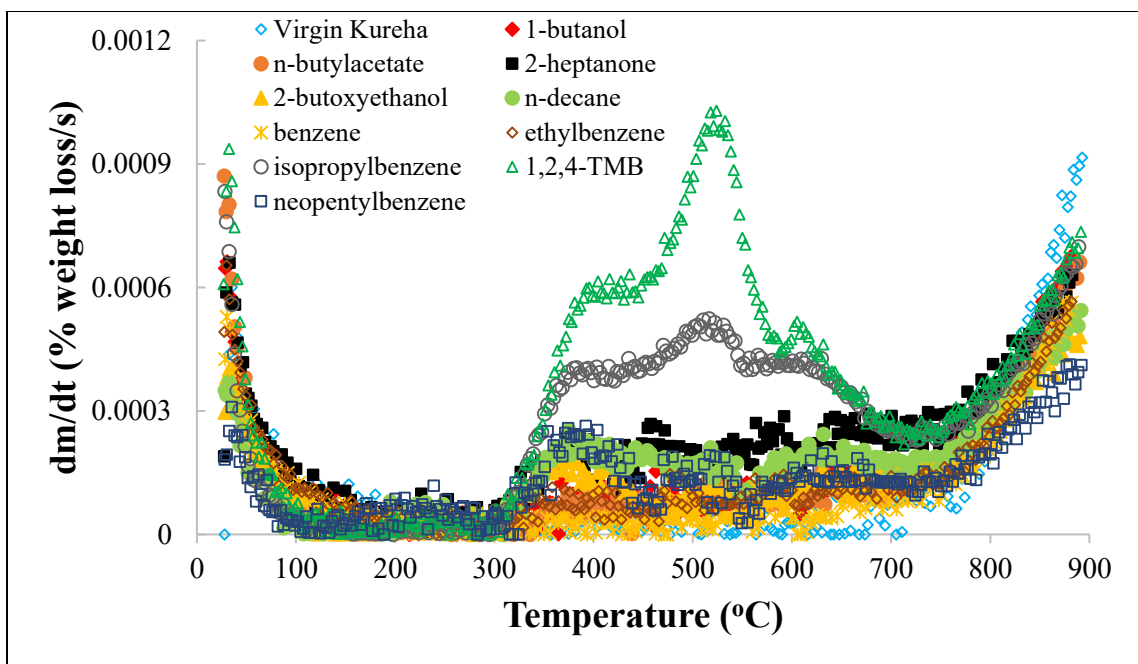


Figure 4-5. DTG analysis of 5-cycle BAC samples regenerated with 10,000 ppm  $\text{O}_2$  in  $\text{N}_2$  purge gas

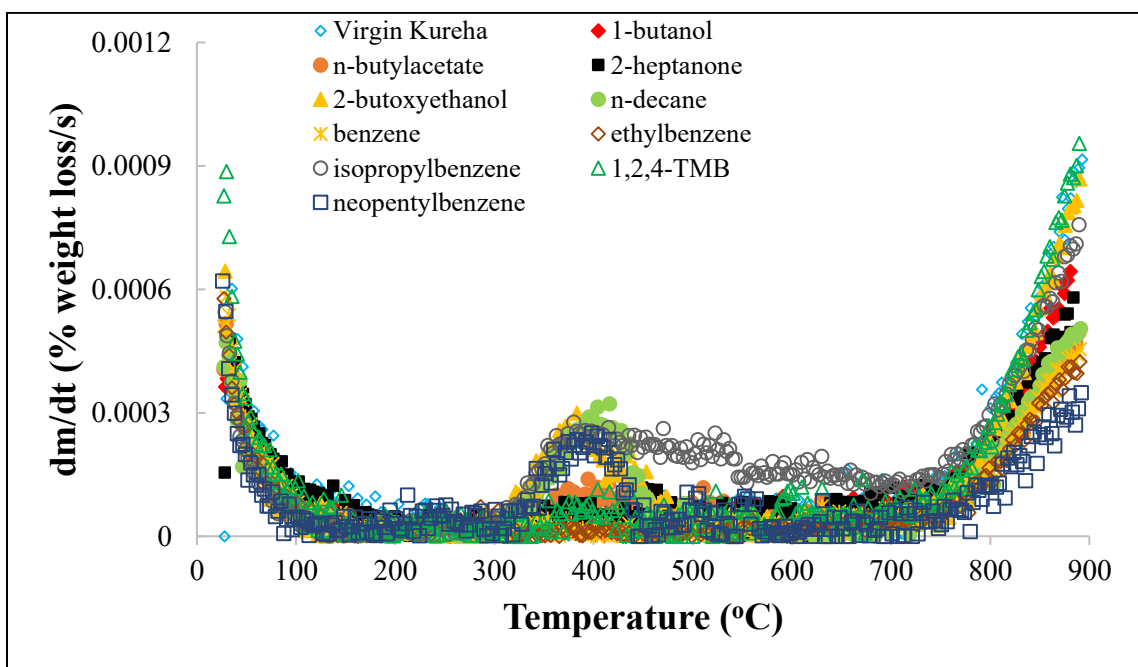
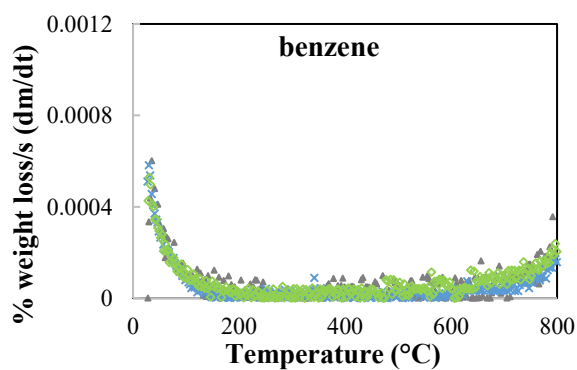
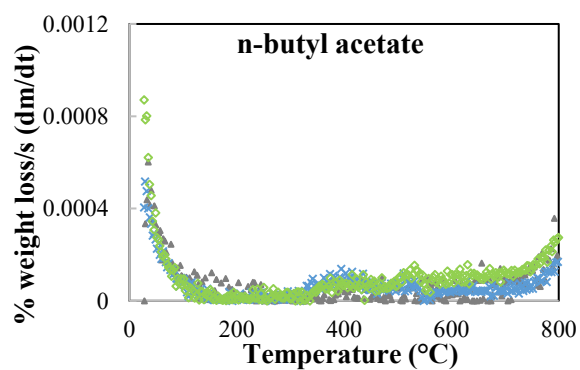
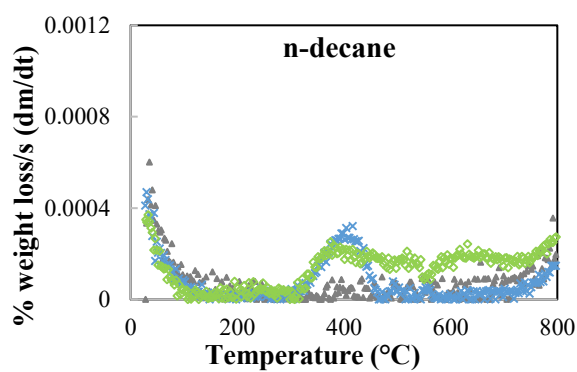
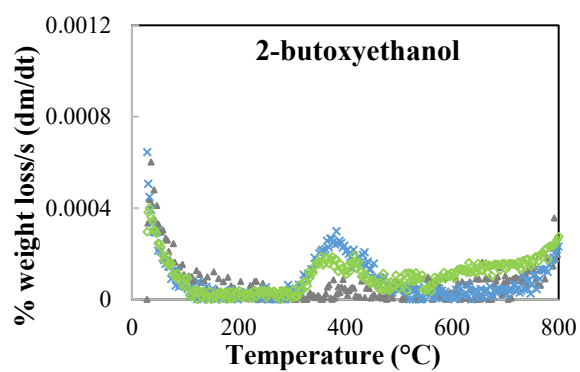
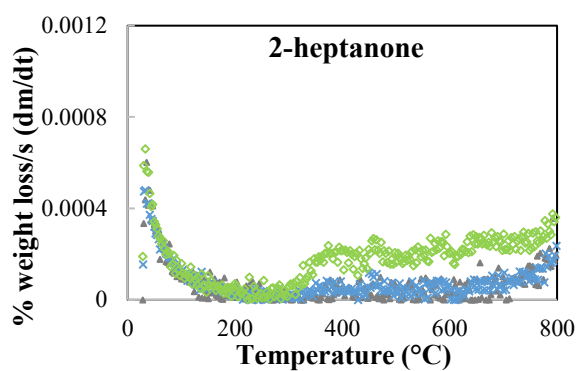
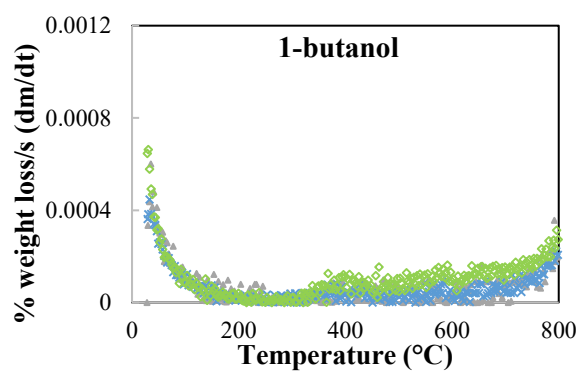


Figure 4-6. DTG analysis of 5-cycle BAC samples regenerated with  $\leq 5$  ppm  $\text{O}_2$  in  $\text{N}_2$  purge gas

▲ Virgin

× ≤ 5 ppm

◇ 10,000 ppm



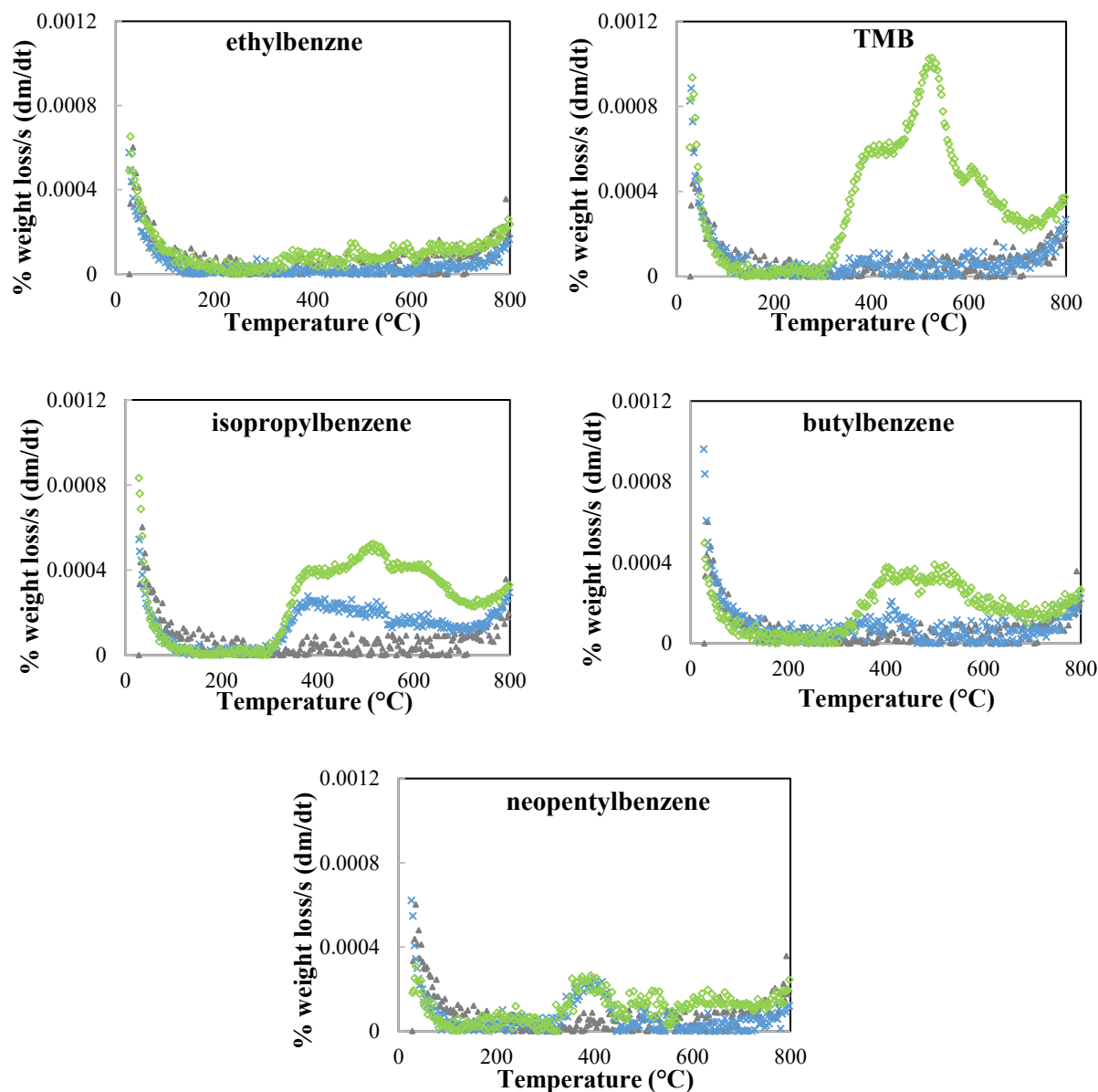


Figure 4-7. DTG analysis of 5-cycle BAC samples saturated with different adsorbates and regenerated at two levels of oxygen concentration in the purge gas ( $\leq 5$  ppm and 10,000 ppm)

Some of the compounds (TMB and isopropylbenzene) show a third peak at 550°C–600°C for samples regenerated at 10,000 ppm O<sub>2</sub> in N<sub>2</sub> but not for samples regenerated at  $\leq 5$  ppm O<sub>2</sub> in N<sub>2</sub> which shows that the compounds being desorbed at this temperature are strongly attached by

chemisorption. A final peak is observed for all compounds starting at about 800°C which is due to carbon loss.

The reduction in pore volume is mostly in the micropore region ( $< 20 \text{ \AA}$ ) since the total pore volume reduction is almost similar to the micropore volume reduction (Table 4-3). This is also supported by the pore size distribution (PSD) graph shown in Figure 4-8. As it can be seen the graphs lie on top of each other for the mesopore region ( $> 20 \text{ \AA}$ ), while for the micropore region the regenerated samples' graphs are placed slightly lower than the virgin graph which shows reduction of pore volume in this region.

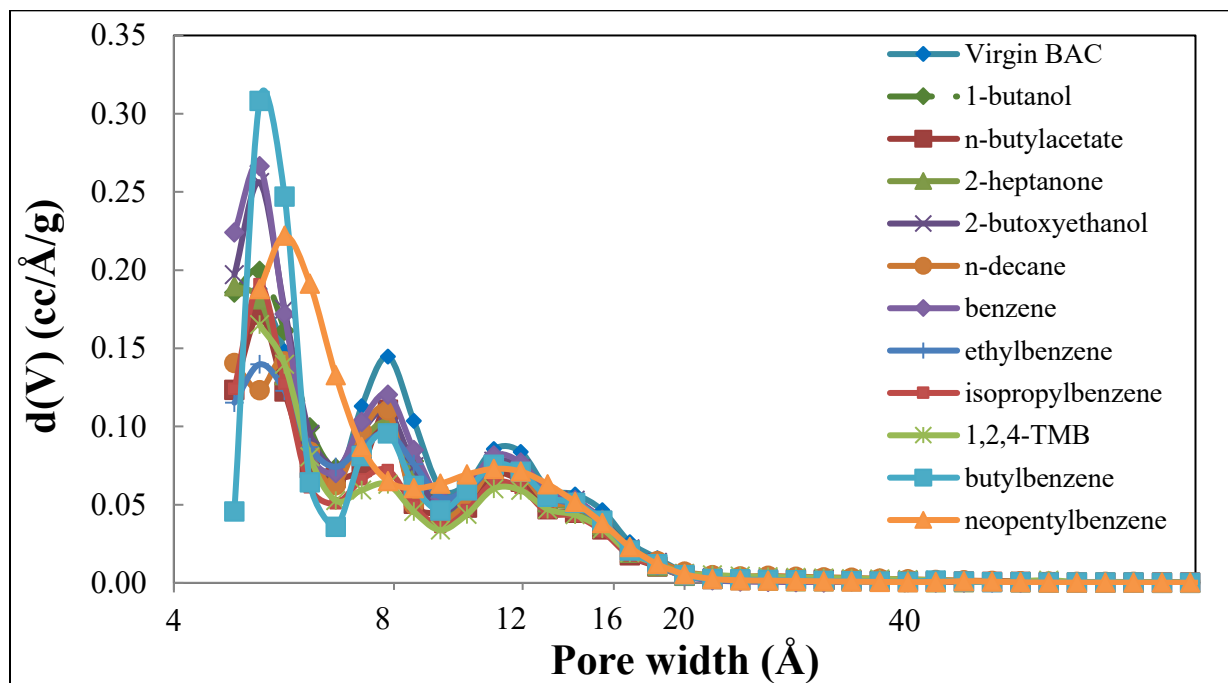


Figure 4-8. PSD of virgin and regenerated BAC samples with 10,000 ppm  $\text{O}_2$  in  $\text{N}_2$  purge gas

## 4.4 Conclusions

Heel formation during cyclic adsorption/regeneration of common VOCs on BAC was investigated focusing on the effect of regeneration purge gas oxygen impurity and adsorbate properties. Regeneration of activated carbon saturated with VOCs in presence of oxygen in the purge gas showed that heel formation is amplified depending on the reactivity of the adsorbate with oxygen in the purge gas. More specifically, regeneration of BACs saturated with alkyl-aromatics with moderate boiling points (TMB, isopropylbenzene, butylbenzene) were prominently affected by the presence of oxygen in the purge gas, resulting in higher heel formation compared to highly pure nitrogen purge gas conditions. This was found to be due to a chemical reaction between the adsorbate and the oxygen in the purge gas possibly producing a polymeric compound which is trapped in the activated carbon pores. However, neopentylbenzene showed lower heel formation compared to the previously mentioned compounds despite having a higher boiling point. This is possibly because the pentyl side chain in neopentylbenzene breaks before the chemical reaction initiates and thus, the regeneration efficiency is satisfactory for this compound.

Aliphatic compounds were not affected by the presence of the purge gas as much as the moderate boiling point aromatics. Highest heel formation for aliphatics was for n-decane resulting in 3.4% and 0.7% in case of 10,000 ppm and  $\leq 5$  ppm oxygen in the purge gas, respectively.

The results from this research help explain heel formation mechanisms and how presence of oxygen impurity in the regeneration purge gas may affect heel formation for different adsorbates (aliphatic and aromatic VOCs) in cyclic adsorption/regeneration systems.

## References

1. Kim, B.R., *VOC Emissions from Automotive Painting and Their Control: A Review*. Environmental Engineering Research, 2011. **16**(1): p. 1-9.
2. Cal, M.P., M.J. Rood, and S.M. Larson, *Removal of VOCs from humidified gas streams using activated carbon cloth*. Gas Separation & Purification, 1996. **10**(2): p. 117-121.
3. Cal, M.P., M.J. Rood, and S.M. Larson, *Gas Phase Adsorption of Volatile Organic Compounds and Water Vapor on Activated Carbon Cloth*. Energy & Fuels, 1997. **11**(2): p. 311-315.
4. Das, D., V. Gaur, and N. Verma, *Removal of volatile organic compound by activated carbon fiber*. Carbon, 2004. **42**(14): p. 2949-2962.
5. Çalışkan, E., et al., *Low temperature regeneration of activated carbons using microwaves: Revising conventional wisdom*. Journal of Environmental Management, 2012. **102**: p. 134-140.
6. Friday, D.K. and M.D. LeVan, *Hot purge gas regeneration of adsorption beds with solute condensation: Experimental studies*. AIChE Journal, 1985. **31**(8): p. 1322-1328.
7. Lashaki, M.J., et al., *Effect of Adsorption and Regeneration Temperature on Irreversible Adsorption of Organic Vapors on Beaded Activated Carbon*. Environmental Science & Technology, 2012. **46**(7): p. 4083-4090.
8. Niknaddaf, S., et al., *Heel formation during volatile organic compound desorption from activated carbon fiber cloth*. Carbon, 2016. **96**: p. 131-138.
9. Hwang, K.S., et al., *Adsorption and thermal regeneration of methylene chloride vapor on an activated carbon bed*. Chemical Engineering Science, 1997. **52**(7): p. 1111-1123.
10. Liu, P.K.T., S.M. Feltch, and N.J. Wagner, *Thermal desorption behavior of aliphatic and aromatic hydrocarbons loaded on activated carbon*. Industrial and Engineering Chemistry Research, 1987. **26**(8): p. 1540-1545.
11. Salvador, F., et al., *Regeneration of carbonaceous adsorbents. Part I: Thermal Regeneration*. Microporous and Mesoporous Materials, 2015. **202**: p. 259-276.
12. Jahandar Lashaki, M., et al., *Effect of desorption purge gas oxygen impurity on irreversible adsorption of organic vapors*. Carbon, 2016. **99**: p. 310-317.

13. Ania, C.O., et al., *Microwave-induced regeneration of activated carbons polluted with phenol. A comparison with conventional thermal regeneration*. Carbon, 2004. **42**(7): p. 1383-1387.
14. Lu, Q. and G.A. Sorial, *Adsorption of phenolics on activated carbon - Impact of pore size and molecular oxygen*. Chemosphere, 2004. **55**(5): p. 671-679.
15. Lu, Q. and G.A. Sorial, *The effect of functional groups on oligomerization of phenolics on activated carbon*. Journal of Hazardous Materials, 2007. **148**(1-2): p. 436-445.
16. Cen, Q., et al., *Thermodynamics and regeneration studies of CO<sub>2</sub> adsorption on activated carbon*. Greenhouse Gases: Science and Technology, 2016. **6**(6): p. 787-796.
17. Yun, J.-H., D.-K. Choi, and H. Moon, *Benzene adsorption and hot purge regeneration in activated carbon beds*. Chemical Engineering Science, 2000. **55**(23): p. 5857-5872.
18. Carratalá-Abril, J., et al., *Regeneration of activated carbons saturated with benzene or toluene using an oxygen-containing atmosphere*. Chemical Engineering Science, 2010. **65**(6): p. 2190-2198.
19. Sabio, E., et al., *Thermal regeneration of activated carbon saturated with p-nitrophenol*. Carbon, 2004. **42**(11): p. 2285-2293.
20. *The Energy Costs Associated with Nitrogen Specifications*. 2017-01-28]; Available from: <http://www.airbestpractices.com/system-assessments/air-treatmentn2/energy-costs-associated-nitrogen-specifications>.
21. Suzuki, M., et al., *Study of thermal regeneration of spent activated carbons: Thermogravimetric measurement of various single component organics loaded on activated carbons*. Chemical Engineering Science, 1978. **33**(3): p. 271-279.
22. Kim, J.-H., et al., *Sorption Equilibrium and Thermal Regeneration of Acetone and Toluene Vapors on an Activated Carbon*. Industrial & Engineering Chemistry Research, 2007. **46**(13): p. 4584-4594.
23. *Kureha Corporation Website*. Available from: [www.kureha.com/pdfs/Kureha-BAC-Bead-Activated-Carbon.pdf](http://www.kureha.com/pdfs/Kureha-BAC-Bead-Activated-Carbon.pdf).
24. Berndt, T. and O. Böge, *Reaction of O(3P) Atoms with Benzene*, in *Zeitschrift für Physikalische Chemie/International journal of research in physical chemistry and chemical physics*. 2004. p. 391.



25. Boocock, G. and R.J. Cvetanović, *Reaction of oxygen atoms with benzene*. Canadian Journal of Chemistry, 1961. **39**(12): p. 2436-2443.
26. Solomons, T.W.G.F., Craig B., *Organic Chemistry*, D. Brennan, Editor. 2003, John Wiley & Sons, inc. p. 453-454.
27. Robaugh, D.A., B.D. Barton, and S.E. Stein, *Thermal decomposition of propyl-, isobutyl-, and neopentylbenzene*. The Journal of Physical Chemistry, 1981. **85**(16): p. 2378-2383.

## **5. CHAPTER 5: Conclusions and Recommendations**

## 5.1 Conclusions

In Chapter 3 the effect of regeneration purge gas oxygen impurity on heel formation during adsorption/regeneration of 1,2,4-trimethylbenzene on beaded activated carbon was studied. 5-cycle adsorption/regeneration experiments were performed with varying oxygen concentrations in the purge gas ( $\leq 5$  ppm, 208 ppm, 625 ppm, 1250 ppm, 2500 ppm, 5000 ppm, 10,000 ppm, and 20,000 ppm). The results showed that heel formation increases from 0.5% to 15.8% at  $\leq 5$  ppm and 20,000 ppm oxygen concentration in the purge gas, respectively. Moreover, lower adsorption capacity, shorter breakthrough time, and loss of BET surface area were observed. DTG analysis of the samples showed that chemisorption is the main heel formation mechanism. It was suggested that formation of polymeric compounds as a result of a chemical reaction between TMB and oxygen, similar to what is reported in the literature, is the main reason for heel formation because the polymeric product is trapped inside the pores due to its larger size.

The effect of regeneration purge gas oxygen impurity on heel formation of different adsorbates was studied in Chapter 4. Eleven adsorbates were tested in 5-cycle adsorption/regeneration experiments with regeneration at two different levels of oxygen impurity. It was found that the nature of the adsorbate and its reactivity with oxygen are the deciding parameters of heel formation in presence of oxygen. The results showed that alkyl-aromatics with moderate boiling points (136-183°C) were prominently affected by presence of oxygen in the purge gas. This was found to be due to a chemical reaction between some adsorbates and oxygen which possibly produce a polymeric compound that traps inside the pores and results in heel formation. Neopentylbenzene however, did not follow a similar behavior as other alkyl-aromatics. It was suggested that the reason for low heel formation of neopentylbenzene is that it decomposes at elevated temperatures and escapes the pores before having a chance to react with oxygen.

## 5.2 Recommendations

This research investigated the effect of regeneration purge gas oxygen impurity on heel formation of different organic vapors. Based on the results obtained, the following recommendations can be made for future research:

- Using a higher heating rate during regeneration may introduce time constraints for diffusion of the adsorbate out of the pores and provide more time for the adsorbate to react with oxygen inside the pores. This may result in higher heel formation and therefore, the effect of heating rate can be investigated to elucidate more on its significance.
- Using microwave regeneration with oxygen containing purge gas may be another topic of interest. Microwave heating directly heats the adsorbate inside the pores of the adsorbent which may result in different desorption behaviors from conventional heating. Hence, investigating the effect oxygen impurity in microwave regeneration of adsorbents could be a potential topic for future studies.
- Understanding the chemical reactions of oxygen with different organic compounds may clarify the heel formation mechanism and make it easier to predict the regeneration behavior of different adsorbates. Thus, it is important to investigate the reaction mechanisms of oxygen with compounds with different functionalities.

## Bibliography

- Ahmad, A. A., & Idris, A. (2014). Preparation and characterization of activated carbons derived from bio-solid: A review. *Desalination and Water Treatment*, 52(25-27), 4848-4862. doi:10.1080/19443994.2013.808797
- Aktaş, Ö., & Çeçen, F. (2007). Bioregeneration of activated carbon: A review. *International Biodeterioration & Biodegradation*, 59(4), 257-272. doi:10.1016/j.ibiod.2007.01.003
- Ania, C. O., Menéndez, J. A., Parra, J. B., & Pis, J. J. (2004). Microwave-induced regeneration of activated carbons polluted with phenol. A comparison with conventional thermal regeneration. *Carbon*, 42(7), 1383-1387. doi:<http://dx.doi.org/10.1016/j.carbon.2004.01.010>
- Ania, C. O., Parra, J. B., Menéndez, J. A., & Pis, J. J. (2007). Microwave-assisted regeneration of activated carbons loaded with pharmaceuticals. *Water Research*, 41(15), 3299-3306. doi:10.1016/j.watres.2007.05.006
- Barrie, J. K. P. j. (1989). *Recent advances in zeolite science*: Elsevier.
- Berenjian, A., Chan, N., & Malmiri, H. J. (2012). Volatile Organic Compounds removal methods: A review. *American journal of biochemistry and biotechnology*, 8(4), 220-229. doi:10.3844/ajbbsp.2012.220.229
- Berndt, T., & Böge, O. (2004). Reaction of O(3P) Atoms with Benzene *Zeitschrift für Physikalische Chemie/International journal of research in physical chemistry and chemical physics* (Vol. 218, pp. 391).
- Boehler, M., Zwicknnpflug, B., Hollender, J., Ternes, T., Joss, A., & Siegrist, H. (2012). Removal of micropollutants in municipal wastewater treatment plants by powder-activated carbon. *Water Science and Technology*, 66(10), 2115-2121. doi:10.2166/wst.2012.353
- Boocock, G., & Cvetanović, R. J. (1961). Reaction of oxygen atoms with benzene. *Canadian Journal of Chemistry*, 39(12), 2436-2443. doi:10.1139/v61-323
- Bowman, F. M., & Seinfeld, J. H. (1995). Atmospheric chemistry of alternate fuels and reformulated gasoline components. *Progress in Energy and Combustion Science*, 21(5), 387-417. doi:10.1016/0360-1285(95)00008-9
- Brunauer, S., Emmett, P. H., & Teller, E. (1938). Adsorption of gases in multimolecular layers. *Journal of the American Chemical Society*, 60(2), 309-319.
- Cal, M. P., Rood, M. J., & Larson, S. M. (1996). Removal of VOCs from humidified gas streams using activated carbon cloth. *Gas Separation & Purification*, 10(2), 117-121. doi:[http://dx.doi.org/10.1016/0950-4214\(96\)00004-7](http://dx.doi.org/10.1016/0950-4214(96)00004-7)
- Cal, M. P., Rood, M. J., & Larson, S. M. (1997). Gas Phase Adsorption of Volatile Organic Compounds and Water Vapor on Activated Carbon Cloth. *Energy & Fuels*, 11(2), 311-315. doi:10.1021/ef960200p
- Çalışkan, E., Bermúdez, J. M., Parra, J. B., Menéndez, J. A., Mahramanlioğlu, M., & Ania, C. O. (2012). Low temperature regeneration of activated carbons using microwaves: Revising conventional wisdom. *Journal of Environmental Management*, 102, 134-140. doi:10.1016/j.jenvman.2012.02.016
- Carratalá-Abril, J., Lillo-Ródenas, M. A., Linares-Solano, A., & Cazorla-Amorós, D. (2010). Regeneration of activated carbons saturated with benzene or toluene using an oxygen-containing atmosphere. *Chemical Engineering Science*, 65(6), 2190-2198. doi:10.1016/j.ces.2009.12.017
- Cen, Q., Fang, M., Wang, T., Majchrzak-Kucęba, I., Wawrzyńczak, D., & Luo, Z. (2016). Thermodynamics and regeneration studies of CO<sub>2</sub> adsorption on activated carbon. *Greenhouse Gases: Science and Technology*, 6(6), 787-796. doi:10.1002/ghg.1621
- CEPA. (1999). Definition of Volatile Organic Compounds (VOCs). Retrieved from <https://www.ec.gc.ca/inrp-npri/default.asp?lang=En&n=EF5C823B-1>

- Chang, K. S., Wang, H. C., & Chung, T. W. (2004). Effect of regeneration conditions on the adsorption dehumidification process in packed silica gel beds. *Applied Thermal Engineering*, 24(5-6), 735-742. doi:10.1016/j.applthermaleng.2003.11.003
- Chatzopoulos, D., Varma, A., & Irvine, R. L. (1993). Activated carbon adsorption and desorption of toluene in the aqueous phase. *AIChE Journal*, 39(12), 2027-2041. doi:10.1002/aic.690391213
- Chiang, Y. C., Chiang, P. C., & Huang, C. P. (2001). Effects of pore structure and temperature on VOC adsorption on activated carbon. *Carbon*, 39(4), 523-534. doi:10.1016/S0008-6223(00)00161-5
- Cooney, D. O., Nagerl, A., & Hines, A. L. (1983). Solvent regeneration of activated carbon. *Water Research*, 17(4), 403-410. doi:10.1016/0043-1354(83)90136-7
- Dąbrowski, A., Podkościelny, P., Hubicki, Z., & Barczak, M. (2005). Adsorption of phenolic compounds by activated carbon—a critical review. *Chemosphere*, 58(8), 1049-1070. doi:<http://dx.doi.org/10.1016/j.chemosphere.2004.09.067>
- Das, D., Gaur, V., & Verma, N. (2004). Removal of volatile organic compound by activated carbon fiber. *Carbon*, 42(14), 2949-2962. doi:<http://dx.doi.org/10.1016/j.carbon.2004.07.008>
- De Jonge, R. J., Breure, A. M., & Van Andel, J. G. (1996). Reversibility of adsorption of aromatic compounds onto powdered activated carbon (PAC). *Water Research*, 30(4), 883-892. doi:10.1016/0043-1354(95)00248-0
- Di Natale, F., Erto, A., & Lancia, A. (2013). Desorption of arsenic from exhaust activated carbons used for water purification. *Journal of Hazardous Materials*, 260, 451-458. doi:10.1016/j.jhazmat.2013.05.055
- Dias, J. M., Alvim-Ferraz, M. C. M., Almeida, M. F., Rivera-Utrilla, J., & Sánchez-Polo, M. (2007). Waste materials for activated carbon preparation and its use in aqueous-phase treatment: A review. *Journal of Environmental Management*, 85(4), 833-846. doi:<http://dx.doi.org/10.1016/j.jenvman.2007.07.031>
- Dobrevski, I., & Zvezdova, L. (1989). Biological regeneration of activated carbon. *Water Science and Technology*, 21(1), 141-143.
- Dombrowski, R. J., Hyduke, D. R., & Lastoskie, C. M. (2000). Pore size analysis of activated carbons from argon and nitrogen porosimetry using density functional theory. *Langmuir*, 16(11), 5041-5050. doi:10.1021/la990827a
- Environment-Canada. (2016-05-25). Volatile Organic Compound Emissions. Retrieved from <https://www.ec.gc.ca/indicateurs-indicators/default.asp?lang=en&n=64B9E95D-1>
- Fayaz, M., Shariaty, P., Atkinson, J. D., Hashisho, Z., Phillips, J. H., Anderson, J. E., & Nichols, M. (2015). Using microwave heating to improve the desorption efficiency of high molecular weight VOC from beaded activated carbon. *Environmental Science and Technology*, 49(7), 4536-4542. doi:10.1021/es505953c
- Friday, D. K., & LeVan, M. D. (1985). Hot purge gas regeneration of adsorption beds with solute condensation: Experimental studies. *AIChE Journal*, 31(8), 1322-1328. doi:10.1002/aic.690310811
- GEO-CENTERS, I. (1984). *The Reaction of Oxygen-Nitrogen Mixtures with Granular Activated Carbons Below The Spontaneous Ignition Temperature*. Retrieved from
- Grant, T. M., & King, C. J. (1990). Mechanism of irreversible adsorption of phenolic compounds by activated carbons. *Industrial and Engineering Chemistry Research*, 29(2), 264-271.
- Guenther, A. (1995). A global model of natural volatile organic compound emissions. *Journal of Geophysical Research*, 100, 8873-8892.
- Guo, D., Shi, Q., He, B., & Yuan, X. (2011). Different solvents for the regeneration of the exhausted activated carbon used in the treatment of coking wastewater. *Journal of Hazardous Materials*, 186(2-3), 1788-1793. doi:10.1016/j.jhazmat.2010.12.068
- Harriott, P., & Cheng, A. T.-Y. (1988). Kinetics of spent activated carbon regeneration. *AIChE Journal*, 34(10), 1656-1662. doi:10.1002/aic.690341009
- Hashisho, Z., Emamipour, H., Rood, M. J., Hay, K. J., Kim, B. J., & Thurston, D. (2008). Concomitant Adsorption and Desorption of Organic Vapor in Dry and Humid Air Streams using Microwave

- and Direct Electrothermal Swing Adsorption. *Environmental Science & Technology*, 42(24), 9317-9322. doi:10.1021/es801285v
- Huang, C. C., Chen, H. M., & Chen, C. H. (2010). Hydrogen adsorption on modified activated carbon. *International Journal of Hydrogen Energy*, 35(7), 2777-2780. doi:10.1016/j.ijhydene.2009.05.016
- Hwang, K. S., Choi, D. K., Gong, S. Y., & Cho, S. Y. (1997). Adsorption and thermal regeneration of methylene chloride vapor on an activated carbon bed. *Chemical Engineering Science*, 52(7), 1111-1123. doi:10.1016/S0009-2509(96)00470-8
- ISO. (2011). ISO 16000-6 *Determination of volatile organic compounds in indoor and test chamber air by active sampling on Tenax TA sorbent, thermal desorption and gas chromatography using MS or MS-FID*.
- Jahandar Lashaki, M., Atkinson, J. D., Hashisho, Z., Phillips, J. H., Anderson, J. E., Nichols, M., & Misovski, T. (2016). Effect of desorption purge gas oxygen impurity on irreversible adsorption of organic vapors. *Carbon*, 99, 310-317. doi:10.1016/j.carbon.2015.12.037
- Khan, F. I., & Kr. Ghoshal, A. (2000). Removal of Volatile Organic Compounds from polluted air. *Journal of Loss Prevention in the Process Industries*, 13(6), 527-545.
- Kim, B. R. (2011). VOC Emissions from Automotive Painting and Their Control: A Review. *Environmental Engineering Research*, 16(1), 1-9. doi:10.4491/eer.2011.16.1.001
- Kim, J.-H., Lee, S.-J., Kim, M.-B., Lee, J.-J., & Lee, C.-H. (2007). Sorption Equilibrium and Thermal Regeneration of Acetone and Toluene Vapors on an Activated Carbon. *Industrial & Engineering Chemistry Research*, 46(13), 4584-4594. doi:10.1021/ie0609362
- Lashaki, M. J., Fayaz, M., Wang, H., Hashisho, Z., Philips, J. H., Anderson, J. E., & Nichols, M. (2012). Effect of Adsorption and Regeneration Temperature on Irreversible Adsorption of Organic Vapors on Beaded Activated Carbon. *Environmental Science & Technology*, 46(7), 4083-4090. doi:10.1021/es3000195
- Li, L., Liu, S., & Liu, J. (2011). Surface modification of coconut shell based activated carbon for the improvement of hydrophobic VOC removal. *Journal of Hazardous Materials*, 192(2), 683-690. doi:10.1016/j.jhazmat.2011.05.069
- Lillo-Ródenas, M. A., Cazorla-Amorós, D., & Linares-Solano, A. (2005). Behaviour of activated carbons with different pore size distributions and surface oxygen groups for benzene and toluene adsorption at low concentrations. *Carbon*, 43(8), 1758-1767. doi:10.1016/j.carbon.2005.02.023
- Liu, P. K. T., Feltch, S. M., & Wagner, N. J. (1987). Thermal desorption behavior of aliphatic and aromatic hydrocarbons loaded on activated carbon. *Industrial and Engineering Chemistry Research*, 26(8), 1540-1545.
- Lu, Q., & Sorial, G. A. (2004). Adsorption of phenolics on activated carbon - Impact of pore size and molecular oxygen. *Chemosphere*, 55(5), 671-679. doi:10.1016/j.chemosphere.2003.11.044
- Lu, Q., & Sorial, G. A. (2007). The effect of functional groups on oligomerization of phenolics on activated carbon. *Journal of Hazardous Materials*, 148(1-2), 436-445. doi:<http://dx.doi.org/10.1016/j.jhazmat.2007.02.058>
- Martin, R. J., & Ng, W. J. (1984). Chemical regeneration of exhausted activated carbon-I. *Water Research*, 18(1), 59-73. doi:10.1016/0043-1354(84)90048-4
- Martin, R. J., & Ng, W. J. (1985). Chemical regeneration of exhausted activated carbon-II. *Water Research*, 19(12), 1527-1535. doi:10.1016/0043-1354(85)90398-7
- Martin, R. J., & Ng, W. J. (1987). The repeated exhaustion and chemical regeneration of activated carbon. *Water Research*, 21(8), 961-965. doi:10.1016/S0043-1354(87)80014-3
- Miyake, Y., Sakoda, A., Yamanashi, H., Kaneda, H., & Suzuki, M. (2003). Activated carbon adsorption of trichloroethylene (TCE) vapor stripped from TCE-contaminated water. *Water Research*, 37(8), 1852-1858. doi:10.1016/S0043-1354(02)00564-X
- Niknaddaf, S., Atkinson, J. D., Shariaty, P., Jahandar Lashaki, M., Hashisho, Z., Phillips, J. H., . . . Nichols, M. (2016). Heel formation during volatile organic compound desorption from activated carbon fiber cloth. *Carbon*, 96, 131-138. doi:10.1016/j.carbon.2015.09.049

- Ondon, B. S., Sun, B., Yan, Z. Y., Zhu, X. M., & Liu, H. (2014). Effect of microwave heating on the regeneration of modified activated carbons saturated with phenol. *Applied Water Science*, 4(4), 333-339. doi:10.1007/s13201-013-0147-5
- Otto, D. A., Hudnell, H. K., House, D. E., Mølhave, L., & Counts, W. (1992). Exposure of Humans to a Volatile Organic Mixture. I. Behavioral Assessment. *Archives of Environmental Health: An International Journal*, 47(1), 23-30. doi:10.1080/00039896.1992.9935940
- Parmar, G. R., & Rao, N. N. (2009). Emerging control technologies for volatile organic compounds. *Critical Reviews in Environmental Science and Technology*, 39(1), 41-78. doi:10.1080/10643380701413658
- Pevida, C., Plaza, M. G., Arias, B., Fermoso, J., Rubiera, F., & Pis, J. J. (2008). Surface modification of activated carbons for CO<sub>2</sub> capture. *Applied Surface Science*, 254(22), 7165-7172. doi:10.1016/j.apsusc.2008.05.239
- Piccot, S. D., Watson, J. J., & Jones, J. W. (1992). A global inventory of volatile organic compound emissions from anthropogenic sources. *Journal of Geophysical Research*, 97(D9), 9897-9912.
- Popescu, M., Joly, J. P., Carré, J., & Danatou, C. (2003). Dynamical adsorption and temperature-programmed desorption of VOCs (toluene, butyl acetate and butanol) on activated carbons. *Carbon*, 41(4), 739-748. doi:[http://dx.doi.org/10.1016/S0008-6223\(02\)00391-3](http://dx.doi.org/10.1016/S0008-6223(02)00391-3)
- Ravikovitch, P. I., & Neimark, A. V. (2006). Density functional theory model of adsorption on amorphous and microporous silica materials. *Langmuir*, 22(26), 11171-11179. doi:10.1021/la0616146
- Robaugh, D. A., Barton, B. D., & Stein, S. E. (1981). Thermal decomposition of propyl-, isobutyl-, and neopentylbenzene. *The Journal of Physical Chemistry*, 85(16), 2378-2383. doi:10.1021/j150616a017
- Ryu, Y.-K., Kim, K.-L., & Lee, C.-H. (2000). Adsorption and Desorption of n-Hexane, Methyl Ethyl Ketone, and Toluene on an Activated Carbon Fiber from Supercritical Carbon Dioxide. *Industrial & Engineering Chemistry Research*, 39(7), 2510-2518. doi:10.1021/ie990673u
- Rzepka, M., Lamp, P., & de la Casa-Lillo, M. A. (1998). Physisorption of Hydrogen on Microporous Carbon and Carbon Nanotubes. *The Journal of Physical Chemistry B*, 102(52), 10894-10898. doi:10.1021/jp9829602
- Sabio, E., González, E., González, J. F., González-García, C. M., Ramiro, A., & Gañan, J. (2004). Thermal regeneration of activated carbon saturated with p-nitrophenol. *Carbon*, 42(11), 2285-2293. doi:10.1016/j.carbon.2004.05.007
- Saha, B. B., Chakraborty, A., Koyama, S., Yoon, S.-H., Mochida, I., Kumja, M., . . . Ng, K. C. (2008). Isotherms and thermodynamics for the adsorption of n-butane on pitch based activated carbon. *International Journal of Heat and Mass Transfer*, 51(7-8), 1582-1589. doi:<http://dx.doi.org/10.1016/j.ijheatmasstransfer.2007.07.031>
- Salvador, F., Martin-Sanchez, N., Sanchez-Hernandez, R., Sanchez-Montero, M. J., & Izquierdo, C. (2015a). Regeneration of carbonaceous adsorbents. Part I: Thermal Regeneration. *Microporous and Mesoporous Materials*, 202, 259-276. doi:10.1016/j.micromeso.2014.02.045
- Salvador, F., Martin-Sanchez, N., Sanchez-Hernandez, R., Sanchez-Montero, M. J., & Izquierdo, C. (2015b). Regeneration of carbonaceous adsorbents. Part II: Chemical, Microbiological and Vacuum Regeneration. *Microporous and Mesoporous Materials*, 202(C), 277-296. doi:10.1016/j.micromeso.2014.08.019
- Salvador, F., Sánchez-Montero, M. J., Salvador, A., & Martín, M. J. (2005). Study of the energetic heterogeneity of the adsorption of phenol onto activated carbons by TPD under supercritical conditions. *Applied Surface Science*, 252(3), 641-646. doi:10.1016/j.apsusc.2005.02.090
- Snoeyink, V. L., Weber Jr, W. J., & Mark Jr, H. B. (1969). Sorption of phenol and nitrophenol by active carbon. *Environmental Science and Technology*, 3(10), 918-926.
- Solomons, T. W. G. F., Craig B. (2003). Organic Chemistry. In D. Brennan (Ed.), (Eight ed., pp. 453-454): John Wiley & Sons, inc.



- Sutikno, T., & Himmelstein, K. J. (1983). Desorption of phenol from activated carbon by solvent regeneration. *Industrial & Engineering Chemistry Fundamentals*, 22(4), 420-425. doi:10.1021/i100012a011
- Suzuki, M., Misic, D. M., Koyama, O., & Kawazoe, K. (1978). Study of thermal regeneration of spent activated carbons: Thermogravimetric measurement of various single component organics loaded on activated carbons. *Chemical Engineering Science*, 33(3), 271-279. doi:[http://dx.doi.org/10.1016/0009-2509\(78\)80085-2](http://dx.doi.org/10.1016/0009-2509(78)80085-2)
- Tamon, H., Saito, T., Kishimura, M., Okazaki, M., & Toei, R. (1990). Solvent Regeneration of Spent Activated Carbon in Wastewater Treatment. *JOURNAL OF CHEMICAL ENGINEERING OF JAPAN*, 23(4), 426-432. doi:10.1252/jcej.23.426
- Tan, C.-S., & Lee, P.-L. (2008). Supercritical CO<sub>2</sub> desorption of toluene from activated carbon in rotating packed bed. *The Journal of Supercritical Fluids*, 46(2), 99-104. doi:<http://dx.doi.org/10.1016/j.supflu.2008.04.012>
- Treybal, R. E. (1981). *Mass-Transfer Operations* (3 ed.).
- Tukur, N. M., & Al-Khattaf, S. (2007). Catalytic Transformation of 1,3,5-Trimethylbenzene over a USY Zeolite Catalyst. *Energy & Fuels*, 21(5), 2499-2508. doi:10.1021/ef7002602
- USEPA. (2016, March 17, 2016). Technical Overview of Volatile Organic Compounds. Retrieved from <https://www.epa.gov/indoor-air-quality-iaq/technical-overview-volatile-organic-compounds>
- Vidic, R. D., & Suidan, M. T. (1991). Role of dissolved oxygen on the adsorptive capacity of activated carbon for synthetic and natural organic matter. *Environmental Science and Technology*, 25(9), 1612-1618.
- Vidic, R. D., Suidan, M. T., & Brenner, R. C. (1993). Oxidative coupling of phenols on activated carbon: impact on adsorption equilibrium. *Environmental Science & Technology*, 27(10), 2079-2085.
- Walker, G. M., & Weatherley, L. R. (1997). Adsorption of acid dyes on to granular activated carbon in fixed beds. *Water Research*, 31(8), 2093-2101. doi:10.1016/S0043-1354(97)00039-0
- Wang, H., Jahandar Lashaki, M., Fayaz, M., Hashisho, Z., Philips, J. H., Anderson, J. E., & Nichols, M. (2012). Adsorption and Desorption of Mixtures of Organic Vapors on Beaded Activated Carbon. *Environmental Science & Technology*, 46(15), 8341-8350. doi:10.1021/es3013062
- Welham, N. J., Berbenni, V., & Chapman, P. G. (2002). Increased chemisorption onto activated carbon after ball-milling. *Carbon*, 40(13), 2307-2315. doi:[http://dx.doi.org/10.1016/S0008-6223\(02\)00123-9](http://dx.doi.org/10.1016/S0008-6223(02)00123-9)
- Yang, J., Zhao, Q., Xu, H., Li, L., Dong, J., & Li, J. (2012). Adsorption of CO<sub>2</sub>, CH<sub>4</sub>, and N<sub>2</sub> on gas diameter grade ion-exchange small pore zeolites. *Journal of Chemical and Engineering Data*, 57(12), 3701-3709. doi:10.1021/jc300940m
- Yin, C. Y., Aroua, M. K., & Daud, W. M. A. W. (2007). Review of modifications of activated carbon for enhancing contaminant uptakes from aqueous solutions. *Separation and Purification Technology*, 52(3), 403-415. doi:10.1016/j.seppur.2006.06.009
- Yonge, D. R., Keinath, T. M., Poznanska, K., & Jiang, Z. P. (1985). Single-solute irreversible adsorption on granular activated carbon. *Environmental Science and Technology*, 19(8), 690-694.
- Yun, J.-H., Choi, D.-K., & Moon, H. (2000). Benzene adsorption and hot purge regeneration in activated carbon beds. *Chemical Engineering Science*, 55(23), 5857-5872. doi:[http://dx.doi.org/10.1016/S0009-2509\(00\)00189-5](http://dx.doi.org/10.1016/S0009-2509(00)00189-5)
- Zhang, H. (2002). Regeneration of exhausted activated carbon by electrochemical method. *Chemical Engineering Journal*, 85(1), 81-85. doi:10.1016/S1385-8947(01)00176-0

## Appendices

### Appendix A: Mass balance cumulative heel tables of Chapter 3

Table A1. Mass balance of 1,2,4-trimethylbenzene adsorption on BAC regenerated at  $\leq 5$  ppm  $O_2$  in  $N_2$  purge gas

Weight of dry virgin BAC: 3.946 g				
Cycle	Amount Adsorbed (g)	Adsorption Capacity (%)	Total Heel (g)	Total Heel (% of Total Heel/g BAC)
1	1.779	45.1	0.009	0.2
2	1.770	44.9	0.014	0.4
3	1.793	45.4	0.025	0.6
4	1.784	45.2	0.026	0.7
5	1.781	45.1	0.029	0.7

Table A2. Mass balance of 1,2,4-trimethylbenzene adsorption on BAC regenerated at 208 ppm  $O_2$  in  $N_2$  purge gas

Weight of dry virgin BAC: 4.049 g				
Cycle	Amount Adsorbed (g)	Adsorption Capacity (%)	Total Heel (g)	Total Heel (% of Total Heel/g BAC)
1	1.756	43.4	0.014	0.4
2	1.745	43.1	0.027	0.7
3	1.747	43.1	0.036	0.9
4	1.730	42.7	0.043	1.1
5	1.705	42.1	0.051	1.3

Table A3. Mass balance of 1,2,4-trimethylbenzene adsorption on BAC regenerated at 625 ppm  
O<sub>2</sub> in N<sub>2</sub> purge gas

Weight of dry virgin BAC: 4.022 g				
Cycle	Amount Adsorbed (g)	Adsorption Capacity (%)	Total Heel (g)	Total Heel (% g Total Heel/g BAC)
1	1.784	44.4	0.043	1.1
2	1.828	45.5	0.079	2.0
3	1.678	41.7	0.099	2.5
4	1.676	41.7	0.131	3.3
5	1.659	41.2	0.167	4.2

Table A4. Mass balance of 1,2,4-trimethylbenzene adsorption on BAC regenerated at 1250 ppm  
O<sub>2</sub> in N<sub>2</sub> purge gas

Weight of dry virgin BAC: 4.012 g				
Cycle	Amount Adsorbed (g)	Adsorption Capacity (%)	Total Heel (g)	Total Heel (% g Total Heel/g BAC)
1	1.750	43.6	0.052	1.3
2	1.710	42.6	0.093	2.3
3	1.668	41.6	0.165	4.1
4	1.651	41.2	0.205	5.1
5	1.626	40.5	0.253	6.3

Table A5. Mass balance of 1,2,4-trimethylbenzene adsorption on BAC regenerated at 2500 ppm O<sub>2</sub> in N<sub>2</sub> purge gas

Weight of dry virgin BAC: 4.032 g				
Cycle	Amount Adsorbed (g)	Adsorption Capacity (%)	Total Heel (g)	Total Heel (% g Total Heel/g BAC)
1	1.785	44.3	0.078	1.9
2	1.722	42.7	0.136	3.4
3	1.694	42.0	0.214	5.3
4	1.646	40.8	0.281	7.0
5	1.595	39.6	0.356	8.8

Table A6. Mass balance of 1,2,4-trimethylbenzene adsorption on BAC regenerated at 5000 ppm O<sub>2</sub> in N<sub>2</sub> purge gas (numbers in parenthesis are from duplicated experiment)

Weight of dry virgin BAC: 4.054 g (4.019 g)				
Cycle	Amount Adsorbed (g)	Adsorption Capacity (%)	Total Heel (g)	Total Heel (% g Total Heel/g BAC)
1	1.757 (1.769)	43.3 (44.0)	0.072 (0.089)	1.8 (2.2)
2	1.755 (1.719)	43.3 (42.8)	0.180 (0.170)	4.4 (4.2)
3	1.678 (1.669)	41.4 (41.5)	0.293 (0.271)	7.2 (6.7)
4	1.591 (1.592)	39.2 (39.6)	0.388 (0.349)	9.6 (8.7)
5	1.546 (1.557)	38.1 (38.7)	0.479 (0.442)	11.8 (11.0)

Table A7. Mass balance of 1,2,4-trimethylbenzene adsorption on BAC regenerated at 10,000 ppm O<sub>2</sub> in N<sub>2</sub> purge gas (numbers in parenthesis are from duplicated experiment)

Weight of dry virgin BAC: 3.969 g (4.000 g)				
Cycle	Amount Adsorbed (g)	Adsorption Capacity (%)	Total Heel (g)	Total Heel (% g Total Heel/g BAC)
1	1.745 (1.747)	44.0 (43.7)	0.103 (0.103)	2.6 (2.6)
2	1.664 (1.675)	41.9 (41.9)	0.210 (0.227)	5.3 (5.7)
3	1.628 (1.601)	41.0 (40.0)	0.327 (0.320)	8.2 (8.0)
4	1.560 (1.554)	39.3 (38.9)	0.433 (0.437)	10.9 (10.9)
5	1.484 (1.471)	37.4 (36.8)	0.514 (0.536)	13.0 (13.4)

Table A8. Mass balance of 1,2,4-trimethylbenzene adsorption on BAC regenerated at 20,000 ppm O<sub>2</sub> in N<sub>2</sub> purge gas

Weight of dry virgin BAC: 4.020 g				
Cycle	Amount Adsorbed (g)	Adsorption Capacity (%)	Total Heel (g)	Total Heel (% g Total Heel/g BAC)
1	1.766	43.9	0.136	3.4
2	1.675	41.7	0.257	6.4
3	1.602	39.9	0.405	10.1
4	1.518	37.8	0.524	13.0
5	1.414	35.2	0.634	15.8

## Appendix B: Adsorption breakthrough curves of Chapter 4

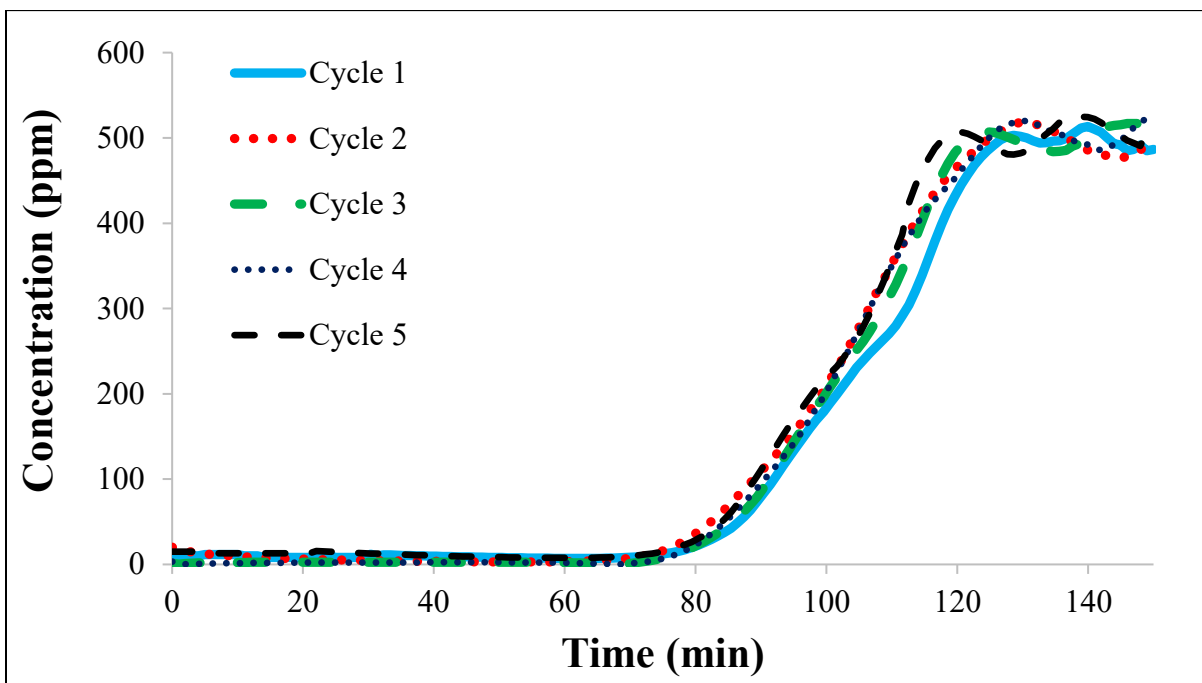


Figure B1. Adsorption breakthrough curves for adsorption of 1-butanol on beaded activated carbon, regenerated at  $\leq 5$  ppm  $O_2$  in  $N_2$

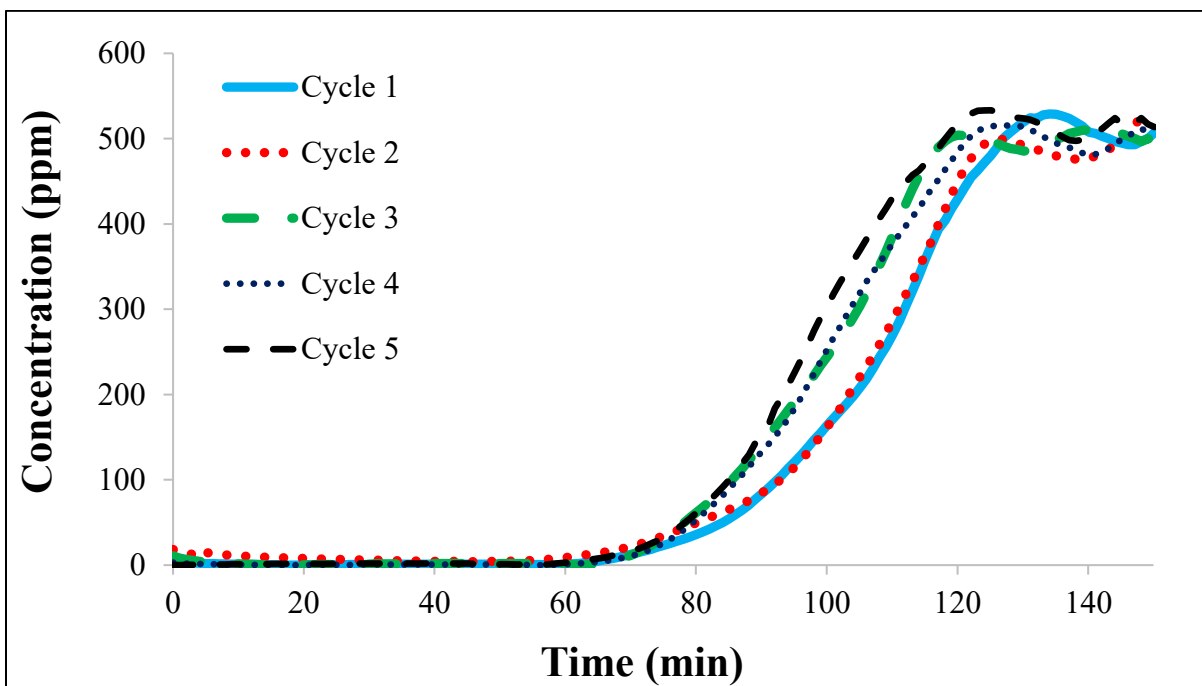


Figure B2. Adsorption breakthrough curves for adsorption of 1-butanol on beaded activated carbon, regenerated at 10,000 ppm  $O_2$  in  $N_2$

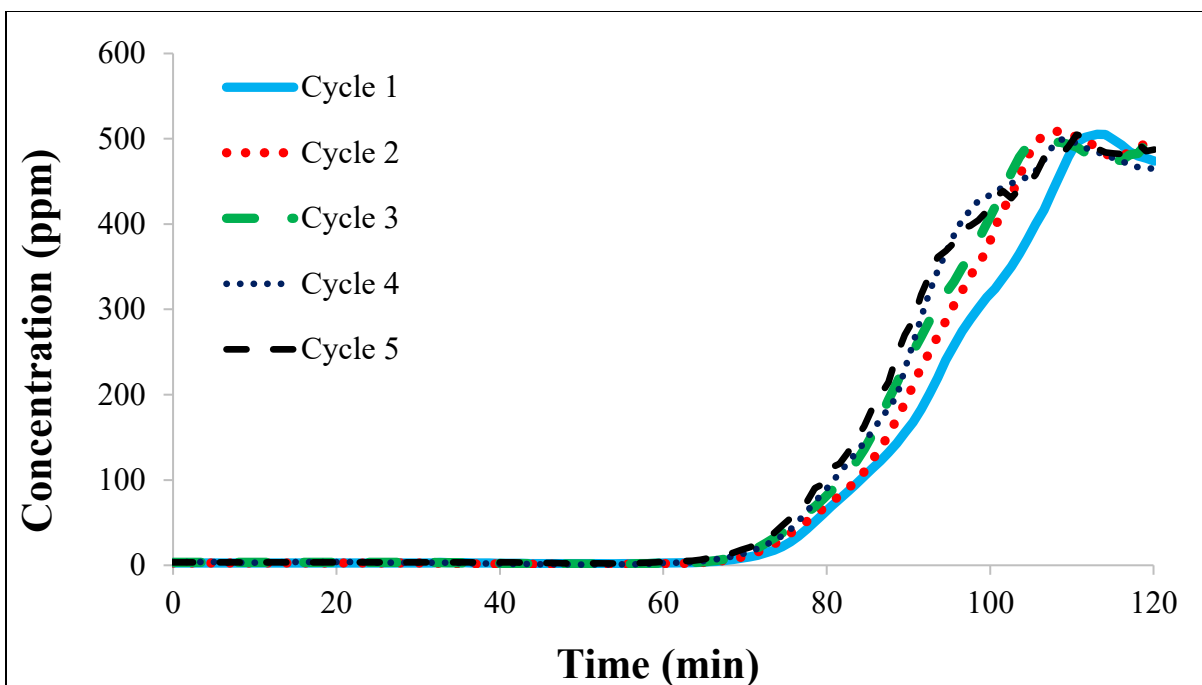


Figure B3. Adsorption breakthrough curves for adsorption of n-butyl acetate on beaded activated carbon, regenerated at  $\leq 5$  ppm  $O_2$  in  $N_2$

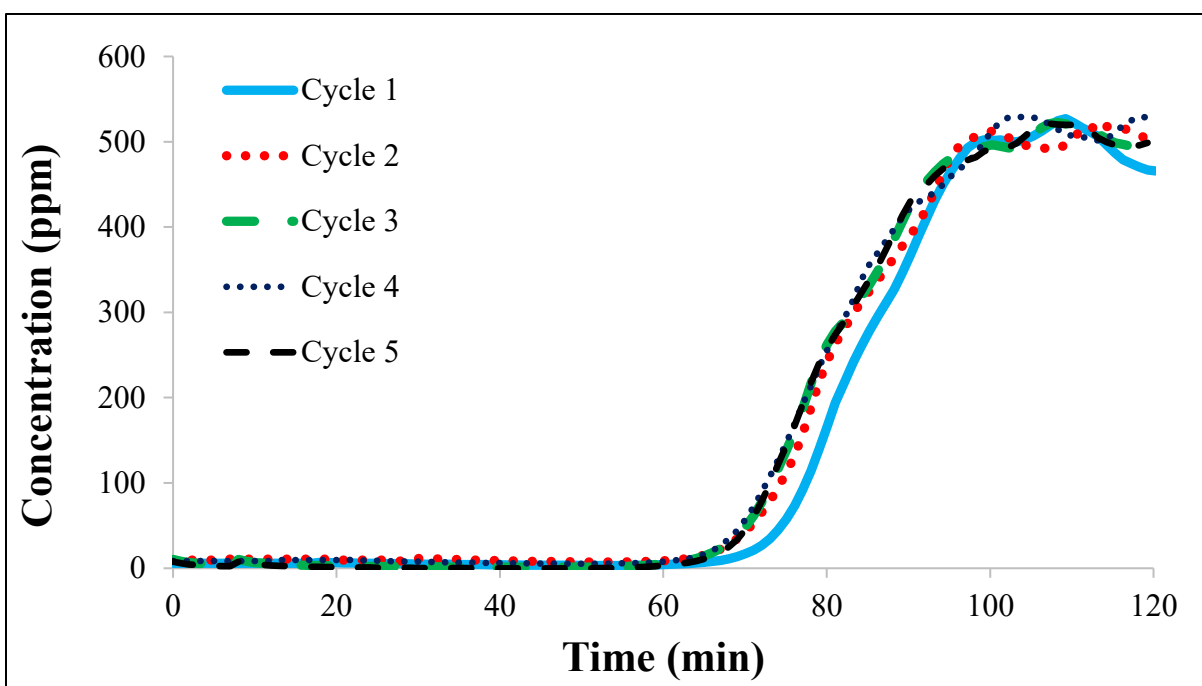


Figure B4. Adsorption breakthrough curves for adsorption of n-butyl acetate on beaded activated carbon, regenerated at 10,000 ppm  $O_2$  in  $N_2$

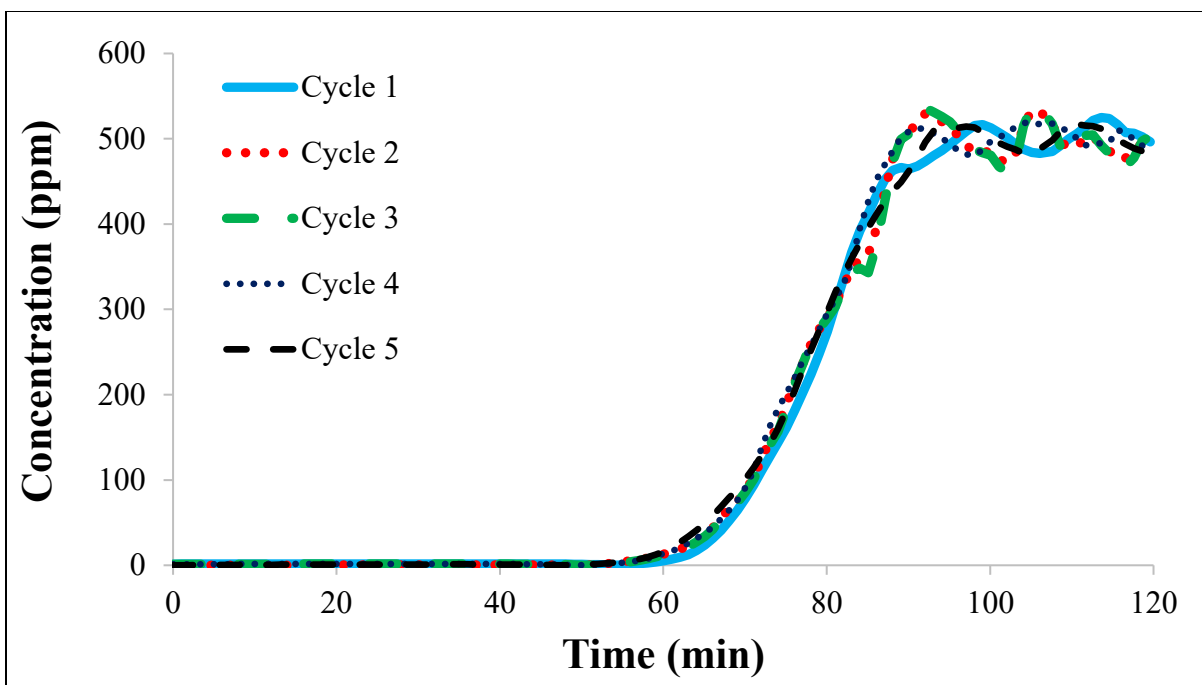


Figure B5. Adsorption breakthrough curves for adsorption of 2-heptanone on beaded activated carbon, regenerated at  $\leq 5$  ppm  $O_2$  in  $N_2$

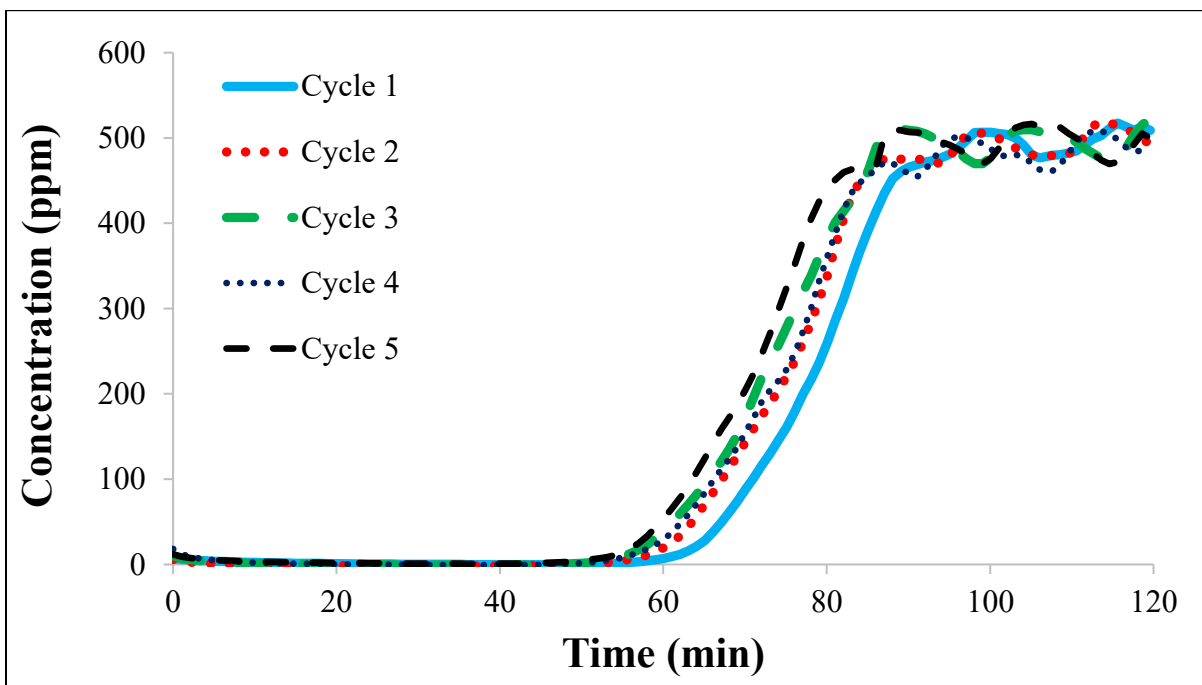


Figure B6. Adsorption breakthrough curves for adsorption of 2-heptanone on beaded activated carbon, regenerated at 10,000 ppm  $O_2$  in  $N_2$



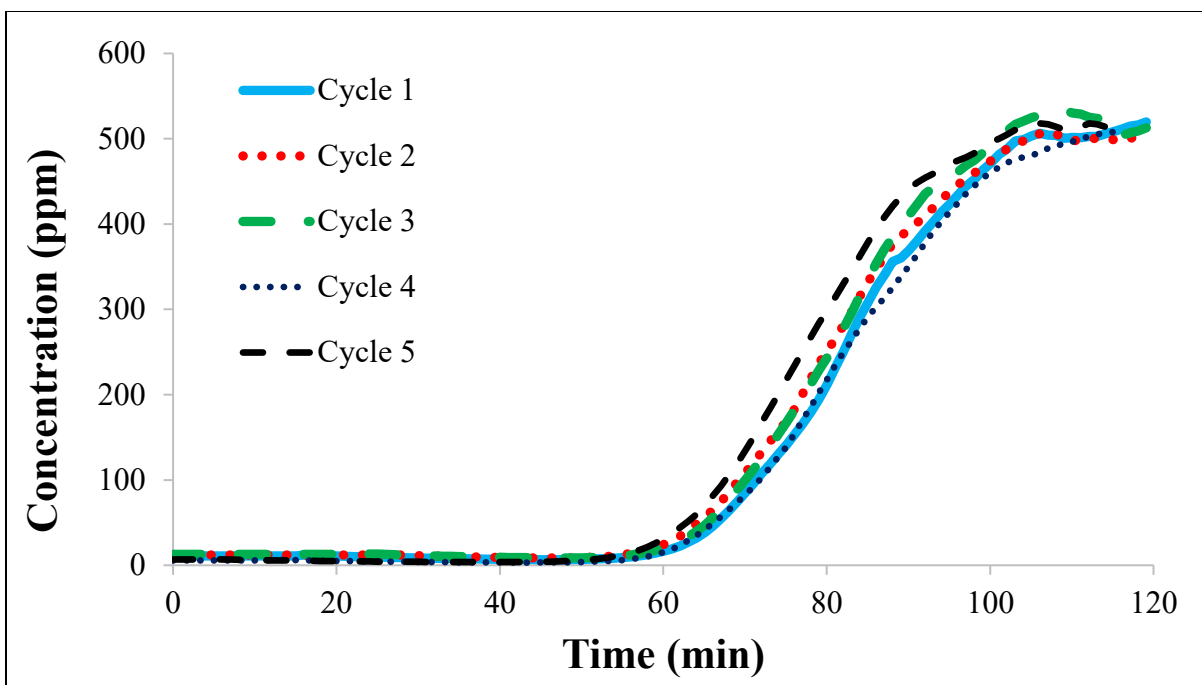


Figure B7. Adsorption breakthrough curves for adsorption of 2-butoxyethanol on beaded activated carbon, regenerated at  $\leq 5$  ppm  $O_2$  in  $N_2$

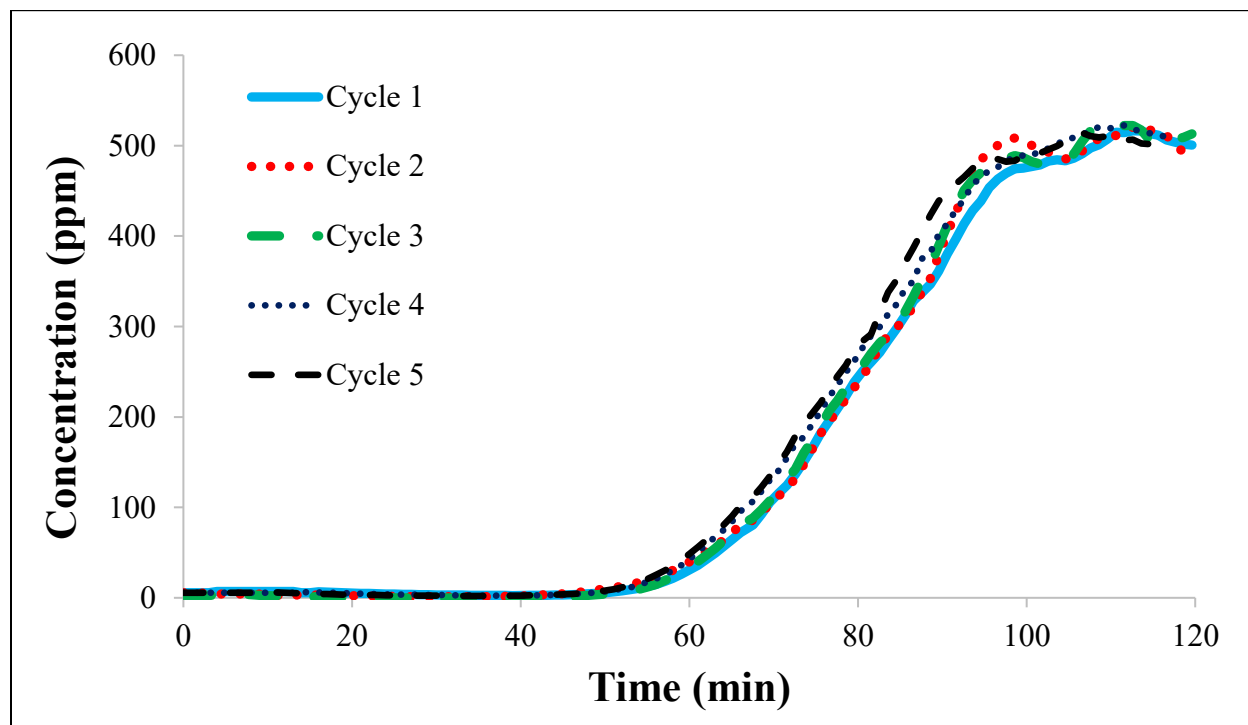


Figure B8. Adsorption breakthrough curves for adsorption of 2-butoxyethanol on beaded activated carbon, regenerated at 10,000 ppm  $O_2$  in  $N_2$

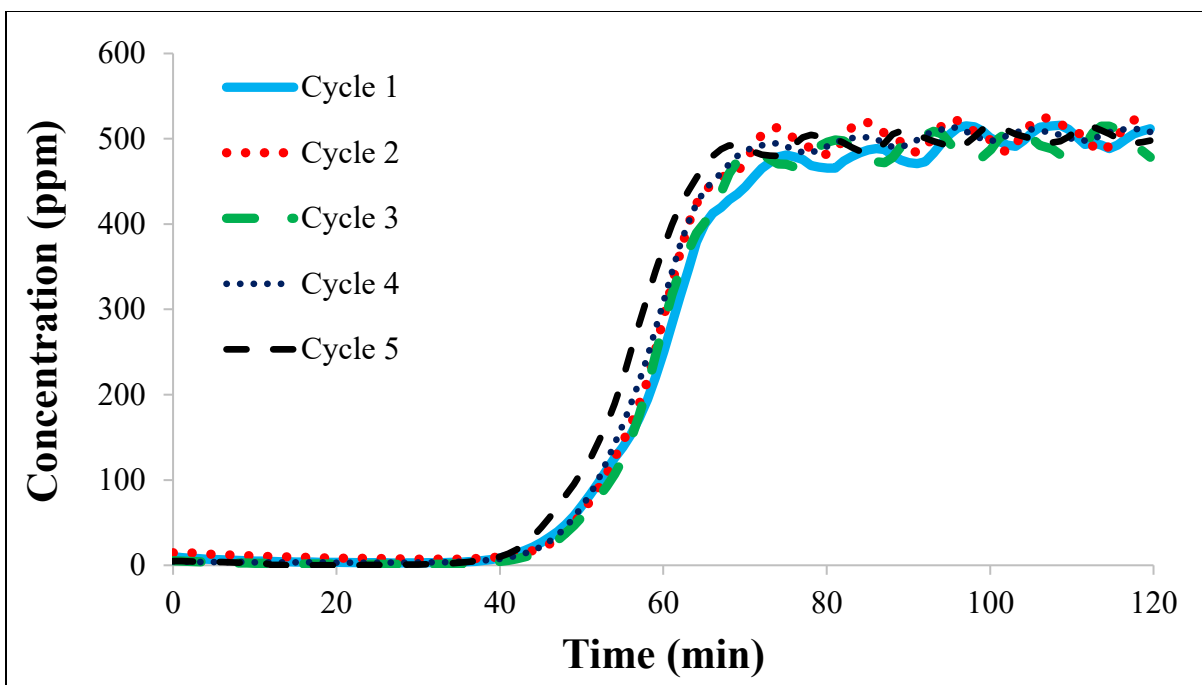


Figure B9. Adsorption breakthrough curves for adsorption of n-decane on beaded activated carbon, regenerated at  $\leq 5$  ppm  $O_2$  in  $N_2$

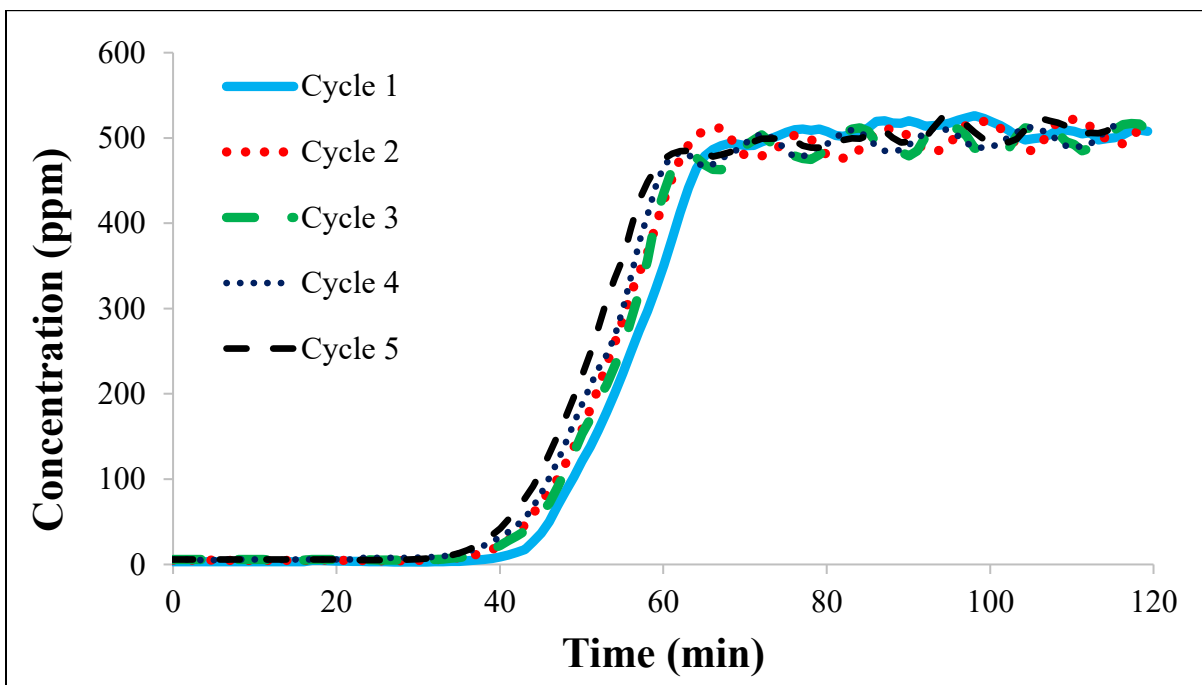


Figure B10. Adsorption breakthrough curves for adsorption of n-decane on beaded activated carbon, regenerated at 10,000 ppm  $O_2$  in  $N_2$

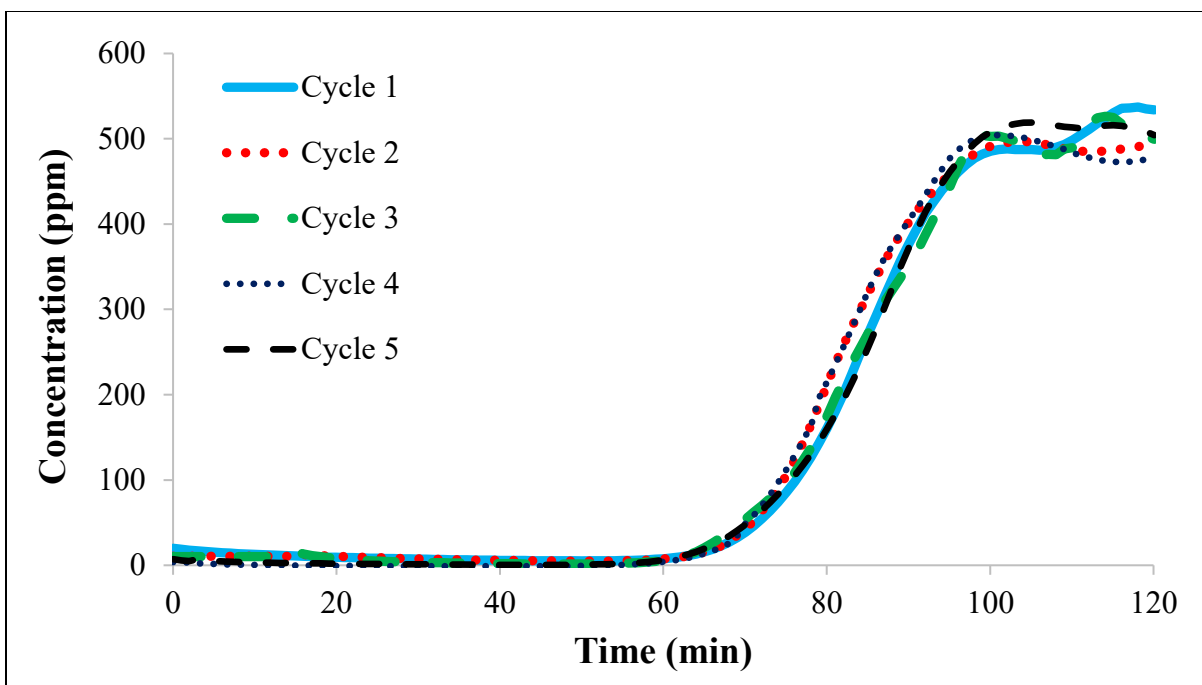


Figure B11. Adsorption breakthrough curves for adsorption of benzene on beaded activated carbon, regenerated at  $\leq 5$  ppm  $O_2$  in  $N_2$

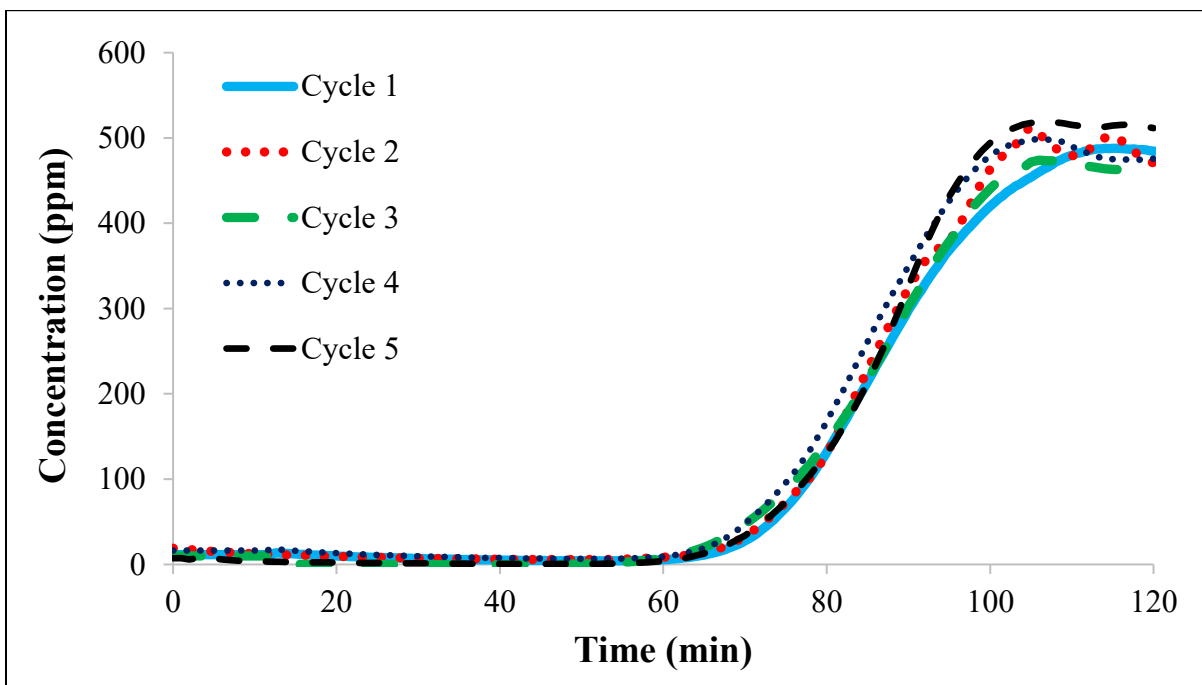


Figure B12. Adsorption breakthrough curves for adsorption of benzene on beaded activated carbon, regenerated at 10,000 ppm  $O_2$  in  $N_2$

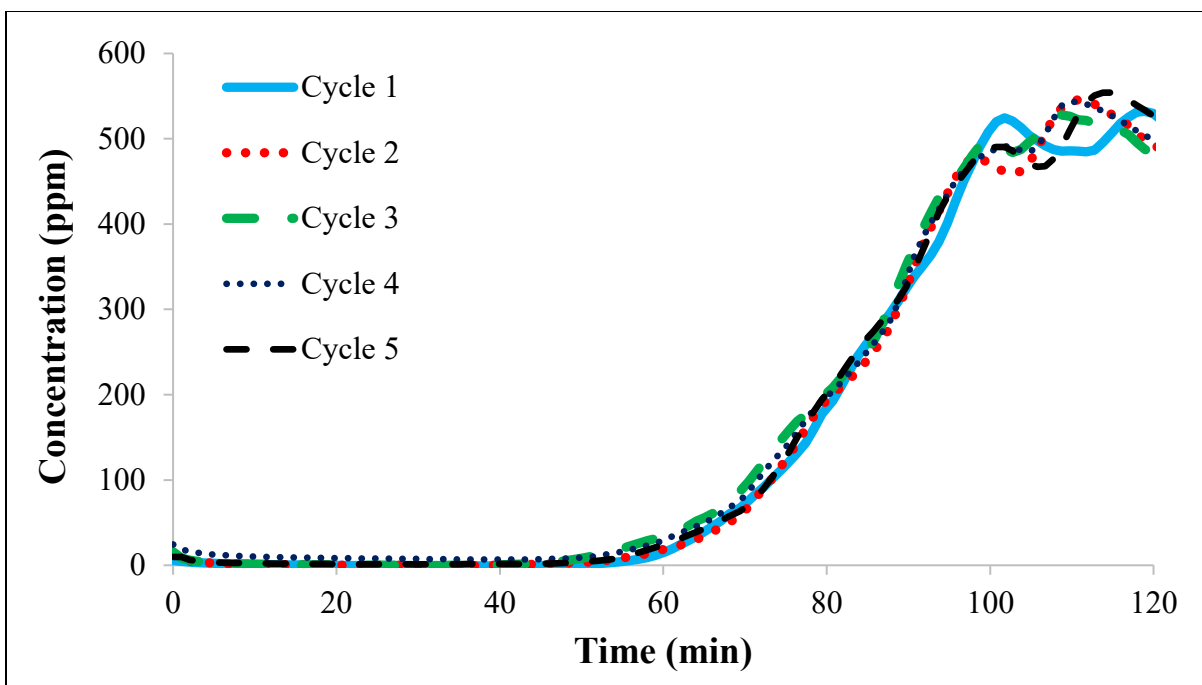


Figure B13. Adsorption breakthrough curves for adsorption of ethylbenzene on beaded activated carbon, regenerated at  $\leq 5$  ppm  $O_2$  in  $N_2$

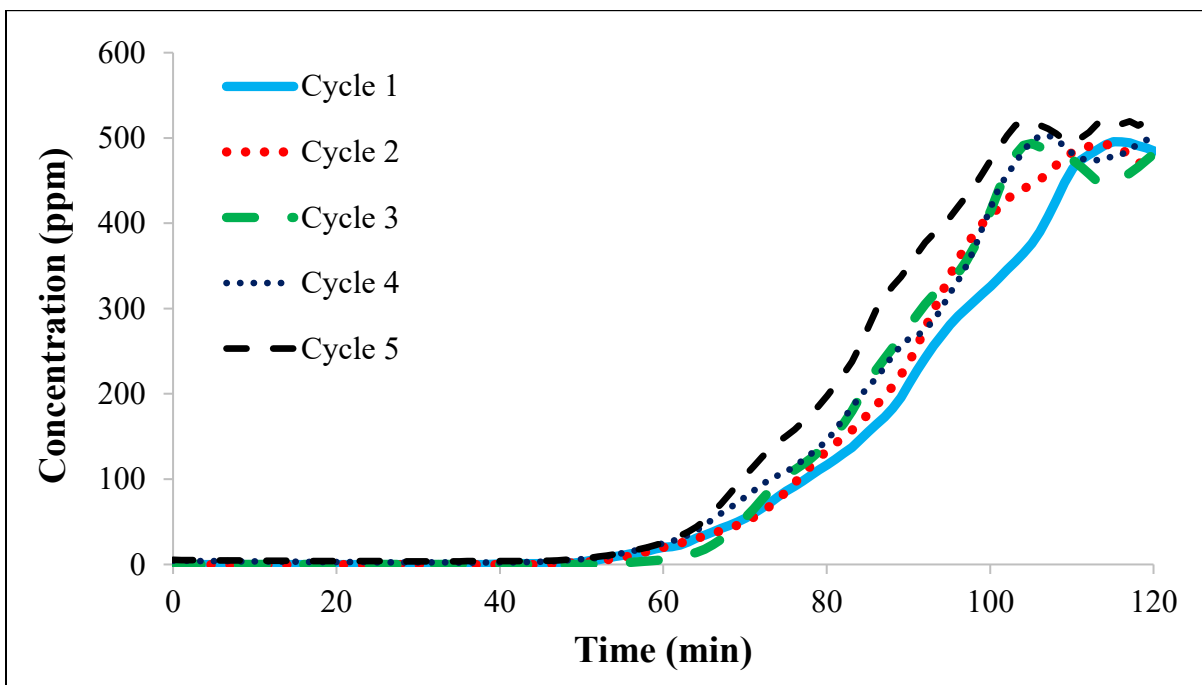


Figure B14. Adsorption breakthrough curves for adsorption of ethylbenzene on beaded activated carbon, regenerated at 10,000 ppm  $O_2$  in  $N_2$

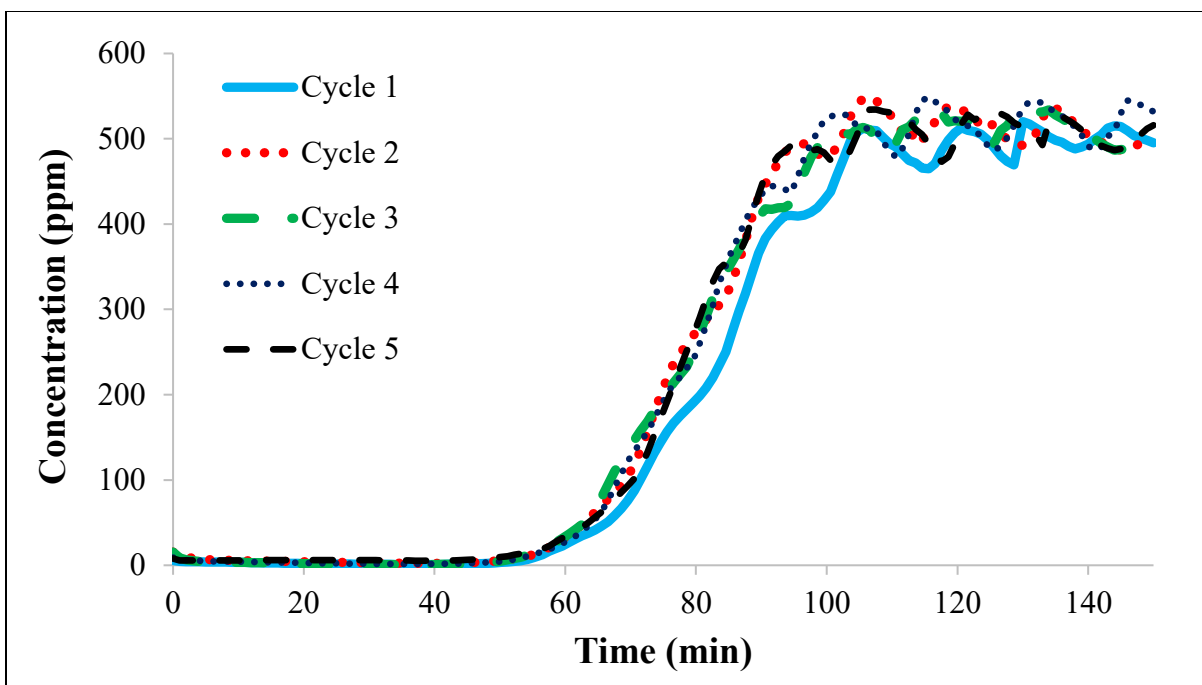


Figure B15. Adsorption breakthrough curves for adsorption of isopropylbenzene on beaded activated carbon, regenerated at  $\leq 5$  ppm  $O_2$  in  $N_2$

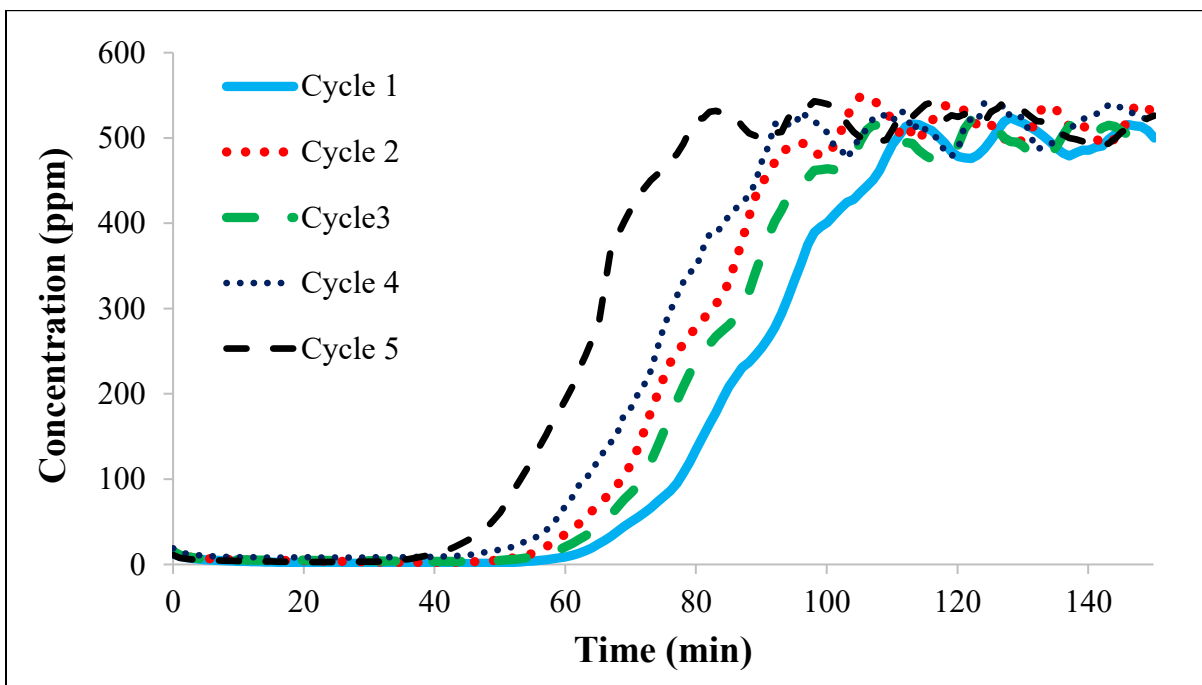


Figure B16. Adsorption breakthrough curves for adsorption of isopropylbenzene on beaded activated carbon, regenerated at 10,000 ppm  $O_2$  in  $N_2$

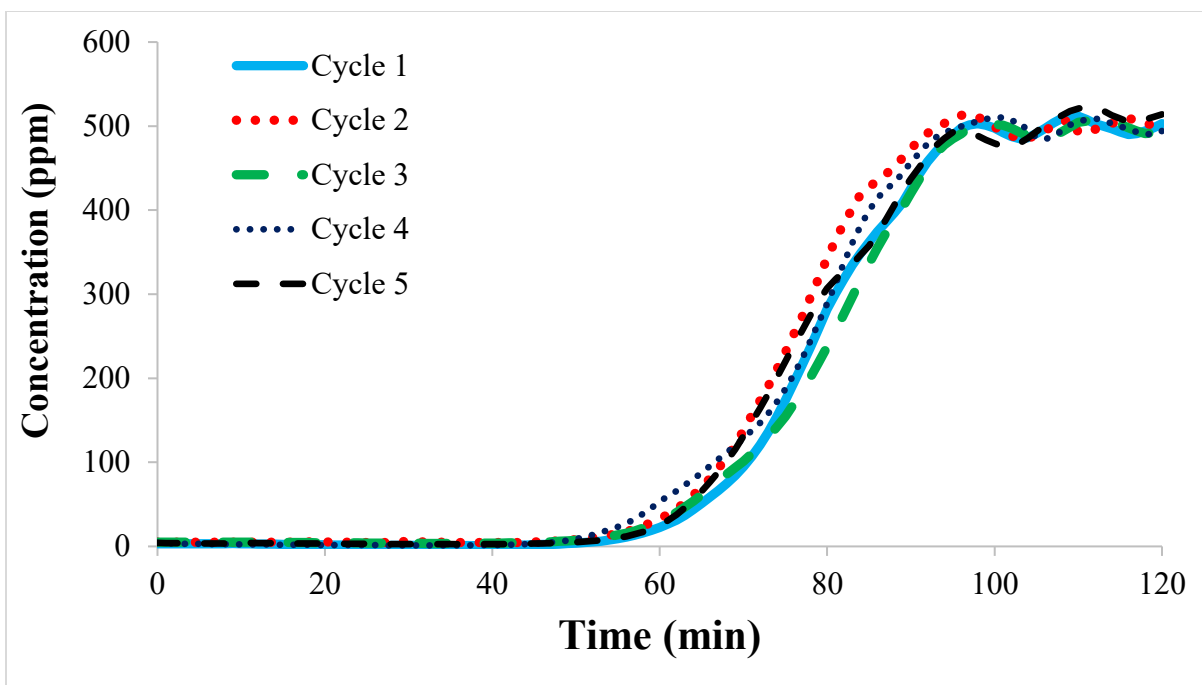


Figure B17. Adsorption breakthrough curves for adsorption of 1,2,4-trimethylbenzene on beaded activated carbon, regenerated at  $\leq 5$  ppm  $O_2$  in  $N_2$

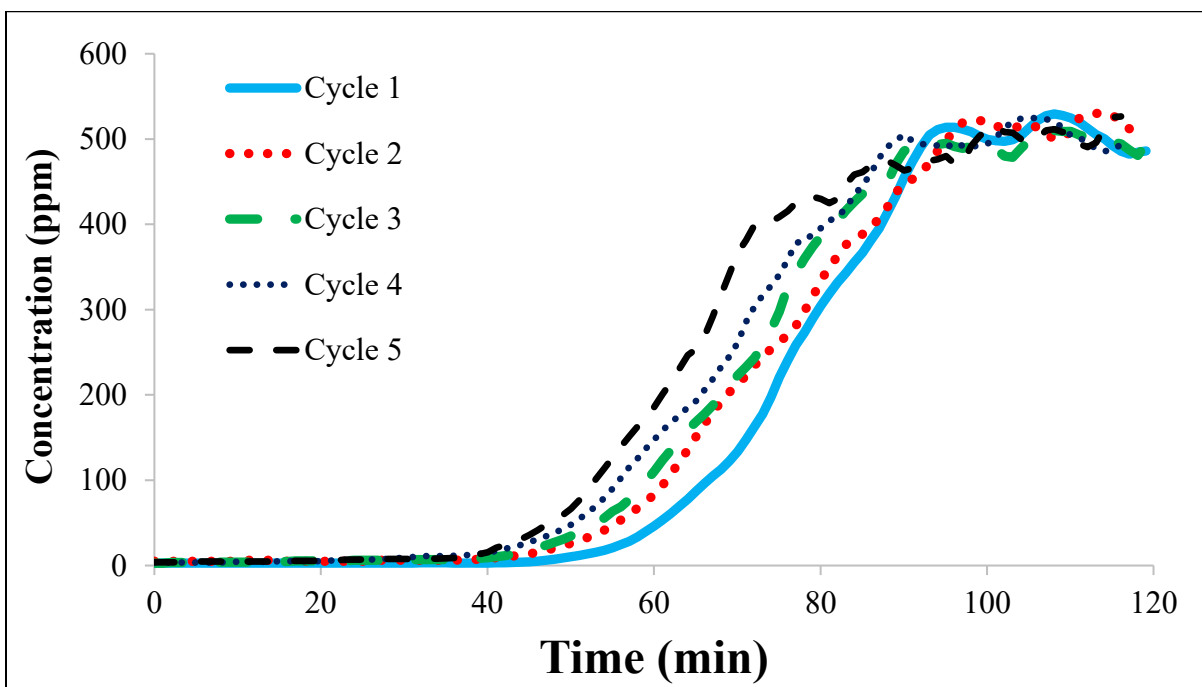


Figure B18. Adsorption breakthrough curves for adsorption of 1,2,4-trimethylbenzene on beaded activated carbon, regenerated at 10,000 ppm  $O_2$  in  $N_2$

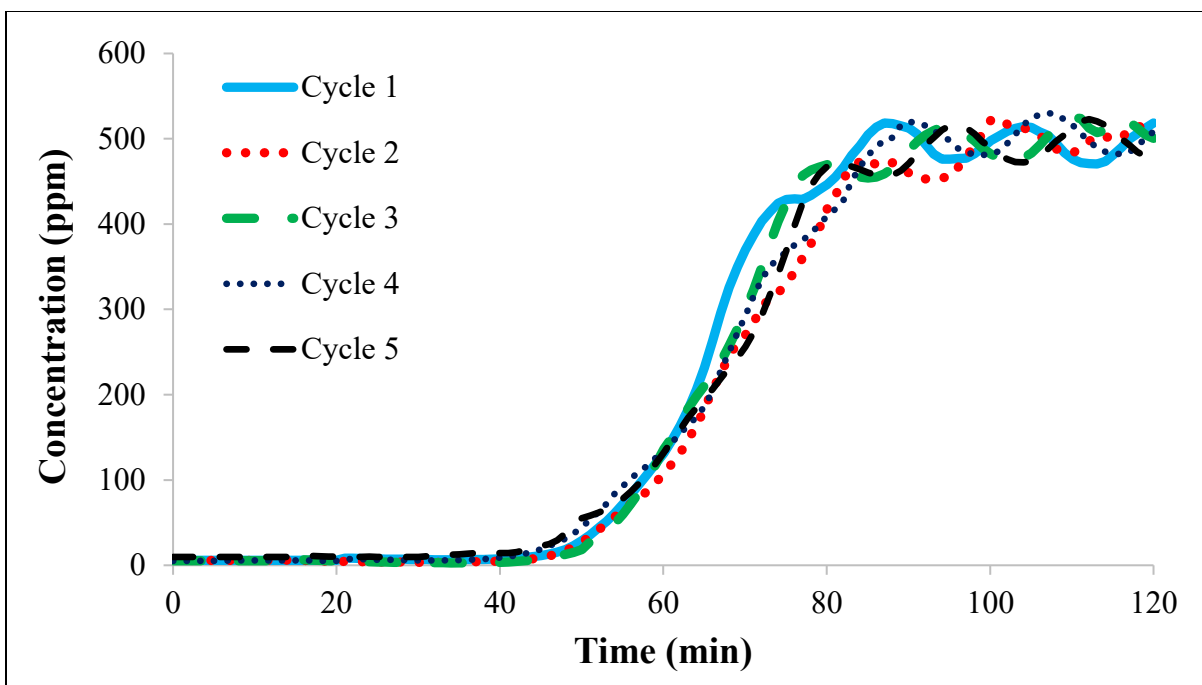


Figure B19. Adsorption breakthrough curves for adsorption of butylbenzene on beaded activated carbon, regenerated at  $\leq 5$  ppm  $O_2$  in  $N_2$

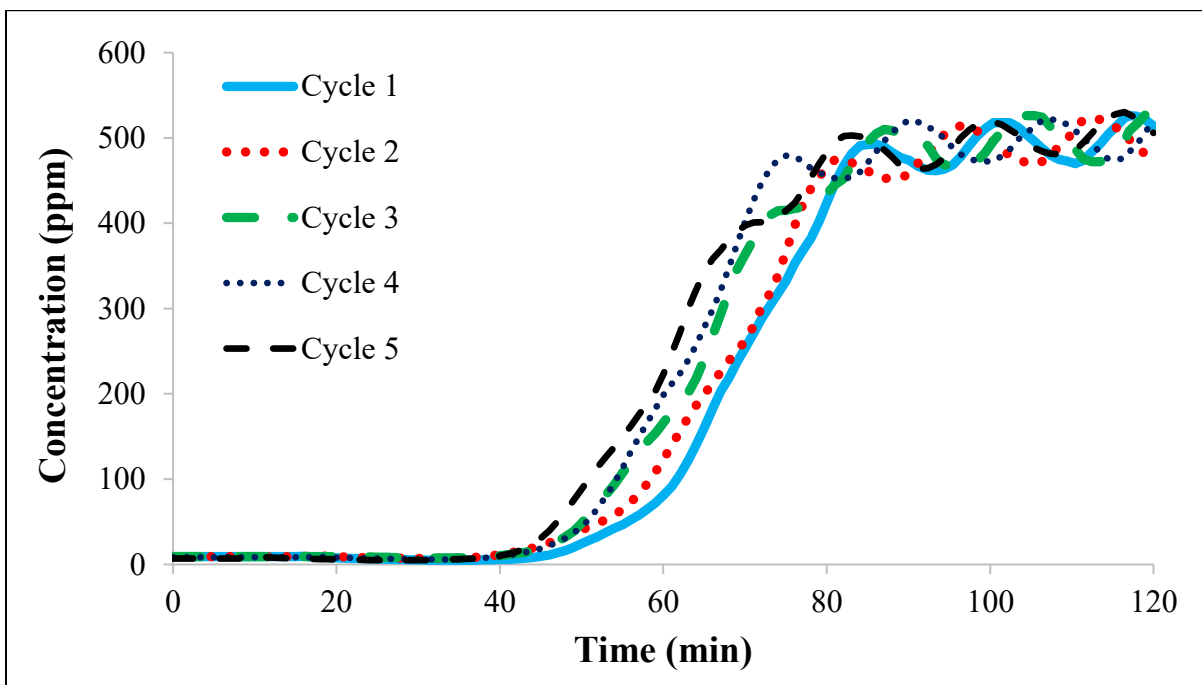


Figure B20. Adsorption breakthrough curves for adsorption of butylbenzene on beaded activated carbon, regenerated at 10,000 ppm  $O_2$  in  $N_2$

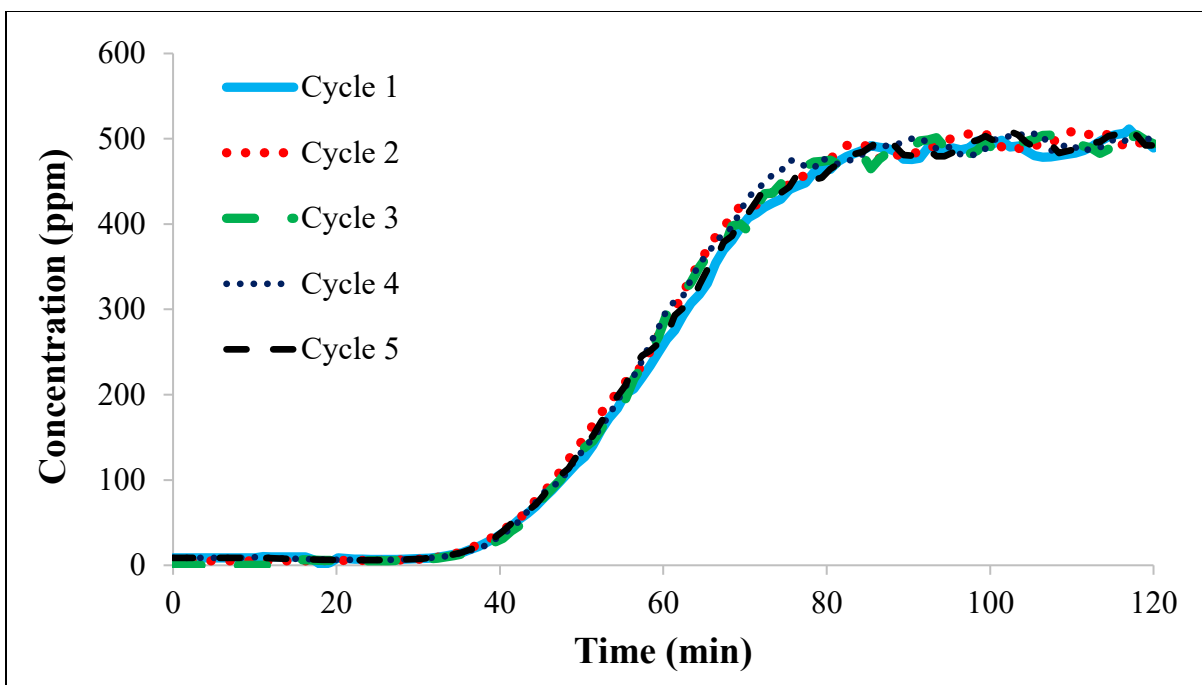


Figure B21. Adsorption breakthrough curves for adsorption of neopentylbenzene on beaded activated carbon, regenerated at  $\leq 5$  ppm  $O_2$  in  $N_2$

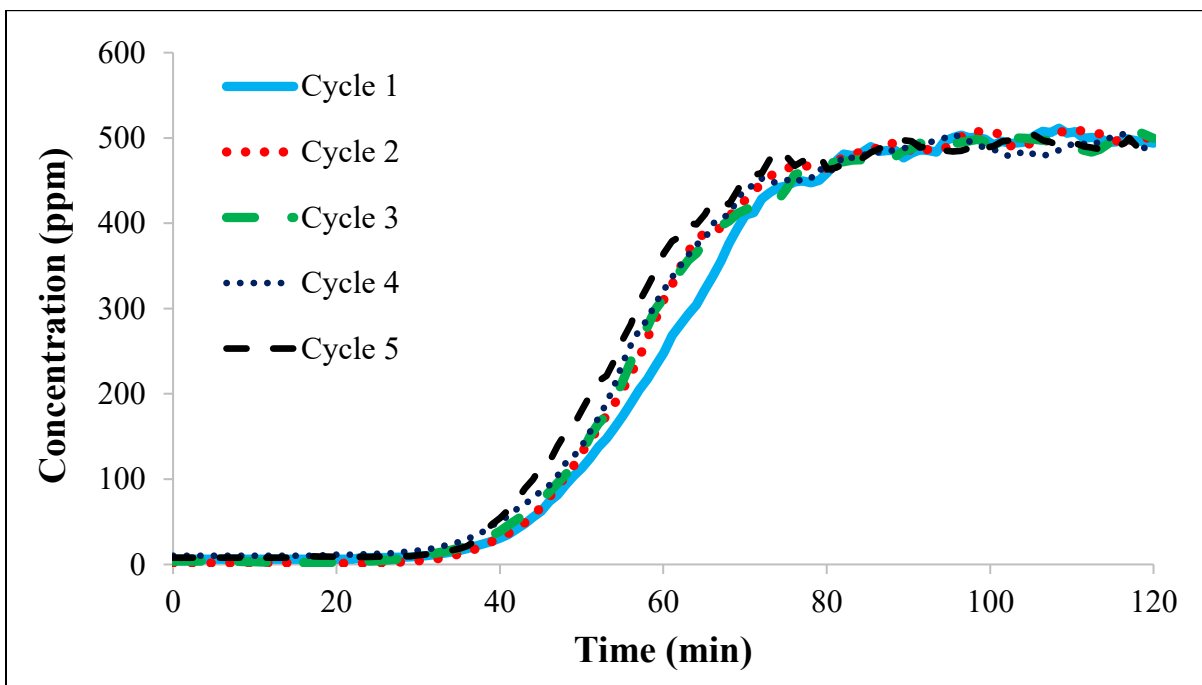


Figure B22. Adsorption breakthrough curves for adsorption of neopentylbenzene on beaded activated carbon, regenerated at 10,000 ppm  $O_2$  in  $N_2$



## Appendix C: Mass balance cumulative heel tables of Chapter 4

Table C1. Mass balance cumulative heel for 1-butanol adsorption on BAC regenerated at  $\leq 5$  ppm O<sub>2</sub> in N<sub>2</sub> purge gas

Weight of dry virgin BAC: 4.047 g				
Cycle	Amount Adsorbed (g)	Adsorption Capacity (%)	Total Heel (g)	Total Heel (% g Total Heel/g BAC)
1	1.475	36.4	0.000	0.0
2	1.467	36.2	0.005	0.1
3	1.432	35.4	0.000	0.0
4	1.474	36.4	0.004	0.1
5	1.471	36.3	0.010	0.2

Table C2. Mass balance cumulative heel for 1-butanol adsorption on BAC regenerated at 10,000 ppm O<sub>2</sub> in N<sub>2</sub> purge gas

Weight of dry virgin BAC: 4.014 g				
Cycle	Amount Adsorbed (g)	Adsorption Capacity (%)	Total Heel (g)	Total Heel (% g Total Heel/g BAC)
1	1.484	37.0	0.018	0.4
2	1.428	35.6	0.021	0.5
3	1.435	35.7	0.024	0.6
4	1.443	35.9	0.022	0.5
5	1.463	36.4	0.028	0.7

Table C3. Mass balance cumulative heel for n-butyl acetate adsorption on BAC regenerated at  $\leq$  5 ppm O<sub>2</sub> in N<sub>2</sub> purge gas

Weight of dry virgin BAC: 4.020 g				
Cycle	Amount Adsorbed (g)	Adsorption Capacity (%)	Total Heel (g)	Total Heel (% of Total Heel/g BAC)
1	1.712	42.6	0.029	0.7
2	1.703	42.4	0.034	0.8
3	1.704	42.4	0.044	1.1
4	1.697	42.2	0.045	1.1
5	1.692	42.1	0.053	1.3

Table C4. Mass balance cumulative heel for n-butyl acetate adsorption on BAC regenerated at 10,000 ppm O<sub>2</sub> in N<sub>2</sub> purge gas

Weight of dry virgin BAC: 4.006 g				
Cycle	Amount Adsorbed (g)	Adsorption Capacity (%)	Total Heel (g)	Total Heel (% of Total Heel/g BAC)
1	1.647	41.1	0.019	0.5
2	1.637	40.9	0.030	0.8
3	1.649	41.2	0.041	1.0
4	1.646	41.1	0.049	1.2
5	1.643	41.0	0.050	1.3

Table C5. Mass balance cumulative heel for 2-heptanone adsorption on BAC regenerated at  $\leq 5$  ppm O<sub>2</sub> in N<sub>2</sub> purge gas

Weight of dry virgin BAC: 4.106 g				
Cycle	Amount Adsorbed (g)	Adsorption Capacity (%)	Total Heel (g)	Total Heel (% of Total Heel/g BAC)
1	1.653	40.3	0.007	0.170
2	1.619	39.4	0.006	0.146
3	1.613	39.3	0.009	0.219
4	1.614	39.3	0.012	0.292
5	1.618	39.4	0.019	0.463

Table C6. Mass balance cumulative heel for 2-heptanone adsorption on BAC regenerated at 10,000 ppm O<sub>2</sub> in N<sub>2</sub> purge gas

Weight of dry virgin BAC: 4.031 g				
Cycle	Amount Adsorbed (g)	Adsorption Capacity (%)	Total Heel (g)	Total Heel (% of Total Heel/g BAC)
1	1.585	39.3	0.039	1.0
2	1.557	38.6	0.063	1.6
3	1.534	38.1	0.078	1.9
4	1.553	38.5	0.103	2.6
5	1.527	37.9	0.117	2.9

Table C7. Mass balance cumulative heel for 2-butoxyethanol adsorption on BAC regenerated at  $\leq 5$  ppm O<sub>2</sub> in N<sub>2</sub> purge gas

Weight of dry virgin BAC: 3.987 g				
Cycle	Amount Adsorbed (g)	Adsorption Capacity (%)	Total Heel (g)	Total Heel (% g Total Heel/g BAC)
1	1.793	45.0	0.022	0.6
2	1.775	44.5	0.025	0.6
3	1.790	44.9	0.027	0.7
4	1.822	45.7	0.031	0.8
5	1.768	44.3	0.044	1.1

Table C8. Mass balance cumulative heel for 2-butoxyethanol adsorption on BAC regenerated at  $\leq 10,000$  O<sub>2</sub> in N<sub>2</sub> purge gas (numbers in parenthesis are from duplicated experiment)

Weight of dry virgin BAC: 4.036 g (4.017 g)				
Cycle	Amount Adsorbed (g)	Adsorption Capacity (%)	Total Heel (g)	Total Heel (% g Total Heel/g BAC)
1	1.803 (1.822)	44.7 (45.4)	0.029 (0.005)	0.7 (0.1)
2	1.763 (1.793)	43.7 (44.6)	0.028 (0.028)	0.7 (0.7)
3	1.685 (1.772)	41.7 (44.1)	0.048 (0.019)	1.2 (0.5)
4	1.775 (1.772)	44.0 (44.1)	0.064 (0.042)	1.6 (1.0)
5	1.752 (1.757)	43.4 (43.7)	0.054 (0.042)	1.3 (1.0)

Table C9. Mass balance cumulative heel for n-decane adsorption on BAC regenerated at  $\leq 5$  ppm O<sub>2</sub> in N<sub>2</sub> purge gas

Weight of dry virgin BAC: 4.051 g				
Cycle	Amount Adsorbed (g)	Adsorption Capacity (%)	Total Heel (g)	Total Heel (% g Total Heel/g BAC)
1	1.486	36.7	0.024	0.592
2	1.464	36.1	0.020	0.494
3	1.467	36.2	0.023	0.568
4	1.464	36.1	0.026	0.642
5	1.465	36.2	0.029	0.716

Table C10. Mass balance cumulative heel for n-decane adsorption on BAC regenerated at 10,000 ppm O<sub>2</sub> in N<sub>2</sub> purge gas (numbers in parenthesis are from duplicated experiment)

Weight of dry virgin BAC: 3.993 g (4.056 g)				
Cycle	Amount Adsorbed (g)	Adsorption Capacity (%)	Total Heel (g)	Total Heel (% g Total Heel/g BAC)
1	1.494 (1.476)	37.4 (36.4)	0.036 (0.040)	0.9 (1.0)
2	1.432 (1.456)	35.9 (35.9)	0.055 (0.063)	1.4 (1.6)
3	1.432 (1.376)	35.9 (33.9)	0.083 (0.073)	2.1 (1.8)
4	1.417 (1.439)	35.5 (35.5)	0.107 (0.093)	2.7 (2.3)
5	1.402 (1.430)	35.1 (35.3)	0.135 (0.125)	3.4 (3.1)

Table C11. Mass balance cumulative heel for benzene adsorption on BAC regenerated at  $\leq 5$  ppm O<sub>2</sub> in N<sub>2</sub> purge gas

Weight of dry virgin BAC: 4.039 g				
Cycle	Amount Adsorbed (g)	Adsorption Capacity (%)	Total Heel (g)	Total Heel (% of Total Heel/g BAC)
1	1.077	26.7	-0.001	0.0
2	1.113	27.6	0.000	0.0
3	1.094	27.1	-0.001	0.0
4	1.099	27.2	0.004	0.1
5	1.104	27.3	0.000	0.0

Table C12. Mass balance cumulative heel for benzene adsorption on BAC regenerated at 10,000 ppm O<sub>2</sub> in N<sub>2</sub> purge gas

Weight of dry virgin BAC: 3.981 g				
Cycle	Amount Adsorbed (g)	Adsorption Capacity (%)	Total Heel (g)	Total Heel (% of Total Heel/g BAC)
1	1.087	27.3	0.006	0.2
2	1.070	26.9	0.009	0.2
3	1.062	26.7	0.009	0.2
4	1.071	26.9	0.010	0.3
5	1.077	27.1	0.008	0.2

Table C13. Mass balance cumulative heel for ethylbenzene adsorption on BAC regenerated at  $\leq$  5 ppm O<sub>2</sub> in N<sub>2</sub> purge gas

Weight of dry virgin BAC: 4.029 g				
Cycle	Amount Adsorbed (g)	Adsorption Capacity (%)	Total Heel (g)	Total Heel (% of Total Heel/g BAC)
1	1.635	40.6	0.004	0.1
2	1.636	40.6	0.004	0.1
3	1.627	40.4	0.001	0.0
4	1.642	40.8	0.003	0.1
5	1.623	40.3	0.004	0.1

Table C14. Mass balance cumulative heel for ethylbenzene adsorption on BAC regenerated at 10,000 ppm O<sub>2</sub> in N<sub>2</sub> purge gas

Weight of dry virgin BAC: 4.077 g				
Cycle	Amount Adsorbed (g)	Adsorption Capacity (%)	Total Heel (g)	Total Heel (% of Total Heel/g BAC)
1	1.663	40.8	0.015	0.4
2	1.655	40.6	0.025	0.6
3	1.659	40.7	0.034	0.8
4	1.641	40.3	0.045	1.1
5	1.645	40.3	0.062	1.5

Table C15. Mass balance cumulative heel for 1,2,4-trimethylbenzene adsorption on BAC regenerated at  $\leq 5$  ppm O<sub>2</sub> in N<sub>2</sub> purge gas

Weight of dry virgin BAC: 4.014 g				
Cycle	Amount Adsorbed (g)	Adsorption Capacity (%)	Total Heel (g)	Total Heel (% g Total Heel/g BAC)
1	1.779	45.1	0.009	0.2
2	1.770	44.9	0.014	0.4
3	1.793	45.4	0.025	0.6
4	1.784	45.2	0.026	0.7
5	1.781	45.1	0.029	0.7

Table C16. Mass balance cumulative heel for 1,2,4-trimethylbenzene adsorption on BAC regenerated at 10,000 ppm O<sub>2</sub> in N<sub>2</sub> purge gas (numbers in parenthesis are from duplicated experiment)

Weight of dry virgin BAC: g				
Cycle	Amount Adsorbed (g)	Adsorption Capacity (%)	Total Heel (g)	Total Heel (% g Total Heel/g BAC)
1	1.745 (1.747)	44.0 (43.7)	0.103 (0.103)	2.6 (2.6)
2	1.664 (1.675)	41.9 (41.9)	0.210 (0.227)	5.3 (5.7)
3	1.628 (1.601)	41.0 (40.0)	0.327 (0.320)	8.2 (8.0)
4	1.560 (1.554)	39.3 (38.9)	0.433 (0.437)	10.9 (10.9)
5	1.484 (1.471)	37.4 (36.8)	0.514 (0.536)	13.0 (13.4)



Table C17. Mass balance cumulative heel for isopropylbenzene adsorption on BAC regenerated at  $\leq 5$  ppm O<sub>2</sub> in N<sub>2</sub> purge gas

Weight of dry virgin BAC: 4.014 g				
Cycle	Amount Adsorbed (g)	Adsorption Capacity (%)	Total Heel (g)	Total Heel (% of Total Heel/g BAC)
1	1.783	44.4	0.040	1.0
2	1.886	47.0	0.071	1.8
3	1.841	45.9	0.109	2.7
4	1.903	47.4	0.155	3.9
5	1.828	45.5	0.185	4.6

Table C18. Mass balance cumulative heel for isopropylbenzene adsorption on BAC regenerated at 10,000 ppm O<sub>2</sub> in N<sub>2</sub> purge gas

Weight of dry virgin BAC: 4.001 g				
Cycle	Amount Adsorbed (g)	Adsorption Capacity (%)	Total Heel (g)	Total Heel (% of Total Heel/g BAC)
1	1.833	45.8	0.112	2.8
2	1.879	47.0	0.224	5.6
3	1.747	43.7	0.303	7.6
4	1.659	41.5	0.389	9.7
5	1.603	40.1	0.448	11.2

Table C19. Mass balance cumulative heel for butylbenzene adsorption on BAC regenerated at  $\leq$  5 ppm O<sub>2</sub> in N<sub>2</sub> purge gas

Weight of dry virgin BAC: 4.002 g				
Cycle	Amount Adsorbed (g)	Adsorption Capacity (%)	Total Heel (g)	Total Heel (% of Total Heel/g BAC)
1	1.729	43.2	0.014	0.3
2	1.703	42.6	0.021	0.5
3	1.623	40.6	0.016	0.4
4	1.731	43.3	0.028	0.7
5	1.714	42.8	0.034	0.8

Table C20. Mass balance cumulative heel for butylbenzene adsorption on BAC regenerated at 10,000 ppm O<sub>2</sub> in N<sub>2</sub> purge gas

Weight of dry virgin BAC: 4.016 g				
Cycle	Amount Adsorbed (g)	Adsorption Capacity (%)	Total Heel (g)	Total Heel (% of Total Heel/g BAC)
1	1.684	41.9	0.079	2.0
2	1.674	41.7	0.132	3.3
3	1.634	40.7	0.180	4.5
4	1.603	39.9	0.230	5.7
5	1.578	39.3	0.282	7.0

Table C21. Mass balance cumulative heel for neopentylbenzene adsorption on BAC regenerated at  $\leq 5$  ppm O<sub>2</sub> in N<sub>2</sub> purge gas

Weight of dry virgin BAC: 3.982 g				
Cycle	Amount Adsorbed (g)	Adsorption Capacity (%)	Total Heel (g)	Total Heel (% of Total Heel/g BAC)
1	1.656	41.6	0.023	0.6
2	1.650	41.4	0.027	0.7
3	1.641	41.2	0.019	0.5
4	1.640	41.2	0.014	0.4
5	1.652	41.5	0.028	0.7

Table C22. Mass balance cumulative heel for neopentylbenzene adsorption on BAC regenerated at 10,000 ppm O<sub>2</sub> in N<sub>2</sub> purge gas

Weight of dry virgin BAC: 4.030 g				
Cycle	Amount Adsorbed (g)	Adsorption Capacity (%)	Total Heel (g)	Total Heel (% of Total Heel/g BAC)
1	1.692	42.0	0.021	0.5
2	1.664	41.3	0.034	0.8
3	1.659	41.2	0.044	1.1
4	1.637	40.6	0.052	1.3
5	1.635	40.6	0.055	1.4